

Aus der Klinik für Dermatologie
des Universitätsklinikums Heidelberg
(Ärztlicher Direktor: Prof. Dr. med. Alexander Enk)

Contribution of B cells to autoimmune blistering diseases in regulatory T cell-deficient scurfy mice

Inauguraldissertation
zur Erlangung des Doctor scientiarum humanarum (Dr. sc. hum.)
an der medizinischen Fakultät Heidelberg
der
Ruprecht-Karls-Universität

vorgelegt von
Elisabeth Marie Vicari

aus
Speyer, Deutschland

2023

Dekan: Herr Prof. Dr. med. Dr. h. c. Hans-Georg Kräusslich

Doktormutter: Frau Prof. Dr. med. Eva Hadaschik

TABLE OF CONTENT

TABLE OF CONTENT	3
ABBREVIATIONS	6
TABLE OF FIGURES	8
1 INTRODUCTION	9
1.1 Autoimmunity	9
1.1.1 Regulatory T cells (Treg)	9
1.1.2 Scurfy mouse model	10
1.1.3 B cells	11
1.2 Architecture of the skin.....	15
1.3 Autoimmune blistering diseases (AIBD)	17
1.3.1 Epidemiological background	17
1.3.2 Diagnostic of AIBD	18
1.3.3 Epidermolysis bullosa acquisita (EBA)	18
1.3.4 Pathological mechanisms of EBA.....	19
1.4 Aims of the project	21
2 MATERIAL AND METHODS	22
2.1 Material	22
2.1.1 Cell culture media and reagents.....	22
2.1.2 Cell lines	23
2.1.3 Primers (Genotyping)	23
2.1.4 Antibodies	24
2.1.5 Kits.....	26
2.1.6 Markers	27
2.1.7 Enzymes	27
2.1.8 Buffers and solutions.....	27
2.1.9 Additional reagents	30
2.1.10 Materials	31

2.1.11	Lab equipment	31
2.1.12	Databases	32
2.1.13	Software	32
2.2	Methods	32
2.2.1	Mice	32
2.2.2	Passive Transfer of monoclonal antibodies into neonatal mice.....	33
2.2.3	Genotyping.....	33
2.2.4	Cell experiments	34
2.2.5	SDS-PAGE.....	36
2.2.6	Bicinchoninic Acid Assay (BCA)	37
2.2.7	Histology	37
2.2.8	Immunofluorescence microscopy	38
2.2.9	Peptide Competition Assay	39
2.2.10	Enzyme linked immunospot assay (ELISpot).....	39
2.2.11	Enzyme linked immunosorbent assay (ELISA).....	40
2.2.12	Flow cytometry	40
2.2.13	LEGENDplex Assay	41
2.2.14	Statistical Analysis.....	41
3	RESULTS	42
3.1	Scurfy mice show altered lymphatic organs	42
3.2	Scurfy mice have altered B cell populations and show restricted B cell maturation in lymph nodes	43
3.3	Spleen of scurfy mice shows impaired marginal zone surrounding follicles	46
3.4	Scurfy mice have elevated frequencies of memory B cells	47
3.5	Germinal center B cells and autoantibody producing cells are highly increased in scurfy mice	49
3.6	Inflamed skin of scurfy mice shows elevated levels of B cells	51
3.7	Serum of scurfy mice contains B cell relevant inflammatory cytokines related to Th2 immune responses	52
3.8	Scurfy mice develop AIBD-related antigen-specific B cells.....	54

3.9	Isolated scurfy autoantibody H510 targets antigen expressed in lower BMZ	56
3.10	Pathogenic autoantibody H510 targets murine vWFA2 of Col7	60
3.11	Pathologic mechanism of H510 is independent of inflammatory immune cells	63
4	DISCUSSION	65
4.1	Treg deficiency leads to altered B cell compartment in scurfy mice	65
4.2	Scurfy mice develop antigen-specific B cells relevant for AIBD onset.....	68
4.3	Injection of autoantibody H510 mimics EBA in mice	68
4.4	H510 induces skin blistering independent from inflammatory immune cells	70
4.5	Conclusion and outlook.....	71
5	SUMMARY	73
6	ZUSAMMENFASSUNG	74
7	REFERENCES	75
8	PERSONAL PUBLICATIONS.....	88
9	ACKNOWLEDGMENTS	89
10	EIDESSTÄTTLICHE VERSICHERUNG	90

ABBREVIATIONS

AF	alexa fluor
AIBD	autoimmune blistering diseases
APC	antigen presenting cell
BAFF	B cell activating factor
BCA	bicinchoninic acid assay
BCR	B cell receptor
BM	bone marrow
BMZ	basement membrane zone
BP	Bullous pemphigoid
BP180	bullous pemphigoid 180
BP230	bullous pemphigoid 230
Breg	regulatory B cell
BSA	bovine serum albumin
CD	cluster of differentiation
Col7	collagen type VII
DAPI	4'6-diamidine-2'-phenylindole dihydrochloride
DC	dendritic cell
DEJ	dermal-epidermal junction
DIF	direct immunofluorescence
DMEM	Dulbecco's modified Eagle's medium
DMSO	dimethyl sulfoxide
DNA	deoxyribonucleic acid
EBA	Epidermolysis bullosa acquisita
ELISA	Enzyme linked immunosorbent assay
ELISpot	Enzyme linked immunospot assay
FACS	fluorescence-activated cell sorting
Fc	crystallizable fragment of an antibody
FcγR	Fcγ-receptor
FCS	fetal calf serum
FO	follicles
Foxp3	forkhead box P3 (transcription factor)
GC	germinal center
h	hour
H&E	hematoxylin and eosin
H510	name of monoclonal scurfy antibody

HEK293T	human embryonic kidney cells 293T
HEPES	4-(2-hydroxyethyl)-1-piperazineethanesulfonic acid
HRP	horseradish peroxidase
IFN	interferon
IgG/A/M	immunoglobulin G/A/M
IIF	indirect immunofluorescence
IL	interleukin
kDa	kilo dalton
MHC	major histocompatibility complex
MZ	marginal zone
NaCl	sodium chloride
NC1/2	non-collagenous domain 1/2
PBS	phosphate buffered saline
PCR	polymerase chain reaction
Pen/Strep	penicillin/streptomycin
PVDF	polyvinylidene fluoride
ROS	reactive oxygen species
RT	room temperature
sBCMA	soluble B cell maturation antigen
SDS	sodium dodecyl sulfate
SLE	systemic lupus erythematosus
TAC1	transmembrane activator calcium modulator and cyclophilin ligand interactor
TAE	tris acetate EDTA
TBS	tris buffered saline
Tfh	follicular T helper cell
TGF	transforming growth factor
Th	T helper cell
THD	triple helical domain
TLR	toll-like receptor
Treg	regulatory T cell
vWFA2	von-Willebrand-Factor-A-like domain 2
WT	wildtype

TABLE OF FIGURES

Figure 1. Schematic illustration of disease progression in scurfy mice.....	11
Figure 2. Schematic illustration of the skin and structures.	16
Figure 3. Pathogenic mechanism of inflammatory EBA.	20
Figure 4. Gating strategy of flow cytometry data.....	41
Figure 5. Scurfy mice show enlarged lymphatic organs and secondary follicles in sdLN.	42
Figure 6. Scurfy mice show altered B1 and B2 B cell populations.....	44
Figure 7. Scurfy mice show impaired B cell maturation in sdLN.....	45
Figure 8. Histology of scurfy spleen shows altered marginal zone structures.	46
Figure 9. Scurfy mice show impaired MZ B cell compartment in spleen and sdLN..	47
Figure 10. Scurfy mice show elevated frequencies of memory B cells in bone marrow and spleen..	48
Figure 11. GC B cells and antibody-producing cells are frequently higher in scurfy mice.....	50
Figure 12. Scurfy mice show inflamed ear skin with B cells present in the tissue.....	51
Figure 13. B cell-related inflammatory cytokines are present in serum of scurfy mice.....	53
Figure 14. Treg deficiency in scurfy mice leads to AIBD-related antigen-specific B cells in spleen and sdLN.	55
Figure 15. mAb H510 targets antigen along dermal-epidermal junction.....	57
Figure 16. Isolated primary murine keratinocytes and fibroblasts are highly purified.....	58
Figure 17. Binding pattern of mAb H510 is co-localized with K14 in murine keratinocytes. ...	59
Figure 18. Binding of H510 was blocked after incubation with vWFA2 protein.	60
Figure 19. mAb H510 recognizes murine vWFA2 of Col7.	62
Figure 20. Complement 3 is not present along the DEJ after H510 injection.	63
Figure 21. H510 induces subepidermal blisters independently from immune cells.....	64
Figure 22. Schematic project summary.....	72

1 INTRODUCTION

1.1 Autoimmunity

The immune system functions as the defense mechanism of the body against infections. After the first protection by the innate immune response, adaptive immune mechanisms specifically recognize pathogens and develop long-term immunological memory (Sakaguchi et al. 2008). While continuous production of new T cells and B cells takes place, incorrect negative selection or inactivation can result in autoreactive antigen-specific immune cells attacking self-antigens and healthy tissues (Elkon and Casali 2008; Nicholson 2016).

Autoreactive T cells, present in the periphery, can recognize peptides of autoantigens presented on specific cells leading to diseases such as autoimmune blistering disease (AIBD) (Hertl et al. 2006). Furthermore, autoimmune diseases such as systemic lupus erythematosus (SLE) are triggered by autoreactive T cells that activate B cells via co-stimulatory molecules and B cell activation via Toll-like receptors (TLRs) (Shlomchik 2008; Theofilopoulos et al. 2017). Activated autoreactive B cells secrete pro-inflammatory cytokines and autoantibodies which results in T cell activation and autoimmune pathology (Chan and Shlomchik 1998; Wong et al. 2004).

To avoid reactivity against self-antigens and the development of autoimmunity, the immune system has established specific mechanisms.

1.1.1 Regulatory T cells (Treg)

For suppression of autoimmunity, regulatory T cells (Treg) play a major role in preventing autoimmune diseases (Ohkura et al. 2013; Sakaguchi et al. 2008). *In vivo* experiments have demonstrated the development of autoimmune diseases in mice after depletion of CD4⁺CD25⁺ Treg and inhibition of disease induction by adoptive transfer of Treg (Sakaguchi et al. 1995).

Treg are characterized by the transcription factor FOXP3 belonging to forkhead transcription factors (Fontenot et al. 2003; Hori et al. 2003). Insertion of missense mutations in the *Foxp3* gene has demonstrated the insurance of regulation, development, and function of Treg by the transcription factor (Sakaguchi et al. 2008). Mutations in the *Foxp3* gene cause a dysfunction of Treg leading to severe autoimmune diseases. Dysfunction in Treg results in the scurfy phenotype (1.1.2) in mice (Haeberle et al. 2018). In humans, these mutations lead to non-

functional Treg resulting in the IPEX (immunodysregulation polyendocrinopathy enteropathy X-linked) syndrome (Ochs et al. 2005; Sakaguchi et al. 2008).

Functionally, $Foxp3^+$ Treg suppress autoreactive T cells by secreting anti-inflammatory cytokines such as TGF- β , IL-10, or IL-35 to influence inflammatory responses (Bettini and Vignali 2009). The exact mechanism for the prevention of autoimmunity is not yet fully understood, but several indirect and direct mechanisms have been described for the regulation of potentially autoreactive $CD4^+$ T cells.

By secreting regulatory cytokines, Treg can change the conformation of antigen-presenting cells (APCs) that shape antigen-specific $CD4^+$ T cells to a regulatory phenotype (Arellano et al. 2016). In addition, direct inhibition of $CD4^+$ T cells by Treg can occur (Shlomchik 2008). Autoreactive $CD4^+$ T cells provide B cell help, which eventually leads to autoantibody production and autoimmune diseases (Linterman et al. 2011; Wollenberg et al. 2011). Furthermore, Treg secrete TGF- β or cytotoxic proteins to initiate apoptosis of autoreactive B cells and finally inhibit autoantibody production (Arellano et al. 2016; Lim et al. 2005).

In summary, Treg are critical to maintain the balance of the immune system by suppressing autoimmunity. Subsequently, the development of autoimmune diseases as a result of dysfunctional Treg will be discussed.

1.1.2 Scurfy mouse model

To get further insights into the development of autoimmune disease, the scurfy mouse model can be used. Scurfy mice have a two base pair insertion in the *Foxp3* gene and therefore non-functional Treg (Brunkow et al. 2001; Godfrey et al. 1991b). Autoreactive $CD4^+$ T cells expand and produce tissue damage (Figure 1). Recently, it was shown that the transfer of $CD4^+$ T cells in Rag2 knock-out mice, lacking B and T cells, leads to interface dermatitis in the skin indicating T cell-mediated autoimmunity (Takahashi et al. 2011). Furthermore, autoreactive $CD4^+$ T cells can indirectly recruit inflammatory immune cells or activate B cells which then produce high titers of autoantibodies detectable in the serum of scurfy mice (Figure 1) (Aschermann et al. 2013; Hadaschik et al. 2015; Huter et al. 2010). Scurfy mice suffer from strong inflammation and progressive immune cell infiltration in lymph nodes, spleen, skin, lung, and liver (Figure 1) (Godfrey et al. 1991b). These mice die 15-40 days after birth due to generalized autoimmune diseases following multi-organ failure (Fontenot et al. 2003; Hadaschik et al. 2015; Haeberle et al. 2018). Considering the *Foxp3* mutation as an X-chromosomal mutation, only male mice develop the typical scurfy phenotype (Godfrey et al. 1991b).

Previously, characterization of scurfy autoantibodies revealed skin-specific antibodies which target different structural skin proteins leading to subepidermal blister formation in the skin relevant for the development of AIBD (Figure 1) (Haerberle et al. 2018; Hashimoto et al. 2018; Muramatsu et al. 2018). Specifically, a reactive pathogenic autoantibody attacking BP230 in the skin, mimicking the human disease bullous pemphigoid (BP), could be isolated from sick scurfy mice (Haerberle et al. 2018).

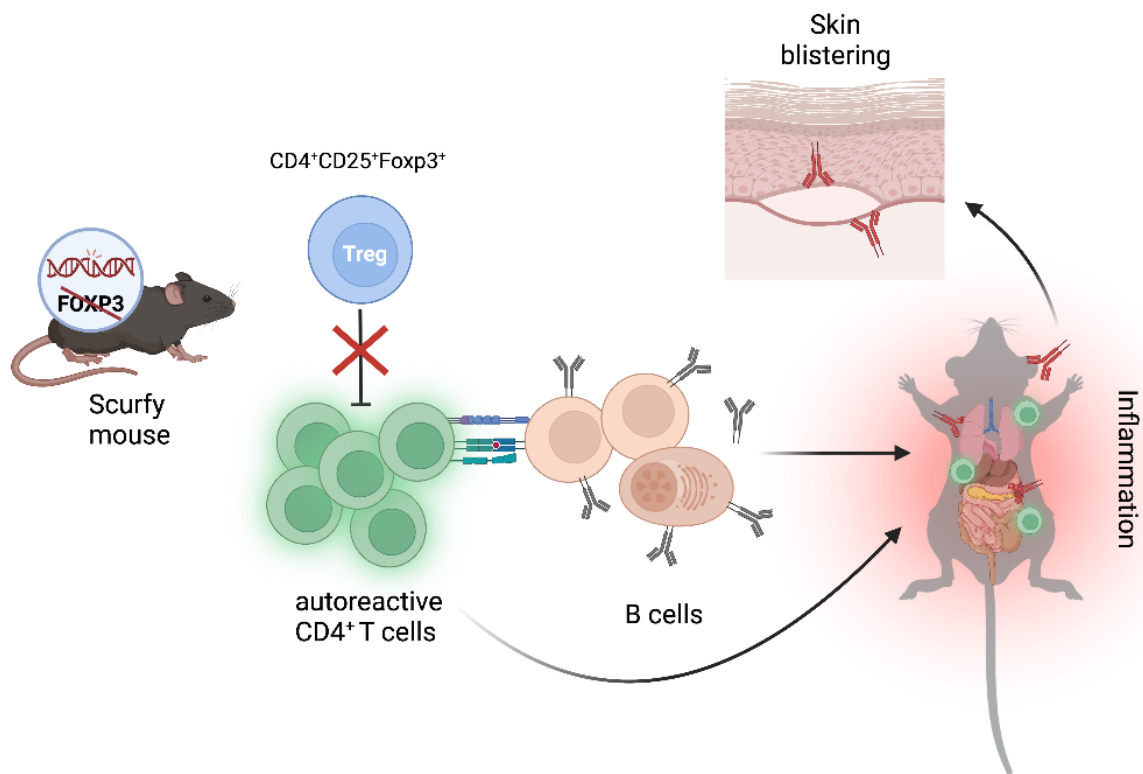


Figure 1. Schematic illustration of disease progression in scurfy mice. *Foxp3* mutation in scurfy mice results in dysfunctional regulatory T cells (Treg). Expansion of autoreactive CD4⁺ T cells cannot be prevented by Treg which leads to activation of autoreactive B cells producing high titers of autoantibodies. Autoantibodies and autoreactive T cells affect several inner organs and lead to strong inflammation and blister formation in the skin (created with BioRender).

1.1.3 B cells

B cells are crucial for autoimmune disease development with antibody contribution as they are capable of antigen presentation and provide co-stimulation to T cells (Hoffman et al. 2016). In addition, B cells are immunomodulatory and regulate immune responses by cytokine secretion (Hoffman et al. 2016).

In this chapter, B cell development, function, and contribution to autoimmunity will be discussed in detail.

1.1.3.1 Development and function of B cells

In mice and humans, two main classes of B lymphocytes derive from hematopoietic stem cells: B1 and B2 B cells. B1 progenitors give rise to B1 cells in fetal liver which migrate to pleural and peritoneal cavities producing low-affinity antibodies to T cell-independent antigens as well as natural IgM and polyreactive IgA antibodies (Hoffman et al. 2016; Montecino-Rodriguez and Dorshkind 2012; Pillai and Cariappa 2009).

B cell progenitors in bone marrow (BM) give rise to transitional 2 B cells acquiring cell surface IgD and CD21 after leaving the BM (Chung et al. 2003). Transitional B cells differentiate into marginal zone (MZ) B cells and follicular B cells occurring in spleen and lymph nodes (Hoffman et al. 2016). While MZ B cells represent a population generating antibodies T cell independently, follicular B cells mirror the conventional B cells of the adaptive immune system (Hoffman et al. 2016). By residing lymphoid follicles of spleen and lymph nodes, most mature B cells respond to foreign antigens presented by follicular dendritic cells (DCs), proliferate, and undergo clonal expansion to plasma cells or enter germinal center (GC) reactions (LeBien and Tedder 2008). GCs develop in secondary lymphoid tissues after antigen activation of mature B cells (LeBien and Tedder 2008). Within the GC, GC B cells interact with follicular T helper cells (T_{fh}) producing IL-21 and other co-stimulatory signals (Shlomchik and Weisel 2012). This results in B cell proliferation and induction of gene expression programs important for somatic hypermutation and class-switch recombination (LeBien and Tedder 2008). High-affinity class-switched memory B cells and plasma cells are generated within GC reactions (Shlomchik and Weisel 2012). Supported by secretion of CXCL12 and the cytokines IL-6 and APRIL plasma cells produce antibodies independently of further exposure to antigens and thereby maintain serologic memory (Nutt et al. 2015). Memory B cells are arranged in follicular groups in lymphoid tissues where they wait for rapid differentiation into plasmablasts ensuring diversified antibody responses (Kurosaki et al. 2015; McHeyzer-Williams et al. 2015).

Besides antibody production, B cells function as mediators for immune homeostasis (LeBien and Tedder 2008). On the one hand, antigen internalization by B cell receptors (BCR) is required for antigen-specific interactions between T and B cells, which was demonstrated by B cell depletion studies in adult wildtype (WT) mice (Bouaziz et al. 2007; Lanzavecchia 1985). Furthermore, the absence of B cells during mouse maturity revealed importance of B cells for the development of a normal immune system (LeBien and Tedder 2008). By releasing immunomodulatory cytokines, B cells are able to regulate the function of T cells, DCs, and other APCs to maintain a normal function of immune responses (Harris et al. 2000).

Abnormalities in B cell development or regulation can lead to autoimmune reactions resulting in severe autoimmune diseases.

1.1.3.2 Autoreactive B cells and scurfy mice

Considering successful treatment of patients with autoimmune diseases like SLE by B cell depletion, B cells play an important role in human autoimmune disorders (Edwards and Cambridge 2005; Yildirim-Toruner and Diamond 2011). Disease induction can be triggered by B cells as APCs, cytokine secretion, or autoantibody production (Giltiay et al. 2012). B cells undergo different regulatory checkpoints for elimination of autoreactive cells during development (Giltiay et al. 2012). In BM, polyreactive and autoreactive immature B cells are eliminated through receptor editing and deletion (Meffre 2011; Pillai et al. 2011). Instead of elimination, immature B cells become mature B cells in the periphery to avoid autoreactivity (Giltiay et al. 2012).

Dysregulation of these control mechanisms can lead to severe autoimmune diseases in patients. TLR-mediated signals together with defective BCR signaling can result in incorrect deletion or editing of autoreactive B cells in BM which expand in the periphery (Giltiay et al. 2012). Furthermore, signaling via CD40 ligand (CD40L) and major histocompatibility complex (MHC) class II seems to be essential for the peripheral control of autoreactivity (Meffre 2011). Recently, it was shown that elevated levels of B cell pro-survival factor BLyS have an impact on the survival of autoreactive B cells escaping regulatory mechanisms (Liu and Davidson 2011; Pillai et al. 2011). Somatic hypermutation is an important mechanism leading to high-affinity B cells but can in contrast result in generation of autoreactive B cells producing autoantibodies as demonstrated in a mouse model for lupus (Guo et al. 2010).

Previous studies of scurfy mice suffering from Treg deficiency revealed a severe malfunction of B lymphopoiesis in BM of adolescent mice including CD19⁺ B cells and immature IgM⁺ cells (Chang et al. 2012; Leonardo et al. 2010). However, it could not be explained how the development of the peripheral pool of self-reactive mature B cells, characterized by increased antibody production against several self-antigens, occurs (Haeberle et al. 2018; Huter et al. 2010; Leonardo et al. 2010; Nguyen et al. 2007). To address this, it has been proposed that GC reactions of B cells are modulated by a regulatory Tfh cell subset which could explain the strong expansion of B cells in later developmental stages in scurfy mice (Aschermann et al. 2013; Chung et al. 2011). Furthermore, using double knock-out mice Aschermann et al. showed a strong reduction in autoimmunity in scurfy mice if B cells and autoantibodies were absent. Disease phenotype could be reconstituted after transfer of mature splenic B cells from WT mice into B cell-deficient scurfy mice to strengthen this point (Aschermann et al. 2013).

1.1.3.3 B cell associated cytokines

Besides antibody production, B cells secrete several cytokines that mediate Th1- or Th2-like immune responses. Depending on their function, different B cell subsets produce diverse cytokines after activation and can be separated into effector and regulatory phenotypes (Lund 2008). Two effector B cell populations can be subdivided based on their priming by T cells (Harris et al. 2000; Lund 2008). B cells primed by Th1 cells (Be-1 cells) secrete IFN- γ and IL-12p70 to promote Th1 differentiation, which is required for defense against pathogens (Harris et al. 2000; Lund et al. 2005). After being primed by Th2 cells, B cells (Be-2 cells) produce IL-4, IL-2, IL-13, IL-6, and TNF- α for induction of Th2 immune responses often associated with allergies (Harris et al. 2000; Lund et al. 2005). Besides T cell priming, the cytokines IL-4 and IL-6 are important for B cell proliferation, survival, and isotype-switching (Rush and Hodgkin 2001; Van Snick 1990). In addition to Th1 cells, Th17 effector cells have been implicated in the pathogenesis of several autoimmune diseases (Damsker et al. 2010; van Bruggen and Ouyang 2014). Moreover, the role of IL-17 in maintaining the humoral immune response as well as promotion of GC development during autoimmunity has been demonstrated, indicating an impact on B cell autoimmune responses (Hsu et al. 2008; Xie et al. 2010).

The cytokines CD40L and B cell activating factor (BAFF) also play critical roles in B cell function (Medgyesi et al. 2014; Thai et al. 2018). CD40L is important for antibody production and isotype-switched memory B cells (Jain et al. 2011; MacLeod et al. 2006). Myeloid innate immune cells express BAFF, which can bind B cells via the BAFF receptor (BAFFR), B cell maturation antigen (BCMA), and transmembrane activator and calcium-modulator and cytophilin ligand interactor (TACI), thereby maintaining peripheral B cell survival (Guo et al. 2021). Overexpression of BAFF has been implicated in autoimmune disorders such as SLE (Groom et al. 2007; Schneider et al. 2001). BCMA is found membrane-bound on activated B cells and IgG-secreting cells that bind BAFF and APRIL and is essential for antibody production but is also involved in autoimmune diseases (Darce et al. 2007; Hiepe et al. 2011; Yang et al. 2005). Previously, direct shedding of the membrane-bound receptor by γ -secretase was confirmed, leading to regulatory mechanisms and plasma cell restriction by soluble BCMA (sBCMA) (Laurent et al. 2015).

To regulate autoimmune responses, regulatory B cells (Breg) are characterized by reduction of autoimmunity and suppression of antigen-specific CD4⁺ T cell proliferation (Mauri et al. 2003; Yang et al. 2010). By secreting the cytokines IL-10 and TGF- β , Breg can convert naive CD4⁺ T cells into Treg or facilitate plasma cell development (Chen et al. 2003; Choe and Choi 1998).

1.1.3.4 Skin associated B cells

The common understanding of autoreactive B cell development comprises self-reactive B cell generation in the BM following escape of central tolerance and circulation to secondary lymphoid organs (Brink 2014; Yurasov et al. 2005). Furthermore, GC reactions can lead to memory B cell differentiation or plasma cells that induce autoimmune disease via pathogenic autoantibodies (Winter et al. 2012). In several cutaneous autoimmune diseases, autoantibodies are critical for diagnosis and various immune cells are known to patrol the skin and directly induce inflammation (Debes and McGettigan 2019; Egbuniwe et al. 2015). Different B cell subsets such as B2 B cells, memory B cells, and plasma cells have been shown to infiltrate the skin and are involved in autoimmune bullous dermatoses such as pemphigus vulgaris (Hennerici et al. 2016; Yuan et al. 2017). B cells may reside tertiary lymphoid structures in inflamed skin being directly in charge to mediate autoimmune responses in the tissue (Fetter et al. 2020).

Previously, Haeberle et al. could display that CD4⁺ T cells and CD11b⁺ cells infiltrate the inflamed skin of sick scurfy mice suffering from severe autoimmune diseases (Haeberle et al. 2017). Whether B cells are also able to recirculate in the skin and directly contribute to autoantibody production and inflammation in scurfy mice leading to AIBD progression will be discussed further.

1.2 Architecture of the skin

To further understand skin-specific autoimmune diseases, the architecture of the skin, including structural proteins, is of great importance. The skin is composed of the epidermis, dermis, and subcutis (Figure 2). The epidermis consists of keratinocytes that form the stratum basale with a layer of keratinocytes just above the basement membrane zone (BMZ) (Figure 2). These basal keratinocytes contain mitotically active stem cells that continuously produce new keratinocytes (Kanitakis 2002). Keratinocytes are separated from the dermis by the basement membrane consisting of the Lamina lucida and Lamina densa (Figure 2). The epidermis acts as a barrier against external mechanical influences, water or pathogenic organisms (Kanitakis 2002).

Therefore, the stability of the skin is important to maintain its structure and functions. The epidermis and dermis are connected by desmosomes and hemidesmosomes (Figure 2). Keratinocytes are interconnected by desmosomal structures that link keratin filaments. Intracellular adhesion of keratinocytes is mediated by Desmoglein 1, Desmoglein 3 and Desmocollin which are cadherins (Amagai et al. 1991; Koch et al. 1990). Basal keratinocytes

are connected to the basement membrane by hemidesmosomes through the dermal-epidermal junction (DEJ) (Figure 2). The cytoplasmic proteins BP230 and Plectin and the transmembrane proteins BP180 and Integrin $\alpha6\beta4$ connect keratinocytes to dermal collagen fibers. Laminin 332 (also called Laminin 5) or Laminin 6 mediate the connection between anchoring fibrils such as Collagen Type VII (Col7) and transmembrane proteins to maintain hemidesmosomal structures (Figure 2) (Yancey 1995).

Targeting these important structural skin proteins results in severe autoimmune skin diseases.

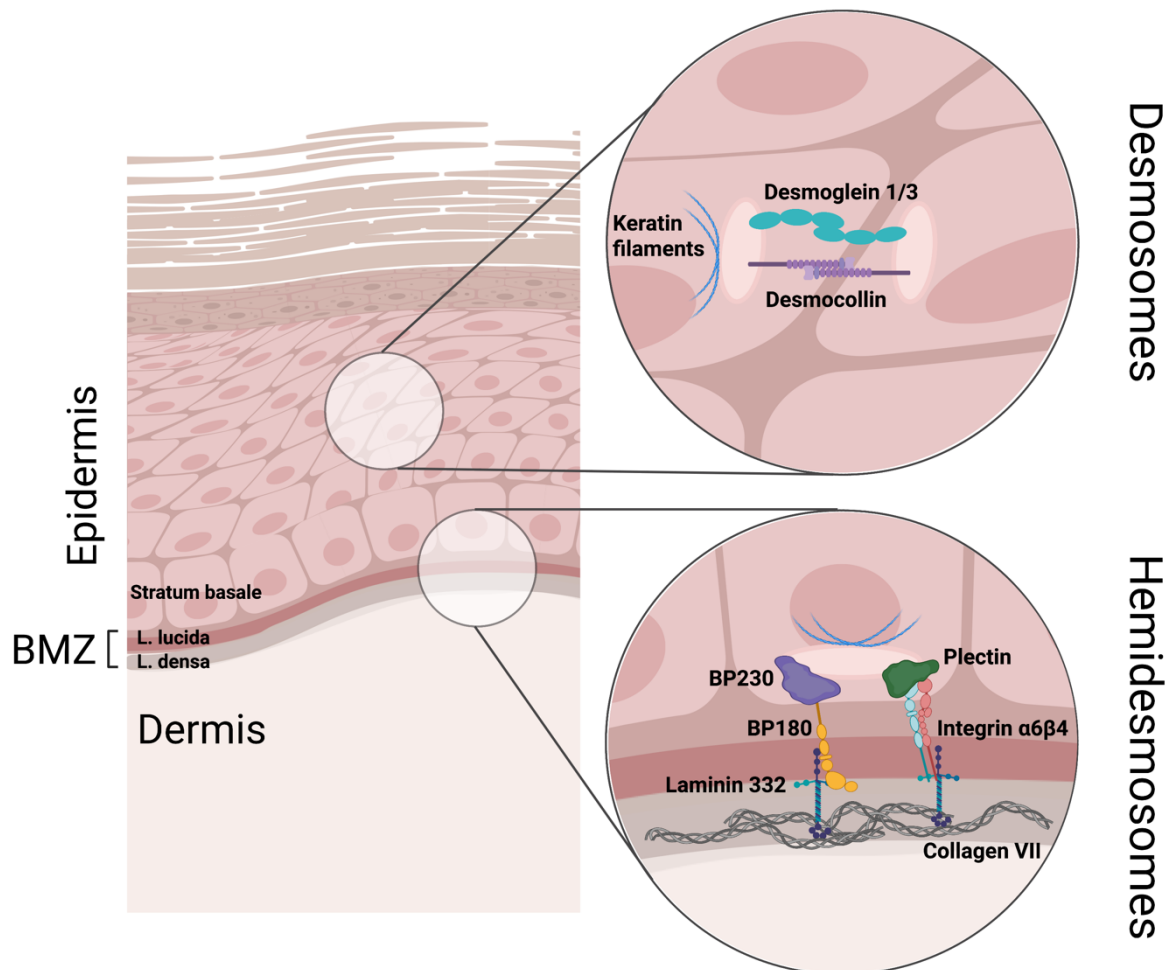


Figure 2. Schematic illustration of the skin and structures. Skin consists of three layers: epidermis, dermis and subcutis. Epidermis consists of keratinocytes which are arranged in different layers. Basal keratinocyte layer above the basement membrane zone (BMZ) is called Stratum basale. Keratinocytes are interconnected via desmosomes consisting of Desmoglein 1, Desmoglein 3, Desmocollin and different anchoring proteins. Connection between epidermis and dermis is called BMZ (Lamina lucida, L. lucida, Lamina densa, L. densa) and consist of hemidesmosomal structures. Hemidesmosomes are built of cytoplasmatic proteins like BP230 or Plectin, transmembrane proteins like BP180 or Integrin $\alpha6\beta4$ which are connected via Laminin 332 to Collagen VII in the lower BMZ (created with BioRender).

1.3 Autoimmune blistering diseases (AIBD)

Autoimmune blistering diseases (AIBD) are a group of human autoimmune disorders that cause severe damage to the skin and mucous membranes (Witte et al. 2018). Characteristically, pathogenic autoantibodies target key structural skin proteins, leading to intraepidermal blistering or blisters around the BMZ in AIBD patients (Hammers and Stanley 2016; Schmidt et al. 2019; Schmidt and Zillikens 2013). Intraepidermal blistering is triggered by autoantibodies that attack desmosomal proteins such as Desmoglein 1 and 3, resulting in acantholysis and pemphigus diseases (Kasperkiewicz et al. 2017).

Pemphigoid diseases are characterized by blistering in the DEJ induced by autoantibodies targeting hemidesmosomal proteins (Hertl et al. 2006; van Beek et al. 2018). Pathologically, several mechanisms have been described that lead to subepidermal AIBD, such as recruitment of mast cells and neutrophils by autoantibodies as well as activation of the complement system (Fang et al. 2018). For most AIBD, the antigens targeted by autoantibodies have been described. Bullous pemphigoid (BP) is the most common form of subepidermal blistering disease induced by autoantibodies targeting BP180 and BP230 in the skin (Georgi et al. 2001; van Beek et al. 2018). Autoantibodies attacking BP180 or Laminin 332 cause mucous membrane pemphigoid (MMP) and severe blistering in the mouth, conjunctiva, or nasal mucosa (Goletz et al. 2017; Schmidt and Zillikens 2013). The clinical features of anti-p200/Laminin γ 1 pemphigoid resemble BP by the production of autoantibodies against the c-terminus of Laminin γ 1 (Goletz et al. 2014). The severe pemphigoid disease epidermolysis bullosa acquisita (EBA) is described in the following.

1.3.1 Epidemiological background

The prevalence of patients suffering from BP reaches 20 per million per year, making it the most common form of subepidermal blistering in central Europe (Witte et al. 2018). The morbidity of BP patients increases with age and most patients are affected between ages of 70 and 80 (Bertram et al. 2009). EBA is estimated to be a rare disease with an incidence of <0.5 per million (Bertram et al. 2009; Zillikens et al. 1995). In contrast to BP, the onset of EBA can occur at any age (Marzano et al. 2013; Trigo-Guzman et al. 2003).

1.3.2 Diagnostic of AIBD

For the diagnosis of AIBD, detection of membrane-bound and circulating autoantibodies is necessary before appropriate therapy can be initiated (van Beek et al. 2018).

Histologic analysis of biopsies of lesional skin helps to differentiate between intraepidermal or subepidermal blistering to define pemphigus or pemphigoid diseases (van Beek et al. 2018). When direct immunofluorescence (DIF) microscopy is applied to the skin of AIBD patients, skin-bound autoantibodies can be detected (Witte et al. 2018). Linear staining along the DEJ indicates antibodies attacking hemidesmosomal proteins, resulting in pemphigoid disease, whereas pemphigus disease is characterized by intraepidermal reticular staining around keratinocytes (Schmidt and Zillikens 2011).

For further identification of antigen localization along the BMZ, indirect immunofluorescence (IIF) microscopy with patient serum on salt-split skin is the gold standard (Gammon et al. 1990). Specifically, linear staining on skin with salt-induced separation of epidermis and dermis reveals antigen localization on the dermal or epidermal side of the BMZ, indicating different forms of AIBD. Target antigens located at the blister roof such as BP180 or BP230, indicate BP diagnosis (van Beek et al. 2018). Autoantibodies against Col7 or Laminin 332 show linear fluorescence at the dermal side of the artificially induced blister specific for EBA or MMP (van Beek et al. 2018).

Final specific analysis of AIBD is performed by Enzyme linked immunosorbent assay (ELISA) and western blot to identify the target antigens for further treatment (Witte et al. 2018).

1.3.3 Epidermolysis bullosa acquisita (EBA)

Autoantibodies directed against Col7 in the skin or mucous membranes indicate blistering disease EBA (Woodley et al. 2005). Patients suffer from chronic inflammation, severe subepidermal blistering and scarring (Koga et al. 2018). Col7 is a large structural skin protein that is the major component of anchoring fibrils in the dermis. Consisting of a central collagenous domain (triple helical domain, THD) and two non-collagenous domains (NC1 and NC2), autoantibodies mainly target the immunodominant NC1 part including the von-Willebrand-Factor-A-like domain 2 (vWFA2) of Col7 (Chen et al. 2007; Gammon et al. 1993). EBA is a chronic skin disease with remissions over years, and the overall prognosis depends on the age and severity of the patients (Koga et al. 2018). The clinical presentation of EBA varies in different subgroups (Koga et al. 2018). The most common disease manifestations are the classical/mechano-bullous and BP-like forms (Koga et al. 2018). The pathologic mechanisms leading to different forms of EBA are discussed in the following.

1.3.4 Pathological mechanisms of EBA

Two main clinical presentations of EBA have been described, non-inflammatory and inflammatory forms.

The classical/mechano-bullous form of EBA is a non-inflammatory manifestation that clinically shows skin fragility, blisters and erosions, as well as non-inflamed scarred skin (Prost-Squarcioni et al. 2018). Blister formation is induced by a still unknown direct pathway mediated by autoantibodies targeting Col7 without recruitment of inflammatory cells or cytokines (Kasperkiewicz et al. 2016; Koga et al. 2018; Prost-Squarcioni et al. 2018).

In contrast, the BP-like form of EBA leads to pruritus, erosions on inflamed skin as well as blister formation via an inflammatory pathway (Koga et al. 2018). The exact mechanisms leading to disease onset are still unknown. The contribution of genetic and environmental factors like genes around the MHC locus or the microbiome are discussed (Gammon et al. 1988). Autoantibody production against Col7 in the skin is initiated by CD4⁺ T cells in experimental EBA (Iwata et al. 2013). Upon binding of autoantibodies to Col7 in the skin, complement is activated and pro-inflammatory immune cells such as monocytes and macrophages are recruited (Figure 3). Cytokines like IL-6 or TNF- α are released within the effector phase of EBA (Samavedam et al. 2013) leading to extravasation of neutrophils into the skin (Figure 3). Neutrophils bind to immune complexes present in the skin via their Fc γ -receptor IV (Fc γ RIV) as a key mediator (Figure 3) (Kasperkiewicz et al. 2012). After stimulation with immune complexes, a signaling cascade is initiated in neutrophils resulting in activation and release of reactive oxygen species (ROS) and metalloproteases (Figure 3) (Hirose et al. 2017). In addition to ROS extravasation into the DEJ, leukocytes, NKT cells, and $\gamma\delta$ T cells are described to reside in the skin contributing to subepidermal blister formation and the clinical EBA phenotype in patients (Figure 3).

Previous studies have shown a positive effect of Treg on the progression of transfer induced EBA (Bieber et al. 2017). Thus, Treg deficiency in scurfy mice may provide further insights into B cell-mediated AIBD onset and pathological mechanisms.

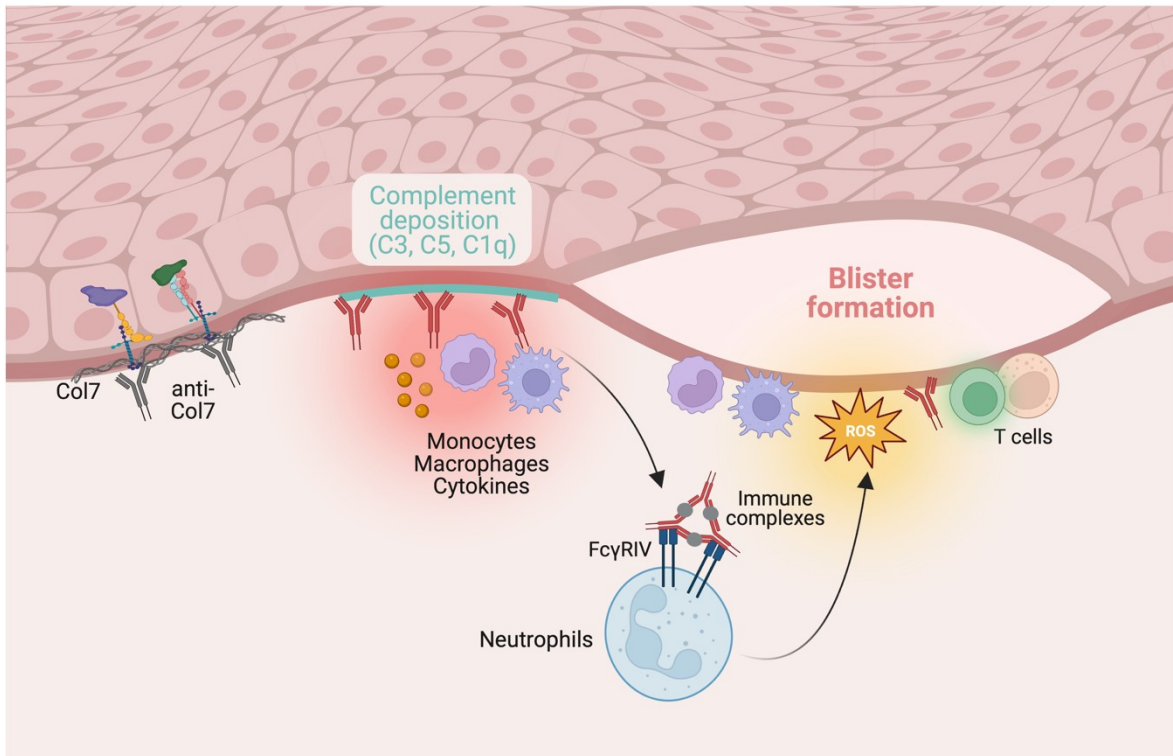


Figure 3. Pathogenic mechanism of inflammatory EBA. Loss of tolerance leads to release of autoantibodies targeting collagen type VII (Col7) at the dermal-epidermal junction (DEJ). Binding of anti-Col7 antibodies leads to complement deposition (C3, C5, C1q), immune cell infiltration and cytokine release at the basement membrane zone (BMZ). Immune complexes (anti-Col7 antibodies and Col7 peptides) bind to Fc γ -receptor IV (Fc γ RIV) on neutrophils resulting in release of reactive oxygen species (ROS) and matrix metalloproteases. In addition, monocytes, macrophages, NKT cells and $\gamma\delta$ T cells are involved in final blister formation in the skin (created with BioRender).

1.4 Aims of the project

The aim of this project is to investigate the role of autoreactive B cells and pathogenic antibodies leading to the onset of AIBD in scurfy mice.

Previous experiments have shown that Treg deficiency in scurfy mice leads to the development of AIBD triggered by autoreactive CD4⁺ T cells (Haeberle et al. 2018). Further studies showed a severe malfunction of B lymphopoiesis in the BM of scurfy mice, while a strong expansion of self-reactive B cells in the periphery was also demonstrated (Chang et al. 2012; Leonardo et al. 2010; Nguyen et al. 2007). These data support the role of B cells in disease pathogenesis.

The objective of the current project is to investigate the contribution of autoreactive B cells in lymphoid organs and skin leading to disease progression in Treg-deficient scurfy mice. Furthermore, the role of antigen-specific autoreactive B cells in the pathogenesis of AIBD is addressed by performing ELISpot assays with AIBD-related antigens and B cells from sick scurfy mice.

Previously, a spontaneously developed scurfy autoantibody targeting BP230 could be isolated which induces BP in WT mice (Haeberle et al. 2018; Muramatsu et al. 2018).

Besides B cell contribution to AIBD, another aim of the current project is to further characterize another autoantibody derived from sick scurfy mice which has been shown to be pathogenic *in vivo* by inducing subepidermal blisters in WT neonatal mice (Vicari 2019, Master thesis): To identify the antigen targeted by this particular autoantibody (H510) and to investigate the pathologic mechanism of blister formation.

Within this project, the objective is to analyze the role of B cells in the immunopathology of scurfy mice involved in the progression of AIBD under Treg deficiency. By characterizing a newly isolated autoantibody from scurfy mice, the potential pathological mechanisms and relevance for AIBD will be elucidated.

Further dissection of the autoimmune responses in scurfy mice that lead to skin disease by focusing on specific B cell subsets and autoantibodies will allow research into novel therapeutic targets for treatment of AIBD patients.

2 MATERIAL AND METHODS

2.1 Material

2.1.1 Cell culture media and reagents

2.1.1.1 Reagents

Fetal calf serum (FCS)	Sigma Aldrich (St. Louis, MO, USA)
Penicillin/Streptomycin (Pen/Strep)	1000 U/ml Penicillin, 10 mg/ml Streptomycin, GE Healthcare (Pasching, Austria)
HEPES	4-(2-hydroxyethyl)-1-piperazineethanesulfonic acid, Biochrom (Berlin, Germany)
Sodium Pyruvate	Sigma Aldrich (St. Louis, MO, USA)
L-Glutamine	GlutaMAX-L (100x), Gibco/Life Technologies (Carlsbad, CA, USA)
β -Mercaptoethanol	Gibco/Life Technologies (Carlsbad, CA, USA)
MEM Amino acids	MEM non-essential Amino acids, Capricorn Scientific (Ebsdorfergrund, Germany)
Gentamycin/Amphotericin B	CnT-GAB10, CELLnTEC (Bern, Switzerland)
Dispase II	CnT-DNP10, CELLnTEC (Bern, Switzerland)
Accutase	CnT-Accutase-100, CELLnTEC (Bern, Switzerland)
Trypsin	Trypsin/EDTA (10x), GE Healthcare (Pasching, Austria)
Collagenase Type Ia	Sigma Aldrich (St. Louis, MO, USA)
DMSO	Dimethylsulfoxid, Sigma Aldrich (St. Louis, MO, USA)

2.1.1.2 Mammalian Cell Culture Media

DMEM	Dulbecco's Modified Eagle Medium, Gibco by Life Technologies (Carlsbad, CA, USA): Containing 10% FCS, 4 mM L-Glutamine, 1 mM Sodium Pyruvate, 10 mM HEPES, 1% Pen/Strep
Complete RPMI	RPMI 1640 Media, Gibco by Life Technologies (Carlsbad, CA, USA): Containing 10% FCS, 2 mM L-Glutamine, 1 mM Sodium Pyruvate, 10 mM HEPES, 1% Pen/Strep, 0.05 mM β -Mercaptoethanol, 1x MEM Amino acids
Epithelial Culture Medium	ready-to-use, CnT-Prime, CELLnTEC (Bern, Switzerland), before use addition of 1x CnT-GAB10

2.1.2 Cell lines

Name	Cell Type	Organism	Growth Properties	Media	Provider
HEK293T	Embryonic kidney cells	Homo sapiens	adherent	DMEM	AG Prof. Schäkel, Heidelberg
Primary murine keratinocytes	Primary keratinocytes	Mus musculus	adherent	Epithelial Culture Medium	Described in 2.2.4.3
Primary murine fibroblasts	Primary fibroblasts	Mus musculus	adherent	DMEM + 0.05 mM β -Mercaptoethanol	Described in 2.2.4.4

2.1.3 Primers (Genotyping)

FoxP3 reverse primer	CATCGGATAAGGGTGGCATA
FoxP3 forward primer Wildtype	CTCAGGCCTCAATGGACAAG
FoxP3 forward primer Mutant	TCAGGCCTCAATGGACAAAA

2.1.4 Antibodies

2.1.4.1 Isolated scurfy antibody

Specificity	Host	Isotype	Clone	Color	Concentration	Company	Dilution
murine vWFA2 of Collagen type VII	mouse	IgG1 k	H510	-	5 mg/ml	Selfmade and purified by Absolute antibody (Cleveland, UK)	Western blot 1:100, IF 1:100

2.1.4.2 Flow cytometry antibodies

Specificity	Host	Isotype	Clone	Color	Concentration	company	Dilution
B220/CD45R	rat	IgG2a k	RA3-6B2	APC	0.2 mg/ml	Biolegend	1:800
CD138	rat	IgG2a k	281-2	BV 421	0.2 mg/ml	Biolegend	1:600
CD16/CD32	rat	IgG2b k	2.4G2	-	5 mg/ml	Bio X Cell	1:100
CD19	rat	IgG2a k	1D3	FITC	0.5 mg/ml	Biolegend	1:200
CD21/CD35	rat	IgG2a k	7E9	PE/Cy7	0.2 mg/ml	Biolegend	1:1000
CD23	rat	IgG2a k	B3B4	BV 421	0.2 mg/ml	Biolegend	1:400
CD27	arm. hamster	IgG	LG.3A10	biotin	0.5 mg/ml	Biolegend	1:2000
CD45	rat	IgG2b λ	I3/2.3	PE/Cy7	0.2 mg/ml	Biolegend	1:200
CD95 (Fas)	mouse	IgG1 k	SA367H8	PE	0.2 mg/ml	Biolegend	1:1600
Cytokeratin 14 (K14)	rabbit	IgG	EPR-17350	PE	0.5 mg/ml	Abcam	1:5000
Fixable viability dye	-	-	-	eFluor 506	-	eBioscience	1:1000
Fixable viability dye	-	-	-	Zombie Aqua	-	Biolegend	1:4000
GL7	rat	IgM k	GL7	PE/Cy7	0.2 mg/ml	Biolegend	1:800

IgD	rat	IgG2a k	11- 26c.2a	APC/ Cy7	0.2 mg/ml	Biolegend	1:1000
IgG1	rat	IgG	RMG1-1	FITC	0.5 mg/ml	Biolegend	1:100
IgM	rat	IgG2a k	RMM-1	PE	0.2 mg/ml	Biolegend	1:200
Strept- avidin	-	-	-	PE	0.5 mg/ml	BD	1:1000
TACI/ CD267	rat	IgG2ak	8F10	PE	0.2 mg/ml	Biolegend	1:200
TCR- β	arm. hamster	IgG	H57-597	PB	0.5 mg/ml	Biolegend	1:400
Vimentin	rabbit	IgG	EPR- 3776	AF647	0.5 mg/ml	Abcam	1:500

2.1.4.3 Immunofluorescence antibodies

Specificity	Host	Isotype	Clone	Color	Concentration	Company	Dilution
anti-mouse C3	goat	IgG	poly- clonal	FITC	4 mg/ml	MP Biomedicals	1:200
anti-mouse K14	rabbit	IgG	EPR- 17350	-	2.2 mg/ml	Abcam	1:250
anti-mouse IgG	goat	IgG	poly- clonal	AF488	2 mg/ml	Invitrogen	1:400
anti-rabbit IgG	goat	IgG	poly- clonal	AF488	2 mg/ml	Invitrogen	1:400
anti-rabbit IgG	donkey	IgG	poly- clonal	AF647	2 mg/ml	Invitrogen	1:400
anti-mouse vimentin	rabbit	IgG	EPR- 3776	-	0.2 mg/ml	Abcam	1:250
anti-mouse vWFA2	rabbit	IgG1	-	-	unknown (serum)	(Iwata et al. 2015)	1:1000
Isotype control (mouse)	mouse	IgG1 k	MOPC- 21	-	2,5 mg/ml	Biolegend	1:100
Isotype control (rabbit)	goat	IgG1	poly- clonal	-	10 mg/ml	Dianova	1:100

2.1.4.4 Western blot antibodies

Specificity	Host	Isotype	Clone	Color	Concentration	Company	Dilution
anti- β -actin	rat	IgG2a k	W16197A	-	0.5 mg/ml	Biolegend	1:1000
anti-mouse Histidine Tag	mouse	IgG1 k	J099B12	HRP	0.5 mg/ml	Biolegend	1:1500
anti-mouse K14	rabbit	IgG	EPR-17350	-	2.2 mg/ml	Abcam	1:20000
anti-mouse IgG Fab	goat	-	poly-clonal	HRP	0.8 mg/ml	Dianova	1:10000
anti-rabbit IgG Fc	goat	-	poly-clonal	HRP	0.8 mg/ml	Dianova	1:10000
anti-mouse vWFA2	rabbit	IgG1	-	-	unknown (serum)	(Iwata et al. 2015)	1:1000
anti-mouse vimentin	rabbit	IgG	EPR-3776	-	0.2 mg/ml	Abcam	1:2500

2.1.4.5 ELISA antibodies

Specificity	Host	Isotype	Clone	Color	Concentration	Company	Dilution
anti-mouse IgG Fc	goat	-	poly-clonal	HRP	0.1 mg/ml	Bethyl	1:10000

2.1.5 Kits

KAPA Express Extract	KAPA Biosystems/Sigma Aldrich (St. Louis, MO, USA)
QIAGEN HotStarTaq Master Mix	QIAGEN (Venlo, Netherlands)
Pierce BCA Protein Assay Kit	Thermo Scientific (Rockford, IL, USA)
eBioscience Foxp3/Transcription Factor Staining Buffer Set	Thermo Scientific (Rockford, IL, USA)
EasySep Mouse B cell Isolation Kit	STEMCELL Technologies (Vancouver, Canada)
Mouse IgG ELISpot Basic Kit (ALP)	Mabtech (Stockholm, Sweden)

LEGENDplex Mouse B cell Panel (12-plex) w/VbP Biolegend (San Diego, CA, USA)

LEGENDplex Mouse B cell Panel (1-plex) w/VbP Biolegend (San Diego, CA, USA)

2.1.6 Markers

ProSieve QuadColor Protein Marker Lonza (Maine, ME, USA)

2-Log DNA Ladder (10 kb) New England BioLabs (Ipswich, UK)

2.1.7 Enzymes

Roche Liberase TL Research grade Sigma Aldrich (St. Louis, MO, USA)

DNase I (bovine pancreas grade II) Sigma Aldrich (St. Louis, MO, USA)

2.1.8 Buffers and solutions

TBS (Tris Buffered Saline) 50 mM Tris, 150 mM NaCl, pH 7.5

TBS-T TBS, 0.1% Tween-20

PBS (Phosphate Buffered Saline) 137 mM NaCl, 2.7 mM KCl, 8.1 mM Na₂HPO₄·2H₂O, 1.4 mM K₂PO₄

PBS-T PBS, 0.1% Tween-20

2.1.8.1 Flow cytometry

FACS Buffer 2% FCS, PBS

1x ACK-Buffer 150 mM NH₄Cl, 10 mM KHCO₃, 1 mM EDTA

2.1.8.2 ELISpot

Isolation buffer 2% FCS, 1 mM EDTA, PBS

Antibody solution 0.5% FCS, PBS

Blocking solution	1% BSA, PBS
Wash buffer I	50 mM EDTA, PBS
Wash buffer II	0.1% Tween-20, PBS

2.1.8.3 Agarose gel electrophoresis

TAE buffer	40 mM Tris, 9.5 mM acetate, 1 mM EDTA
4% MIDORI Green Advance	NIPPON Genetics (Düren, Germany)

2.1.8.4 Lysis buffer

NP40 lysis buffer	20 mM Tris, 137 mM NaCl, 2 mM EDTA, 1% Nonidet-P40 (NP40), 1x Protease Inhibitors (Complete Mini)
-------------------	---

2.1.8.5 SDS-PAGE

Separating gel	6-12% acryl-bisacrylamid mix, 25% 1.5 M Tris (pH 8.8), 0.1% SDS, 0.1% ammonium persulfate (APS), 0.04% TEMED
Stacking gel	5% acryl-bisacrylamid mix, 12,5% 1.5 M Tris (pH 6.8), 0.1% SDS, 0.1% ammonium persulfate (APS), 0.1% TEMED
SDS loading buffer	0.15 M Tris, 12% SDS, 4 mM glycerol, 2 mM β - mercaptoethanol, 0,02 μ M bromphenolblue, pH 6.8
1x SDS Running buffer	250 mM Tris, 192 mM glycine, 0.1% SDS

2.1.8.6 Western blot

1x Transfer buffer	48 mM Tris, 38 mM glycine, 0.13 mM SDS, 20% methanol
5% Milk blocking buffer	TBS-T, 5% non-fat milk powder
5% BSA blocking buffer	TBS-T, 5% BSA
Wash buffer	TBS-T
Developing	ECL Select Western Blotting Detection Reagent, GE Healthcare (Little Chalfont, UK)
Stripping buffer	6.3% 1 M Tris (pH 6.7), 0.7 % β -mercaptoethanol, 2% SDS

2.1.8.7 ELISA

Coating buffer	50 mM Na ₂ CO ₃ , 50 mM NaHCO ₃ , pH 9.6
Blocking buffer	4% Goat serum, 0.5% Tween-20, PBS
Wash buffer	0.1 % BSA, 0.05% Tween-20, PBS

2.1.8.8 Histology

Xylene	Carl Roth (Karlsruhe, Germany)
Ethanol 99.9%/96%/70%	Carl Roth (Karlsruhe, Germany)
Gill 3 Hematoxylin	Thermo Scientific (Waltham, MA, USA)
Eosin	0.5% Eosin (C ₂₀ H ₆ Br ₄ Na ₂ O ₅), Merck (Darmstadt, Germany), 3 drops acetate
Differentiating solution	0.1% HCl
Xylene based mounting medium	Consul-Mount, Thermo Scientific (Waltham, MA, USA)

2.1.9 Additional reagents

Protease Inhibitors	Complete Mini, Sigma Aldrich (St. Louis, MO, USA)
DAPI	4',6-Diamidine-2-phenylindole, Sigma Aldrich (St. Louis, MO, USA)
Tissue-Tek	O.C.T. Compound, Sakura Finetek (AV Alphen aan den Rijn, Netherlands)
Dako Fluorescence Mounting Medium	Dako – Agilent Technologies (Santa Clara, CA, USA)
AEBSF	4-(2-Aminoethyl)benzensulfonyl fluorid, Sigma Aldrich (St. Louis, MO, USA)
Collagen Type I	isolated from rat, University Hospital Heidelberg – Immunology
BSA	Bovine Serum Albumin, Carl Roth (Karlsruhe, Germany)
Non-fat milk powder	Carl Roth (Karlsruhe, Germany)
Tween-20	GERBU Biotechnik (Heidelberg, Germany)
Agarose	Eurogentec (Lüttich, Belgium)
Goat serum	GE Healthcare (Pasching, Austria)
Donkey serum	GE Healthcare (Pasching, Austria)
Triton X-100	Carl Roth (Karlsruhe, Germany)
Lipofectamine 2000	Thermo Scientific (Waltham, MA, USA)
BCIP/NBT-plus for ALP	5-Brom-4-chlor-3'-indolylphosphate p-toluidinsalt, ELISpot substrate, Mabtech (Stockholm, Sweden)
TMB Chromogen solution	3,3',5,5'-3,3,5,5-Tetramethylbenzidine, ELISA substrate, Thermo Scientific (Waltham, MA, USA)

2.1.10 Materials

ELISA plates (MaxiSorp)	Thermo Scientific (Waltham, MA, USA)
ELISpot plates	96-Well Filtration Plate MultiScreen HTS IP Sterile MSIP Plates, Merck Millipore (Burlington, MA, USA)
Cell Culture Slides	Nunc Lab-Tek Chamber Slides, Thermo Scientific (Waltham, MA, USA)
4-15% Mini-Protean TGX Precast gel	Gradient gel, Bio-Rad (Hercules, CA, USA)
BD Microlance 3 (22 G)	BD Biosciences (Franklin Lakes, NJ, USA)

2.1.11 Lab equipment

Tabletop centrifuge	Hermle Z233 MK-2, Hermle Labortechnik GmbH (Wehingen, Germany)
Centrifuge	Multifuge 3S-R, Heraeus (Newport, UK)
Cryotome	CM1850 UV, LEICA (Wetzlar, Germany)
Microtome	SLIDE 2003, pfm AG (Köln, Germany)
Microplate Reader for ELISA	Multiskan EX, Thermo Electron Corporation (Waltham, MA, USA)
ImmunoSpot Analyzer for ELISpot	S6 Universal M2, ImmunoSpot (Cleveland, OH, USA)
iBright Imaging System	iBright FL1000, Thermo Scientific (Waltham, CA, USA)
Invitrogen Evos	
Flow Cytometer	Gallios 4L, Beckman Coulter (Sinsheim, Germany)

2.2.2 Passive Transfer of monoclonal antibodies into neonatal mice

The passive transfer of antibodies was performed on the first day of life. 0.5-1.5 mg of total purified monoclonal antibody H510 or the corresponding isotype control IgG1 was injected subcutaneously into FcγR^{-/-} mice. 48 to 55 hours (h) after injection, the mice were sacrificed and the back skin, skin of extremities and tail were analyzed by histology (2.2.7) or direct immunofluorescence (2.2.8.1).

2.2.3 Genotyping

2.2.3.1 DNA isolation

To identify the genotypes of scurfy and WT mice pieces of the tails were collected. DNA isolation was performed using the KAPA Express Extract Kit (2.1.5) according to the manufacturer's instructions.

2.2.3.2 Polymerase chain reaction (PCR)

After isolation of the DNA a PCR of the samples was performed using the HotStarTaq Kit (2.1.5) according to the manufacturer's protocol. To identify the mutant and WT allele two different primer sets (2.1.3) were used for PCR.

	<u>WT</u>	<u>Mutant</u>
Tissue DNA	1 µl	1 µl
HotStarTaq Master Mix	10 µl	10 µl
ddH ₂ O	5 µl	5 µl
Coral Loading Dye	2 µl	2 µl
100 µM FP (WT)	1 µl	-
100 µM FP (Mutant)	-	1 µl
100 µM Reverse Primer	1 µl	1 µl

The PCR cycles were performed as follows:

Pre denaturation:	95°C	5 min	1 cycle
Denaturation:	95°C	1 min	} 33 cycles
Annealing:	67°C	1 min	
Elongation:	72°C	1 min	
Post-Elongation:	72°C	10 min	1 cycle
Holding:	4°C		

2.2.3.3 Agarose gel electrophoresis

The analysis of the PCR samples generated in 2.2.3.2 was performed using 1% agarose gels containing 4% MIDORI Green Advance to visualize the bands. DNA was separated for 45 min in TAE buffer at 120 V. DNA bands were identified using UV light in the iBright Imaging System.

2.2.4 Cell experiments

2.2.4.1 Culture of murine and human cells

Frozen cells were thawed in a water bath at 37°C and immediately diluted with 10 ml of the appropriate medium. After centrifugation at 300 x g for 7 min, cell pellet was resuspended in medium. Cells were cultivated at 37°C in a humidified 5% CO₂ incubator in the appropriate media in T25, T75 or T175 cell culture flasks. HEK293T cells and primary murine fibroblasts were split every two to four days and detached with 1x Trypsin/EDTA. Primary murine keratinocytes were seeded in cell culture flasks which were pre-coated with collagen type I (1:1000 in PBS) for 1 h room temperature (RT). Keratinocytes were split every three days by gentle detachment with accutase. For long-term storage, 1 x 10⁶ cells/ml were detached and centrifuged (300 x g, 7 min). Cell pellets were resuspended in appropriate freezing medium (700 µl medium, 200 µl FCS, 100 µl DMSO) and immediately frozen at -80°C in an isopropanol container.

2.2.4.2 Transfection of HEK293T cells

HEK293T cells were cultured in DMEM with 10% FCS, detached and seeded in a 6-well cell culture plate and cultured overnight. Confluent cells were transiently transfected for 18 hours with Lipofectamine 2000 in a ratio of 3:1 to the plasmids for Col7 (NC1, NC2, THD) (with His-Tags, synthesized by BioCat, Heidelberg, Germany). The transfected cells were scraped off with a disposable cell scraper, lysed by freeze-and-thaw and used for western blot analysis.

Successful expression of the proteins was checked in western blot by using anti-His-Tag antibody.

2.2.4.3 Isolation of murine primary keratinocytes

Primary murine keratinocytes were isolated from skin of WT neonatal mice. Reagents and media were purchased from CELLnTEC and the isolation was performed according to their protocol. Separation of epidermis from dermis was induced by incubation in dispase solution at 4°C overnight. Skin was split in epidermis and dermis using forceps. Epidermis was incubated in 500 µl accutase for 30 min RT and afterwards diluted with epithelial culture medium. Keratinocytes were dissolved by rubbing the epidermis with forceps and centrifuged at 180 x g for 5 min. Cell pellet were resuspended in epithelial culture medium and seeded in a density of 4×10^4 cells/cm² in appropriated cell culture flasks which were pre-coated with collagen type I (2.2.4.1).

2.2.4.4 Isolation of murine primary fibroblasts

Primary murine fibroblasts were isolated from adult WT mouse ears. Ears were disinfected with 70% ethanol and placed in 6-well plate with 4 ml 10% DMEM (3x Pen/Strep). The ears were cut into very small pieces with sharp scissors and incubated with collagen type Ia (final 1 mg/ml) at 37°C in a humified 5% CO₂ incubator overnight. Cells were dissolved by pipetting into a 5 ml pipette until the solution became turbid. After centrifugation at 300 x g for 7 min to remove cell debris, the cell pellet was resuspended in 8 ml of 10% DMEM (3x Pen/Strep) and divided into two wells of a 6-well cell culture plate. Cells were cultured in a humified 5% CO₂ incubator at 37°C overnight before the medium was changed. Depending on growth, fibroblasts were cultured for one to two weeks before splitting and further culturing in a T75 cell culture flask.

2.2.4.5 Generation of cell lysates

Confluent cells were washed with PBS and detached with a disposable cell scraper. Cell suspension was centrifuged at 300 x g for 7 min and resuspended in NP40 lysis buffer. Cells were lysed for 20 min on ice and centrifuged at 2000 x g for 10 min. Supernatant was transferred in a new Eppendorf tube and stored at -20°C.

2.2.4.6 Isolation of skin immune cells

Skin immune cells for flow cytometry analysis were isolated from scurfy and WT ears. 2 ml Eppendorf tubes were prepared with 300 μ l digestion mix containing RPMI, 0.5 mg/ml Liberase TL and 0.05 mg/ml DNase I on ice. Ears were flipped open with forceps, placed in the digestion mix and cut into very small pieces with sharp scissors. After 700 μ l of digestion mix was added the samples were digested for 1 h at 37°C shaking at 750 rpm. Digestion was stopped by adding 100 μ l of FCS to the tissue. Tubes were placed on ice and the tissue was homogenized through a 22 G cannula until turbid. Tissue suspension was filtered through a 40 μ m cell strainer and washed with 30 ml FACS buffer. After centrifugation for 30 min at 400 x g cells could be analyzed by flow cytometry.

2.2.5 SDS-PAGE

Sodium dodecyl sulfate polyacrylamide gel electrophoresis (SDS-PAGE) was performed to separate and afterwards identify different proteins.

2.2.5.1 Polyacrylamide Gel preparation

Larger proteins such as Col7 (290 kDa) were separated on a 6% SDS gel. Smaller proteins like vWFA2 (21 kDa) were separated using a 12% SDS gel. These gels were self-made. For simultaneous separation of proteins with different molecular weights (transfected HEK293T cells with different Col7 domains) a 4-15% Mini-Protean TGX gradient gel (2.1.10) was purchased.

Separating and stacking gels were prepared (2.1.8.5). Protein samples were mixed with denaturing 5x SDS loading buffer and boiled for 5 min at 95°C. Samples and protein marker were applied to the gel to determine protein sizes. Proteins were separated in 1x SDS running buffer (2.1.8.5) starting at 80 V for 15 min and at 120 V for 60-90 min. Afterwards the SDS-PAGES were further analyzed using western blot.

2.2.5.2 Western blot

Proteins separated by SDS-PAGE were identified by western blot. Proteins were transferred to a polyvinylidene fluoride (PVDF) membrane. Wet transfer was used for large proteins (>200 kDa) and semi-dry transfer for smaller proteins (<200 kDa). First, the membrane was activated with methanol and filter papers were soaked in 1x transfer buffer (2.1.8.6). The PVDF membrane was applied to three filter papers, the SDS gel was placed on top and again three

soaked filter papers were placed. The proteins were blotted at 250 mA continuously for 30 min. After transfer, the membrane was blocked for 1 h RT shaking with 5% milk blocking buffer. Dilutions for primary antibody incubation were described in 2.1.4.1 and 2.1.4.4. Antibodies were diluted in 5% BSA blocking buffer at appropriate dilutions and incubated with blots for 1 h RT shaking. His-tagged proteins after transfection were detected using the anti-Histidine tag antibody diluted in 5% milk blocking buffer for 1 h RT shaking. Membranes were washed 3 x with wash buffer for 5 min. Secondary antibodies were used in appropriate concentrations (2.1.4.4) diluted in 5% milk blocking buffer and incubated for 1 h RT shaking. After washing, signals were visualized with ECL-developing solution and documented using the iBright imaging system.

2.2.6 Bicinchoninic Acid Assay (BCA)

The concentrations of different proteins or cell lysates were evaluated using the Pierce BCA Protein Assay Kit (2.1.5). The assay was performed according to the manufacturer's protocol. 25 µl of BSA standards were pipetted in duplicates and samples were depending on the concentration 1:5 or 1:10 diluted in PBS. 200 µl of working solution was added to the standards and samples and incubated at 37°C for 30 min. Afterwards the absorption at 550 nm could be measured on the microplate reader and the protein concentration was obtained with help of the standard curve.

2.2.7 Histology

For the histological evaluation of tissue samples (blisters in skin, inflammation in spleen or sdLN) the samples were taken and fixed in 4% neutral buffered formalin at 4°C overnight. Tissue samples were dehydrated and embedded in paraffin. 2 µm sections were cut with the microtome and dried at 37°C overnight. To perform a hematoxylin and eosin staining (H&E staining) the sections were deparaffinized by xylene and rehydrated by a series of alcohols (99,9%, 96%, 70%). After incubation with hematoxylin (DNA, nuclei) and a short differentiation time the sections were washed in running tap water. After staining with eosin (proteins, cytoplasm) and the ascending alcohol series with final xylene, the sections were embedded in xylene based mounting medium.

2.2.8 Immunofluorescence microscopy

2.2.8.1 Direct immunofluorescence (DIF)

The presence of autoantibodies in the skin was determined by direct immunofluorescence (DIF) microscopy. Skin from neonatal mice was collected and embedded in Tissue-Tek medium in a cryotome at -22°C. 7 µm cryosections of the tissues were fixed in ice-cold acetone for 10 min and blocked with 5% goat serum in TBS for 30 min before staining with secondary antibodies (2.1.4.3 anti-mouse C3-FITC, anti-mouse IgG-AF488) at appropriate dilutions with TBS for 1 h RT in a dark humidified chamber. After washing with TBS, the sections were embedded in Dako Fluorescence mounting medium prior to analysis.

2.2.8.2 Indirect immunofluorescence (IIF)

To observe antibody reactivity in tissues, indirect immunofluorescence (IIF) was performed on palatal tissue, skin, and various internal organs of WT mice. Tissue was collected, sectioned, fixed, and blocked as described in 2.2.8.1. The scurfy antibody H510, sera from scurfy or WT mice or different primary antibodies (2.1.4.3) were diluted in TBS and incubated on the sections for 1 h RT in a dark humidified chamber. After washing, secondary antibodies (2.1.4.3 anti-mouse IgG-AF488, anti-rabbit IgG-AF488) were diluted appropriately in TBS and incubated for 1 h RT. Sections were embedded as described in 2.2.8.1.

2.2.8.3 Immunofluorescence on primary murine cells

For IIF staining of isolated and cultured primary murine keratinocytes (2.2.4.3) and fibroblasts (2.2.4.4), cells were seeded at appropriate densities on collagen type I pre-coated (1:1000 in PBS) cell culture chamber slides. Confluent cells were washed with PBS and fixed with 4% neutral buffered formalin for 20 min. To further characterize the specific intracellular antigen expression in these cell types, cells were permeabilized for 10 min with 0.1% Triton X-100 in PBS. Cells were blocked for 10 min with 5% goat or donkey serum and then incubated with primary antibodies (2.1.4.3) at appropriate dilutions for 20 min. After washing with PBS-T, cells were blocked again and incubated with suitable secondary antibodies for 1 h RT. Cells were washed and DAPI staining was performed for 5 min to visualize nuclei of the cells. The chamber was removed and the slides were embedded with Dako Fluorescence mounting medium.

2.2.9 Peptide Competition Assay

To further characterize the binding capacity and specificity of an antibody, the peptide competition assay was used. First, mAb H510, control isotype IgG1 and anti-vWFA2 were incubated with murine vWFA2 protein in a 1:10 ratio. The antibody-peptide mixtures were incubated at 4°C overnight on a rotator. The suspensions were centrifuged at 12.500 rpm for 15 min to sediment immune complexes. The supernatant was used as primary antibody for IIF on WT neonatal skin (2.2.8.2). Fluorescence intensity was evaluated using ImageJ to calculate the mean fluorescence value for statistical analysis.

2.2.10 Enzyme linked immunospot assay (ELISpot)

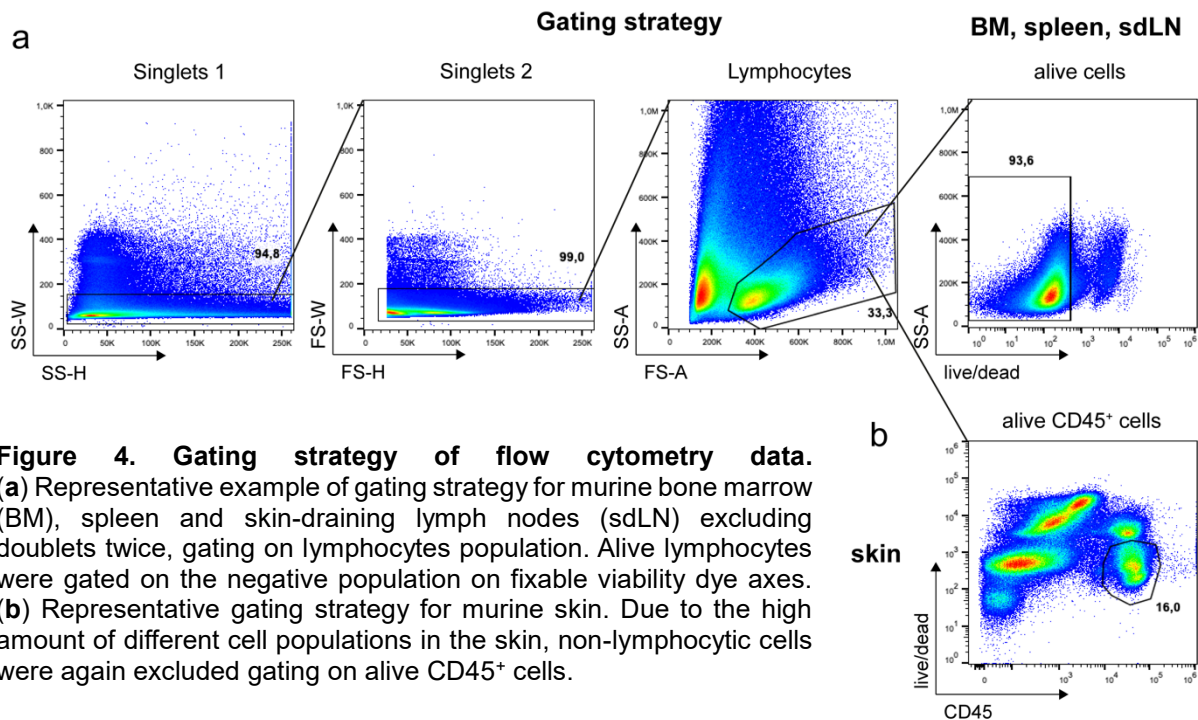
Enzyme linked immunospot assays (ELISpot) were performed to detect antigen-specific IgG-secreting B cells in scurfy mice that may be relevant for the induction of AIBD in these mice. ELISpot plates were first activated with 35% ethanol for 1 min and washed 5x with dH₂O. Plates were coated at 4° overnight with three proteins that are known antigens in AIBD (vWFA2, BP180 c-terminal and Laminin α 3). Proteins were diluted in PBS to a final concentration of 10 μ g/ml and 100 μ l diluted antigen was added to the wells. Cells were harvested from the spleen and sdLN of 10-day-old scurfy and WT littermates. Single cell suspensions were prepared. For sdLN, the whole suspension was used for the assay. Three different approaches were tested for the splenocytes. One part of total splenocytes was taken, erythrocytes were lysed with 1x ACK buffer and the cell suspension was used for the assay. The other part of the splenocytes was used for B cell isolation using the EasySep Mouse B cell isolation Kit according to the manufacturer's protocol. Purified B cells and the remaining cells (termed non-B cells) were then used for the ELISpot assay. After cell isolation, the ELISpot plate was washed five times with wash buffer II and afterwards blocked for 2 h RT with 1% BSA in PBS. After blocking the different cell suspensions were added to the wells at a concentration of 200.000 cells/well and incubated at 37°C with 5% CO₂ in a humidified incubator overnight. The Mouse IgG ELISpot Basic Kit (ALP) was used for spot detection according to manufacturer's instructions. To visualize spots, representing single antigen-specific B cells, wells were incubated with the chemical reagent BCIP/NBT for 10 min. Spots were counted using the ImmunoSpot Analyzer for ELISpots.

2.2.11 Enzyme linked immunosorbent assay (ELISA)

To analyze the antigen specificity of mAb H510, Enzyme linked immunosorbent assay (ELISA) was performed using murine vWFA2 protein and murine laminin γ 1 (kindly provided by Prof. Enno Schmidt – University of Lübeck), as negative control. ELISAs were performed in 96-well plates. Plates were coated with proteins (5 μ g/well) diluted in coating buffer (50 mM carbonate/bicarbonate) overnight at 4°C. Wells were blocked with 4% goat blocking buffer and incubated with mAb H510 (5 μ g/ml) for 1 h RT with shaking. Plates were washed followed by secondary antibody incubation (2.1.4.5) for 1 h RT shaking on an orbital shaker. After washing the plates were developed by 50 μ l TMB chromogen solution to the wells, stopped by adding of 1 M sulfuric acid. Absorbance was measured at 450 nm using a microplate reader.

2.2.12 Flow cytometry

For analysis of different B cell populations in BM, spleen, sdLN and skin, single cell suspensions of the different tissues were prepared for staining. To isolate cells from BM, femur bones were removed and rinsed with ice-cold PBS using a syringe. Flushed BM was resuspended and filtered through a 70 μ m cell strainer. After centrifugation at 400 x g for 7 min, erythrocytes were lysed with 1x ACK buffer and washed with FACS buffer. For spleen single cell suspensions, erythrocytes were also lysed with 1x ACK buffer prior to staining. Single cell suspensions of sdLN were taken immediately after isolation and skin immune cells were isolated as described in 2.2.4.6. For each staining, 1.000.000 cells were used. For background control, single staining, and fluorescence-minus-one (FMOs) were prepared. The Fc receptors of the cells were first blocked with anti-CD16/CD32 antibody for 15 min at 4°C. Cells were then stained with different antibodies (2.1.4.2) for 30 min at 4°C. For characterization of IgG1-producing germinal center B cells, the cells were fixed and permeabilized with the FOXP3/Transcription Factor Staining Buffer Kit (2.1.5) according to the manufacturer's instructions and stained afterwards. The cells were measured on the flow cytometer and data were analyzed using FlowJo software. The measured cells were gated as follows: doublets were excluded twice, lymphocyte population was gated, and then alive cells were gated from BM, spleen and sdLN (Figure 4 a). Due to the high number of different cell populations, skin immune cells (Figure 4 b) were additionally gated on CD45⁺ population.



2.2.13 LEGENDplex Assay

To further characterize B cells in scurfy mice, the LEGENDplex B cell panel was performed to simultaneously analyze 13 essential biomarkers involved in B cell function, activation, and survival. For this assay, the fluorescence-labeled Beads A and Beads B were used to discriminate between the different cytokines in the flow cytometer. Serum from 18–20-day old scurfy mice and WT littermates was collected for analysis. Two LEGENDplex kits (2.1.5) were used to quantify the cytokines IL-4, IL-6, IL-17p70, IL-17A, IL-2, TNF- α , free active TGF- β 1, IL-13, IFN- γ , BAFF, sBCMA, sCD40L and IL-10. Buffers, antibodies and standards were included in the kits and experiments were performed according to the manufacturer's protocol, including analysis of samples and standard curves. Samples were measured using the flow cytometer and data were analyzed using the LEGENDplex Data Analysis Software.

2.2.14 Statistical Analysis

The experiments were analyzed using GraphPad 8 Prism Software and data are expressed as mean \pm standard deviation (SD). For statistical analysis of peptide competition assay, ELISA, LEGENDplex, and flow cytometry data with only two groups, the two-tailed unpaired *t* test with Welch's correction was used considering *P*-values <0.05 as significant. For ELISpot and flow cytometry data with more than two groups, one-way ANOVA followed by Bonferroni's multiple comparisons test was used with *P*-values <0.05 considered significant.

3 RESULTS

3.1 Scurfy mice show altered lymphatic organs

Due to the missing Treg control, scurfy mice spontaneously develop several autoimmune diseases. Autoreactive CD4⁺ T cells are expanded in these mice and activate B cells, which produce autoreactive autoantibodies that primarily attack the skin and inner organs of these mice (Figure 1). To further characterize the strong immune responses in scurfy mice, a histological examination of lymphatic organs was necessary. Histological sections and H&E staining were performed on spleens and skin-draining lymph nodes (sdLN) of sick scurfy mice and WT littermates. The spleen of scurfy mice showed severe enlargement compared to WT littermates (Figure 5 a). Enlargement of the sdLN was also observed in scurfy mice (Figure 5 b). Furthermore, a close-up of the scurfy lymph nodes revealed secondary follicles (Figure 5 b, close-up, white mark) that were not present in the WT sdLN.

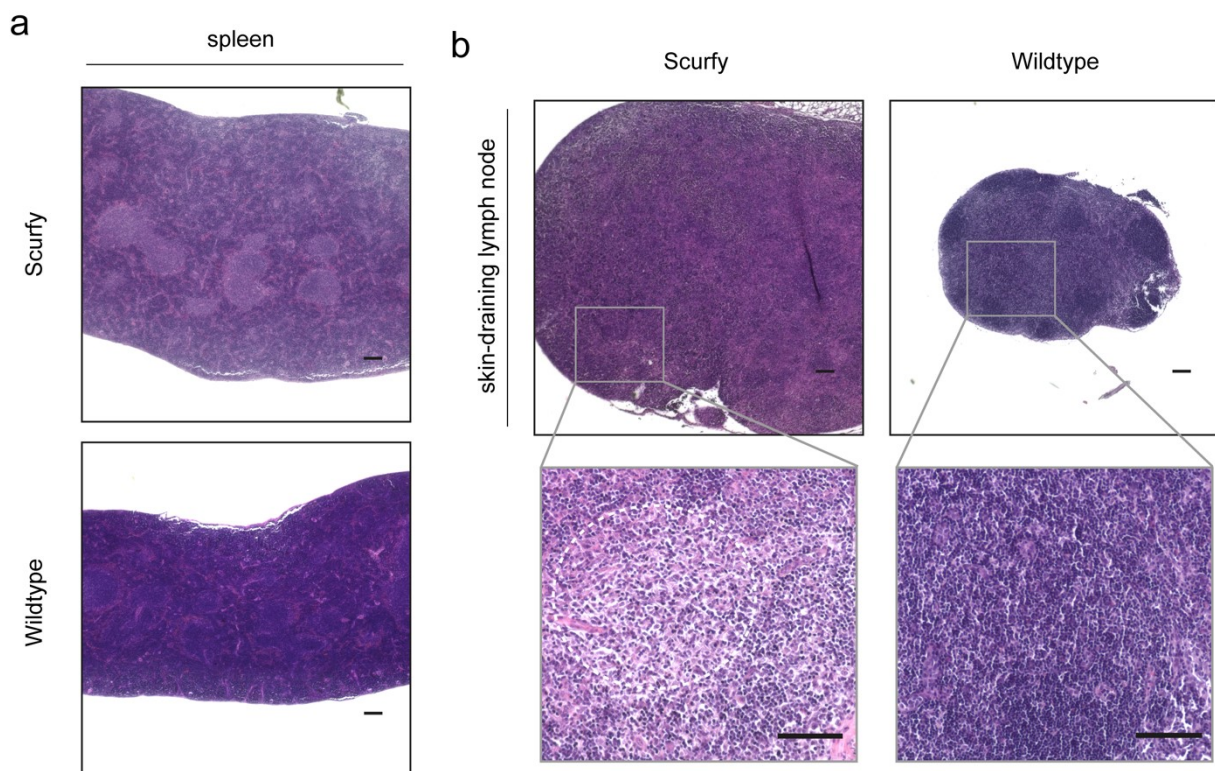


Figure 5. Scurfy mice show enlarged lymphatic organs and secondary follicles in sdLN. (a) H&E staining of spleen of 18-day old scurfy mice and WT littermates. Scurfy mice show a strong enlargement of the spleen compared to WT spleen. Bar = 100 μ m. (b) Representative H&E staining of skin-draining lymph nodes (sdLN) of 18-day old scurfy mice and WT littermates and close-up of secondary follicle. Scurfy mice show enlarged sdLN and apparent secondary follicles (marked by white line) compared to WT mice. Bar = 100 μ m.

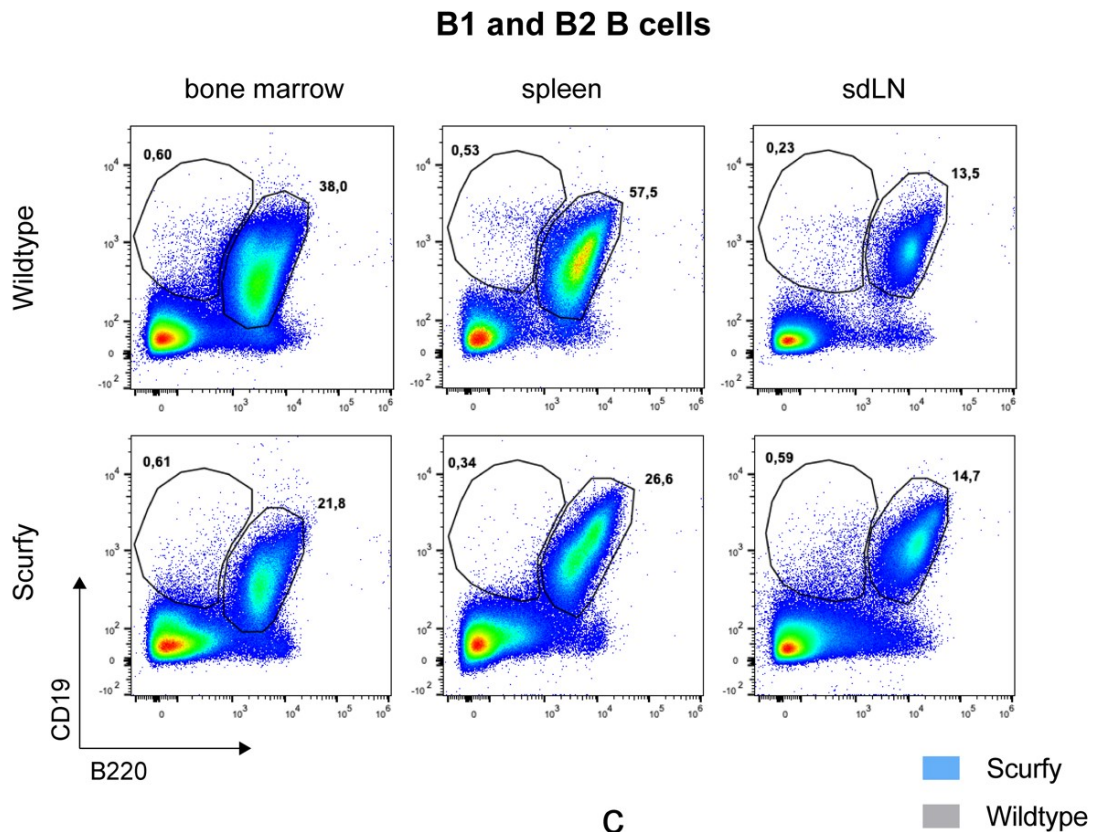
3.2 Scurfy mice have altered B cell populations and show restricted B cell maturation in lymph nodes

Characterization of the disease leading to the scurfy phenotype revealed a primarily CD4⁺ T cell-driven pathology (Godfrey et al. 1991a; Godfrey et al. 1991b). In addition, it has been previously investigated that scurfy mice develop high titers of autoantibodies relevant for development of autoimmune blistering diseases (Hadaschik et al. 2015; Haeberle et al. 2018; Muramatsu et al. 2018).

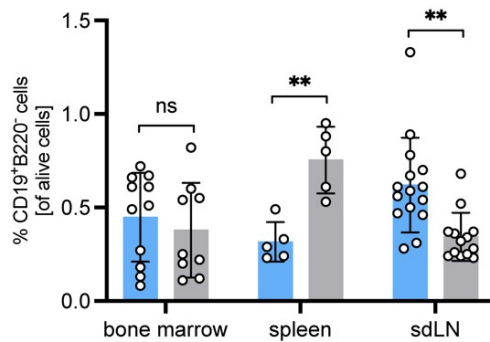
To further elucidate the contribution of B cells to disease in scurfy mice, flow cytometry (FACS) analysis of 18-21-day old scurfy mice and WT littermates was performed.

Immune cells were isolated from BM, spleen and sdLN of scurfy and WT mice and used for FACS analysis to identify B1 and B2 B cells. Representative dot plots show the gating of B1 and B2 B cells with the markers CD19 and B220 within the different tissues (Figure 6 a). B1 B cells were characterized as CD19⁺B220⁻ cells, which showed no significant difference in the BM of scurfy mice as compared to WT littermates (Figure 6 b). Analysis of the spleen revealed a significantly higher frequency of B1 B cells in WT mice (Figure 6 a). In contrast, the sdLN showed higher frequencies of B1 B cells in scurfy mice (Figure 6 b). B2 B cells were identified by the double expression of CD19 and B220 (Figure 6 a). In BM and spleen, scurfy mice showed decreased levels of B2 B cells compared to WT mice (Figure 6 c). In contrast, no difference was observed in the sdLN (Figure 6 c).

a



b



c

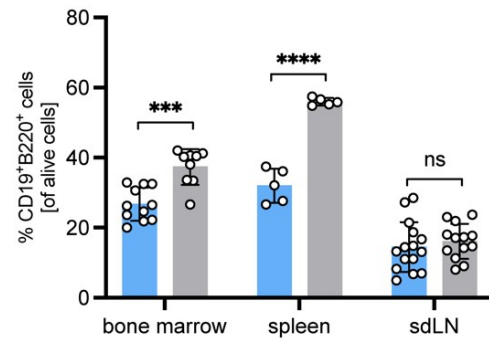


Figure 6. Scurfy mice show altered B1 and B2 B cell populations. (a) Representative dot plots showing alive B1 B cells (CD19⁺B220⁻) and B2 B cells (CD19⁺B220⁺) gated on alive lymphocytes in bone marrow, spleen, and skin-draining lymph nodes (sdLN) of scurfy mice and WT littermates. (b) Quantification of B1 B cells shown as percentage of CD19⁺B220⁻ cells. (c) Quantification of B2 B cells shown as percentage of CD19⁺B220⁺ cells. Data presented as mean ± SD, one-way ANOVA followed by Bonferroni's multiple comparisons test was performed (**p<0.01, ***p<0.001, ****p<0.0001, ns, not significant).

In scurfy mice, it was previously shown that the development of normal B cells in BM and spleen is impaired due to their *Foxp3* deficiency (Riewaldt et al. 2012).

To investigate whether the maturation of B cells in the sdLN is also affected in scurfy mice and to get an idea of the frequency of mature and transitional B cells in our mice, immune cells from BM, spleen and sdLN were analyzed by FACS. Representative dot plots show the gating strategy to identify mature B cells (IgD⁺) and transitional B cells (IgD^{low}) (Figure 7 a). No significant difference in mature and transitional B cells could be detected in BM and spleen of

scurfy and WT littermates (Figure 7 b, c). In contrast, analysis of the sdLN revealed a strong decrease in mature B cell frequencies in scurfy mice compared to WT (Figure 7 b). In line, scurfy mice showed an increase of transitional B cells in sdLN compared to WT littermates (Figure 7 c).

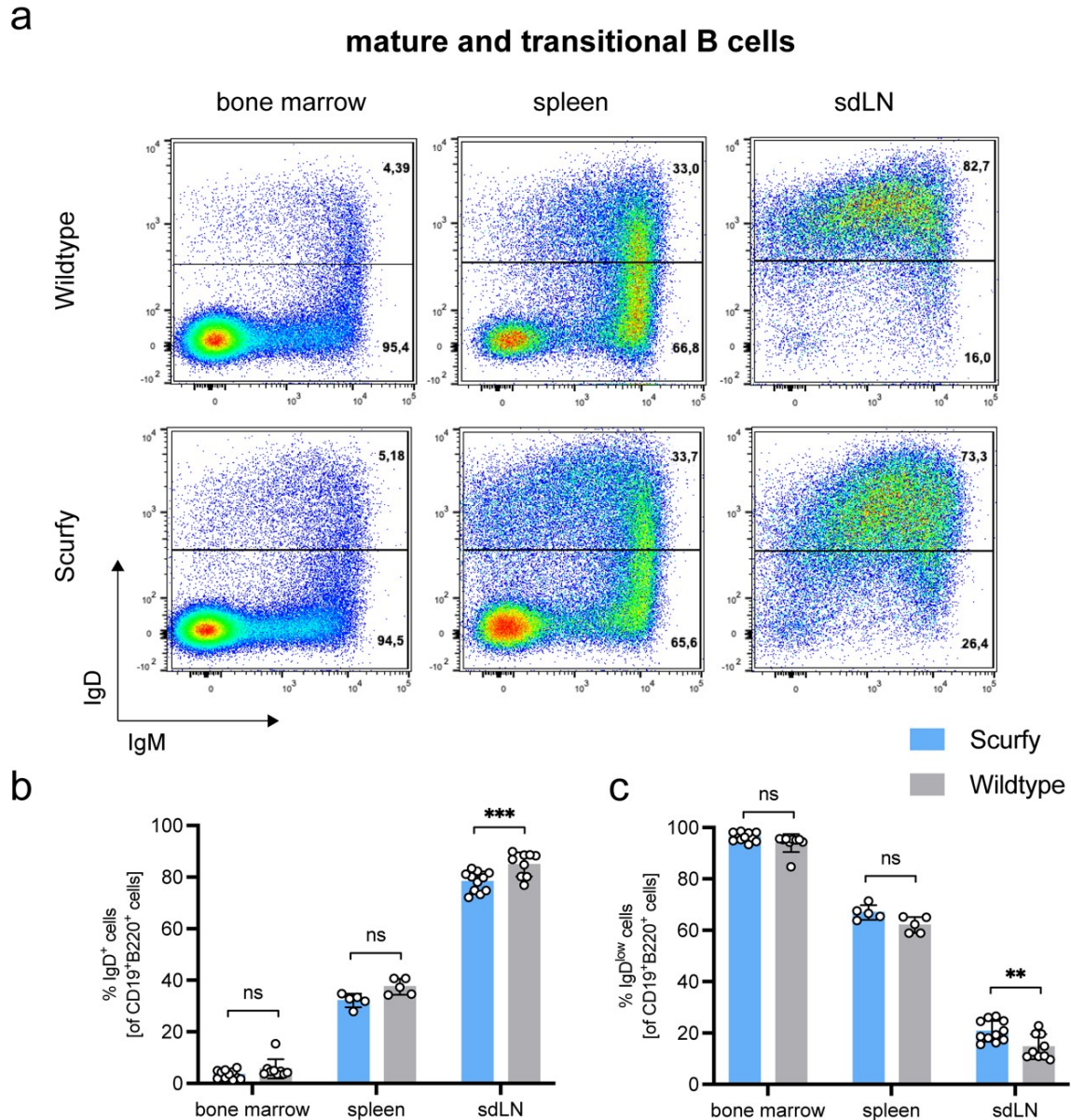


Figure 7. Scurfy mice show impaired B cell maturation in sdLN. (a) Representative dot plots showing alive mature B cells (IgD⁺) and transitional B cells (IgD^{low}) gated on alive CD19⁺B220⁺ cells in bone marrow, spleen, and skin-draining lymph nodes (sdLN) of scurfy mice and WT littermates. (b) Quantification of mature B cells shown as percentage of IgD⁺ cells. (c) Quantification of transitional B cells shown as percentage of IgD^{low} cells. Data presented as mean ± SD, one-way ANOVA followed by Bonferroni's multiple comparisons test was performed (**p<0.01, ***p<0.001, ns, not significant).

3.3 Spleen of scurfy mice shows impaired marginal zone surrounding follicles

The splenic marginal zone (MZ) is structurally a barrier between the lymphoid and innate compartments (Kraal and Mebius 2006). The MZ is located around the follicles (FO) and is characterized by specific MZ macrophages and MZ B cells that function as defense against blood-borne pathogens (Martin et al. 2001; Oliver et al. 1997).

To further investigate these structures in scurfy mice, H&E staining was performed on the spleens of 18-day old scurfy mice and WT littermates. Histologically, follicular structures were seen in both mice (Figure 8, indicated by white circles). The spleens of WT mice showed MZ structures surrounding the FO, which were not detected in scurfy mice (Figure 8).

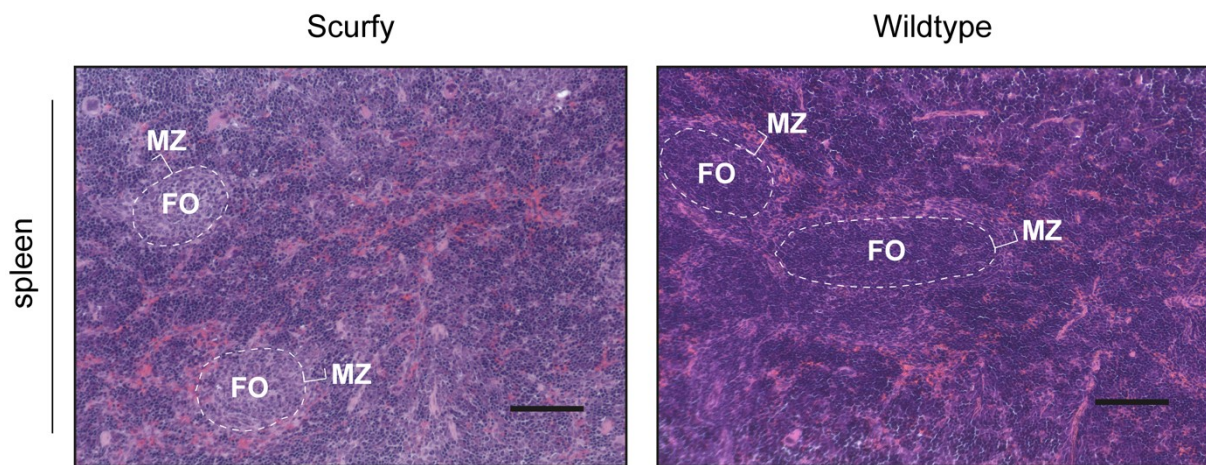


Figure 8. Histology of scurfy spleen shows altered marginal zone structures. Representative H&E staining of spleen of 18-day old scurfy and WT mice. Follicular (FO) structures (white circle) are surrounded by marginal zones (MZ) in WT mice. MZ were not visible in scurfy mice. Bar = 100 μ m.

To analyze B cells located in the MZ and FO, spleen and sdLN were examined by FACS analysis. Representative dot plots showed the gating of follicular B cells ($CD23^+CD21^+$) and MZ B cells ($CD23^-CD21^+$) in scurfy and WT mice gated on mature IgD^+ B cells (Figure 9 a). Quantitative analysis revealed no significant differences in the frequencies of follicular B cells in the sdLN and spleen of scurfy mice and WT littermates (Figure 9 b). In contrast, significantly lower frequencies of MZ B cells were detected in scurfy mice compared to WT mice in both spleen and sdLN (Figure 9 c).

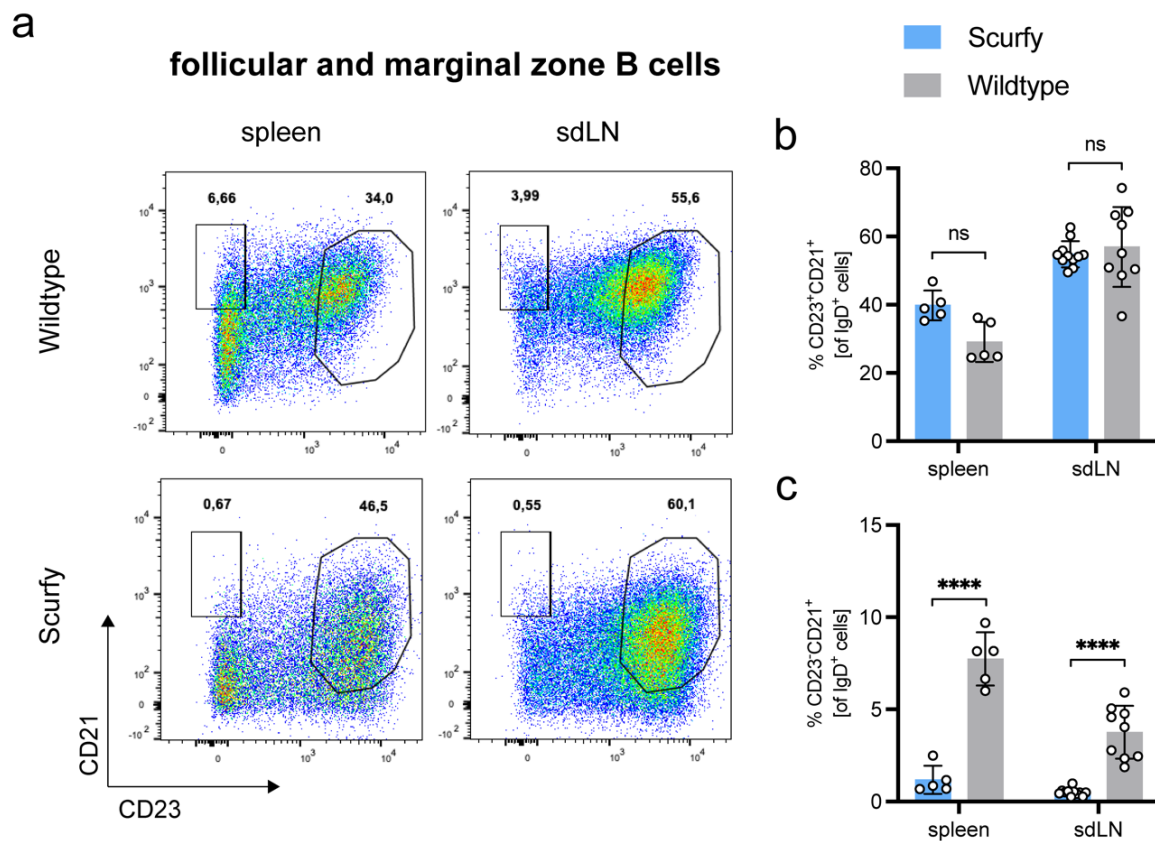


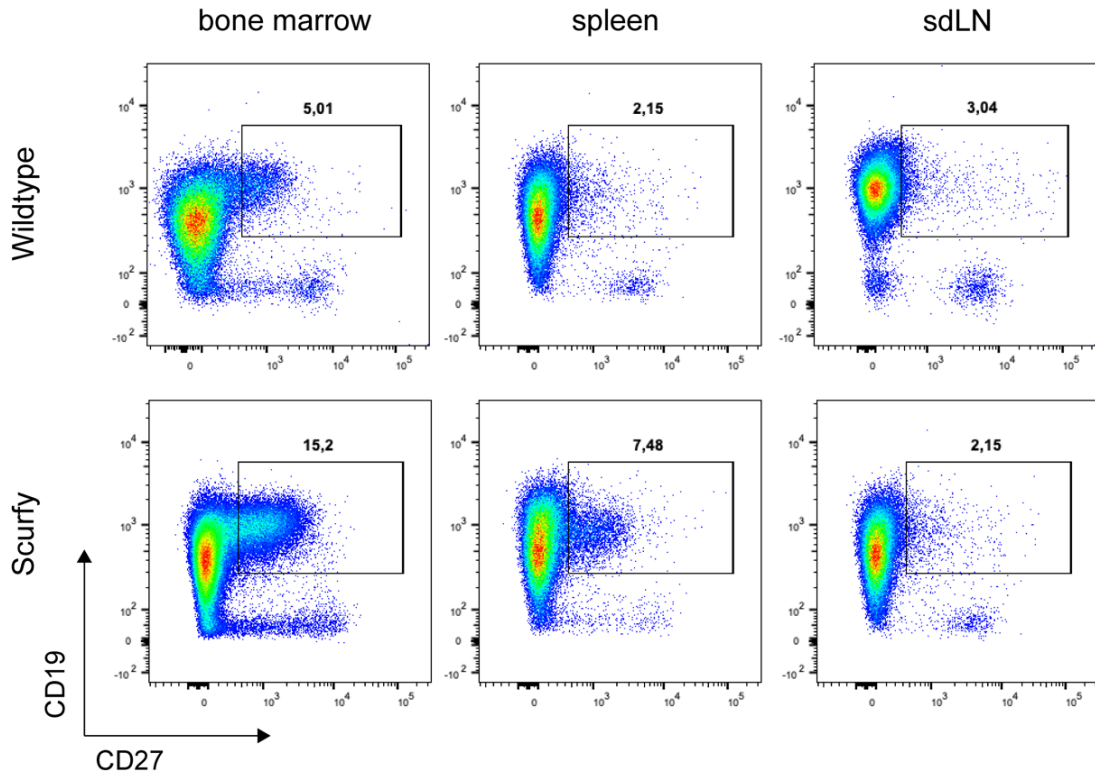
Figure 9. Scurfy mice show impaired MZ B cell compartment in spleen and sdLN. (a) Representative dot plots showing alive follicular B cells (CD23⁺CD21⁺) and marginal zone B cells (CD23⁻CD21⁺) gated on mature B cells (IgD⁺) in spleen and skin-draining lymph nodes (sdLN) of scurfy mice and WT littermates. (b) Quantification of follicular B cells shown as percentage of CD23⁺CD21⁺ cells. (c) Quantification of marginal zone B cells shown as percentage of CD23⁻CD21⁺ cells. Data presented as mean ± SD, one-way ANOVA followed by Bonferroni's multiple comparisons test was performed (****p<0.0001, ns, not significant).

3.4 Scurfy mice have elevated frequencies of memory B cells

Memory B cells are known to be readily reactivated and do not require continuous antigen stimulation to survive (Martin and Goodnow 2002; Maruyama et al. 2000). To investigate whether the memory B cell compartment is altered by autoimmunity due to Treg deficiency in scurfy mice, FACS analysis of BM, spleen, and sdLN of sick scurfy mice and their WT littermates was performed. Gating of memory B cells (CD19⁺CD27⁺) was shown by representative dot plots of scurfy and WT mice in BM, spleen and sdLN (Figure 10 a). Quantitative analysis revealed significantly higher frequencies of memory B cells in BM and spleen of scurfy mice compared to WT mice (Figure 10 b). The memory B cell compartment in the sdLN was not altered in scurfy mice (Figure 10 b).

a

memory B cells



b

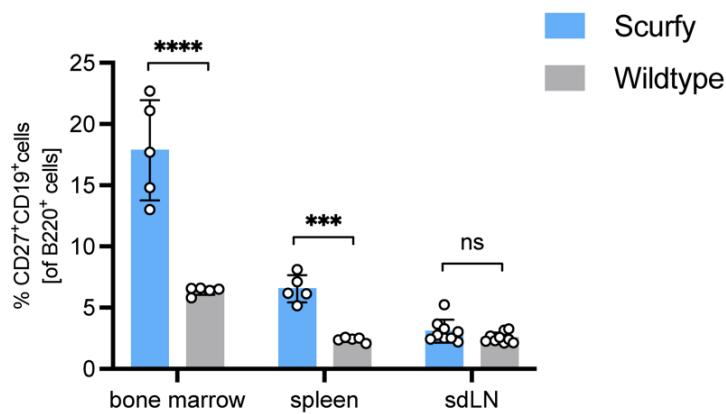


Figure 10. Scurfy mice show elevated frequencies of memory B cells in bone marrow and spleen. (a) Representative dot plots showing alive memory B cells (CD19⁺CD27⁺) gated on alive B220⁺ B cells in bone marrow, spleen, and skin-draining lymph nodes (sdLN) of scurfy mice and WT littermates. (b) Quantification of memory B cells shown as percentage of CD19⁺CD27⁺ cells. Data presented as mean ± SD, one-way ANOVA followed by Bonferroni's multiple comparisons test was performed (**p<0.001, ****p<0.0001, ns, not significant).

3.5 Germinal center B cells and autoantibody producing cells are highly increased in scurfy mice

GC reactions are taking place in secondary lymphoid tissues, where GC B cells closely interact with Tfh cells (Stebegg et al. 2018). B-T cell interactions are regulated by Foxp3⁺ T follicular regulatory cells (Stebegg et al. 2018). Due to the *Foxp3* mutation in scurfy mice, the development of GC B cells in these mice was of interest. To investigate the GC B cell populations in scurfy mice, immune cells of spleen and sdLN of 18-day old scurfy mice and WT littermates were measured by FACS and subsequently analyzed. Representative FACS plots show the gating strategy of GC B cells in the spleen and sdLN of WT and scurfy mice (Figure 11 a). Quantitative analysis revealed significantly higher frequencies of GC B cells in both secondary lymphoid organs in scurfy mice (Figure 11 c).

Scurfy mice are known to develop high titers of autoantibodies that lead to severe autoimmune reactions in these mice, particularly of the IgG1 isotype. To further prove that GC B cells are involved in autoantibody production, FACS analysis of IgG1-producing GC B cells from sdLN and spleen was performed. Representative contour plots showed the strategy of gating IgG1⁺B220⁺ GC B cells (Figure 11 b). Quantitatively, this analysis showed significantly higher frequencies of IgG1-producing GC B cells in scurfy spleen and sdLN compared to WT littermates (Figure 11 d).

FACS analysis of BM, spleen and sdLN was performed to examine plasma cells, which are the major producers of autoantibodies which are highly abundant in sick scurfy mice. Plasma cells were characterized by double expression of the specific markers CD138 and TACI (Figure 11 e). Analysis of BM and spleen showed no significant differences in plasma cell frequency between scurfy and WT mice (Figure 11 f). In contrast, the sdLN of scurfy mice revealed significantly higher frequencies of plasma cells compared to WT littermates (Figure 11 f).

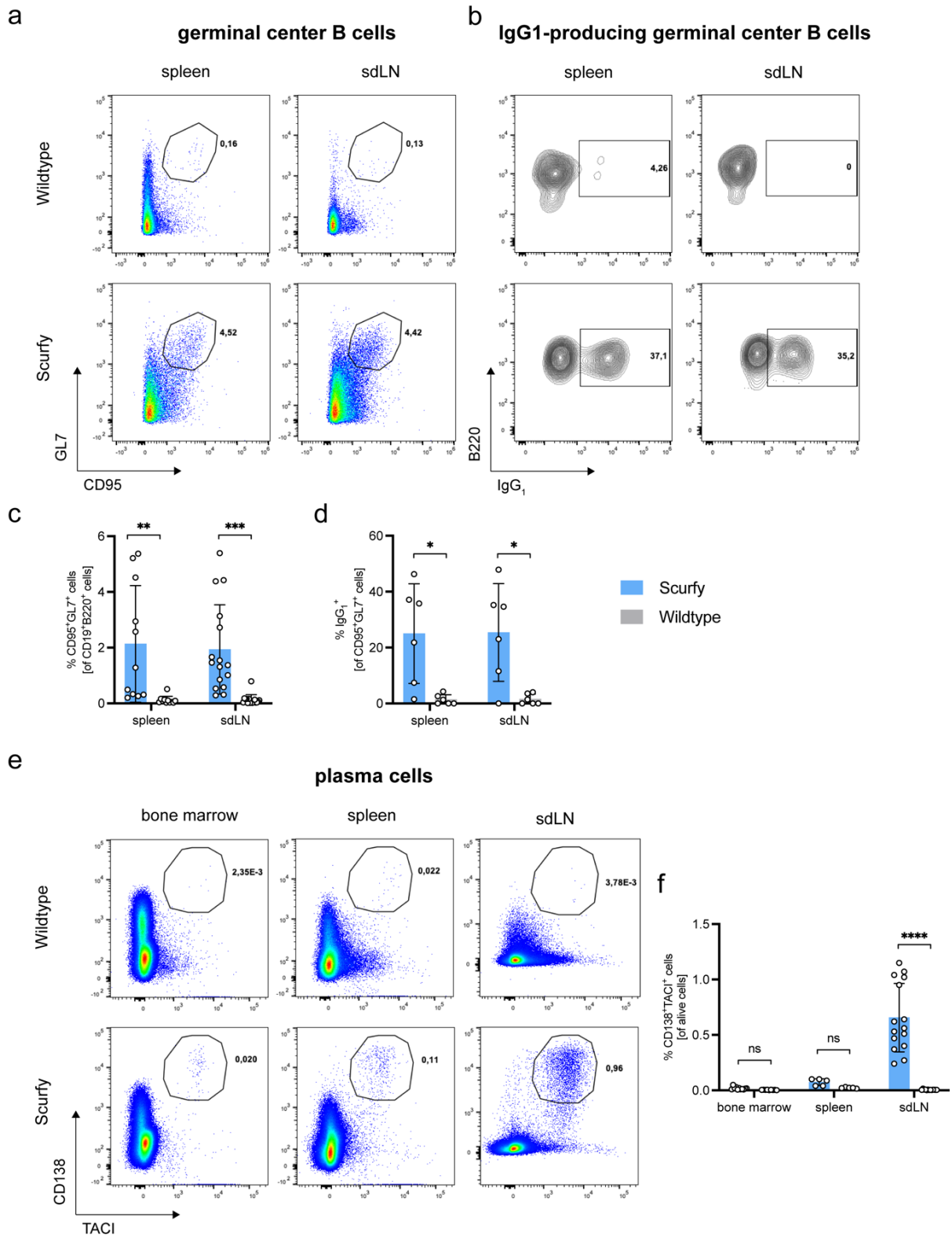


Figure 11. GC B cells and antibody-producing cells are frequently higher in scurvy mice. (a) Representative dot plots showing alive germinal center (GC) B cells (GL7⁺CD95⁺) gated on CD19⁺B220⁺ B cells in spleen and skin-draining lymph nodes (sdLN) of scurvy mice and WT littermates. (b) Representative contour plots show gating of IgG1-producing GC B cells (IgG1⁺B220⁺) gated on GL7⁺CD95⁺ GC B cells. (c) Quantification of GC B cells shown as percentage of GL7⁺CD95⁺ cells. (d) Quantification of IgG1-producing GC B cells shown as percentage of IgG1⁺B220⁺ cells. (e) Representative dot plots show gating of plasma cells (CD138⁺TAC1⁺) gated on alive lymphocytes. (f) Quantification of plasma cells shown as percentage of CD138⁺TAC1⁺ cells. Data presented as mean ± SD, one-way ANOVA followed by Bonferroni's multiple comparisons test was performed (*p<0.05, **p<0.01, ***p<0.001, ****p<0.0001, ns, not significant).

3.6 Inflamed skin of scurfy mice shows elevated levels of B cells

Skin pathology in scurfy mice lacking functional Treg was previously examined and showed thickening of the epidermis, immune infiltration in various parts of the skin, severe inflammation, and hyperkeratosis and erosions (Haerberle et al. 2017; Haerberle et al. 2018). Since scurfy mice develop autoimmune diseases leading to autoantibody induced skin blistering, ears were analyzed by FACS for B cell infiltration.

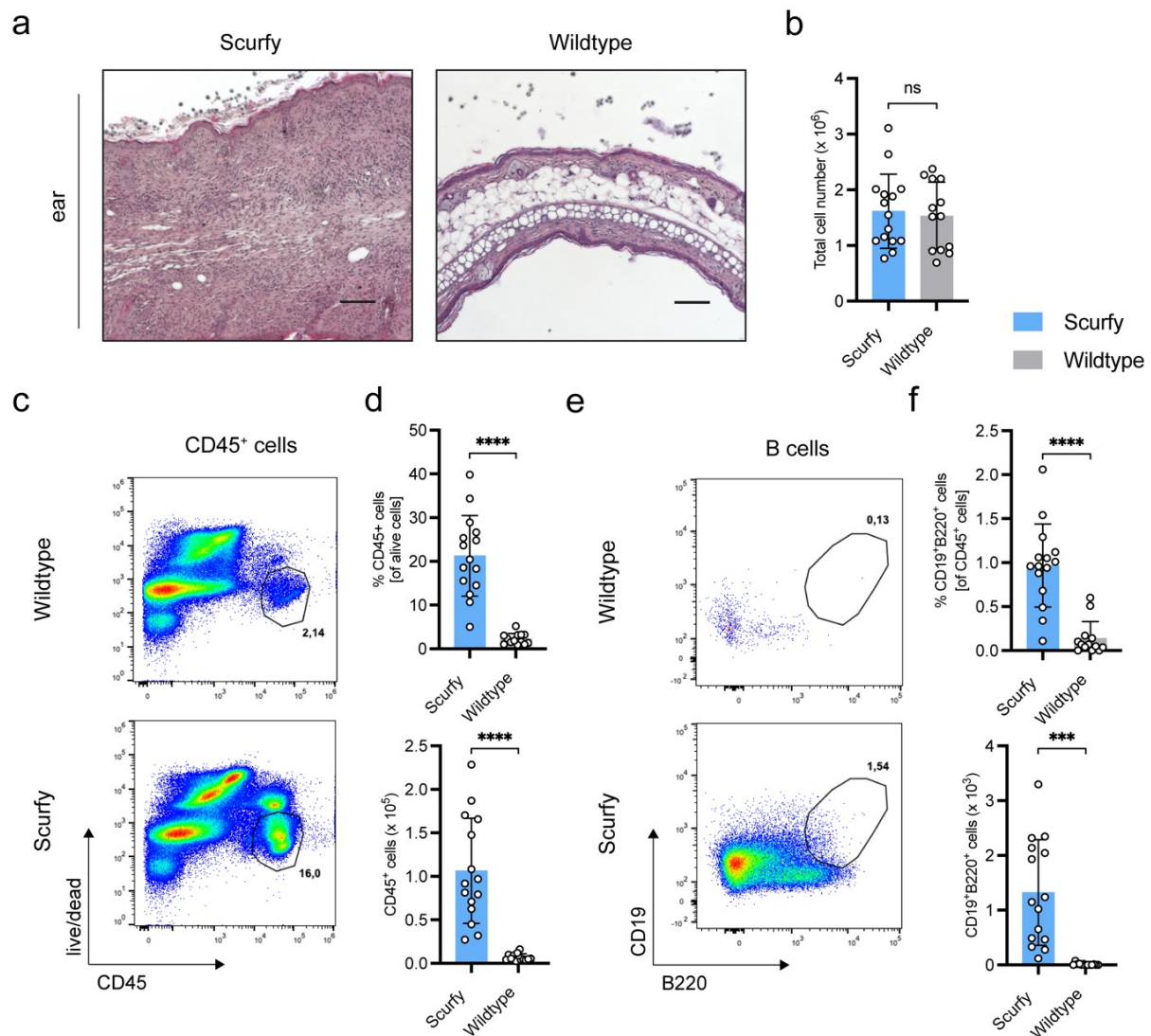


Figure 12. Scurfy mice show inflamed ear skin with B cells present in the tissue. (a) Representative H&E staining of ear of 18-day old scurfy and WT mice showing strong ear thickening and inflammation. Bar = 100 μ m. (b) Quantitative analysis of total cell numbers per two ears of 18-day old scurfy mice and WT littermates. (c) Representative dot plots show gating of alive CD45⁺ cells in skin immune infiltrate. (d) Quantification of alive CD45⁺ cells analyzed as percentage (upper plot) and total cell numbers per two ears (lower plot). (e) Representative dot plots indicate gating of CD19⁺B220⁺ B cells present in ear immune infiltrate. (f) Quantification of CD19⁺B220⁺ B cells gated on alive CD45⁺ cells as percentage (upper plot) and total cell numbers per two ears (lower plot). Data presented as mean \pm SD, two-tailed unpaired *t* test with Welch's correction was used (****p*<0.001, *****p*<0.0001, ns, not significant).

Performing H&E staining of the ears showed a strong thickening of the epidermis and an increased immune infiltrate in 18-day old scurfy mice compared to WT littermates (Figure 12 a). For FACS analysis, ears were digested with Liberase TL and DNase I to isolate the immune infiltrate for staining with surface antibodies. Initially, the total cell number from two ears per mouse was determined to show that cell extraction and measurement was successful. Quantitative analysis showed no significant differences in the total number of cells extracted from scurfy and WT mice (Figure 12 b). By performing FACS analysis of the ears, the lymphocyte infiltrate was examined by staining with anti-CD45 antibody. Representative dot plots showed gating of live CD45⁺ lymphocytes from scurfy and WT ears (Figure 12 c). Quantitative analysis revealed significantly higher frequencies of CD45⁺ cells in scurfy ears compared to WT ears (Figure 12 d). In line, the total number of CD45⁺ lymphocytes per two ears was significantly higher in scurfy mice (Figure 12 d). To evaluate B cells present in the tissue, FACS analysis of CD19⁺B220⁺ B cells in the ears was performed. Representative dot plots indicated gating of CD19⁺B220⁺ B cells gated on alive CD45⁺ lymphocytes from scurfy mice and WT littermates (Figure 12 e). The frequency of B cells in the ears of scurfy mice was significantly higher compared to WT mice (Figure 12 f). In addition, the total number of B cells per two ears was significantly elevated in sick scurfy mice (Figure 12 f).

3.7 Serum of scurfy mice contains B cell relevant inflammatory cytokines related to Th2 immune responses

Previously, skin-infiltrating CD4⁺ T cells of scurfy mice were found to secrete Th2-type inflammatory cytokines (Haeberle et al. 2017). Since B cells are highly contributive to autoimmune diseases in these mice (Aschermann et al. 2013), LEGENDplex assays were performed to characterize cytokines in the sera of these mice that are relevant for B cell development, function and activation. This multiplex assay allowed simultaneous quantification of 13 different cytokines followed by FACS analysis. Representative gating of beads by positive control is shown in Figure 13. Two populations of beads were gated following cytokine discrimination, with fluorescently labeled A Beads and B Beads showing separate populations in the histogram (Figure 13 a). After gating different cytokine populations and calculating data based on standard curves, quantitative analysis was performed. For IL-6, IL-12p70, IL-17A, TGF- β 1, sBCMA and sCD40L, no significant differences between scurfy and WT serum were observed (Figure 13 c, d, e, h, k, l). In contrast, significantly higher levels of IL-4, IL-2, TNF- α , IL-13, IFN- γ , IL-10 and BAFF were present in the serum of sick scurfy mice compared to WT littermates (Figure 13 b, f, g, i, j, m, n).

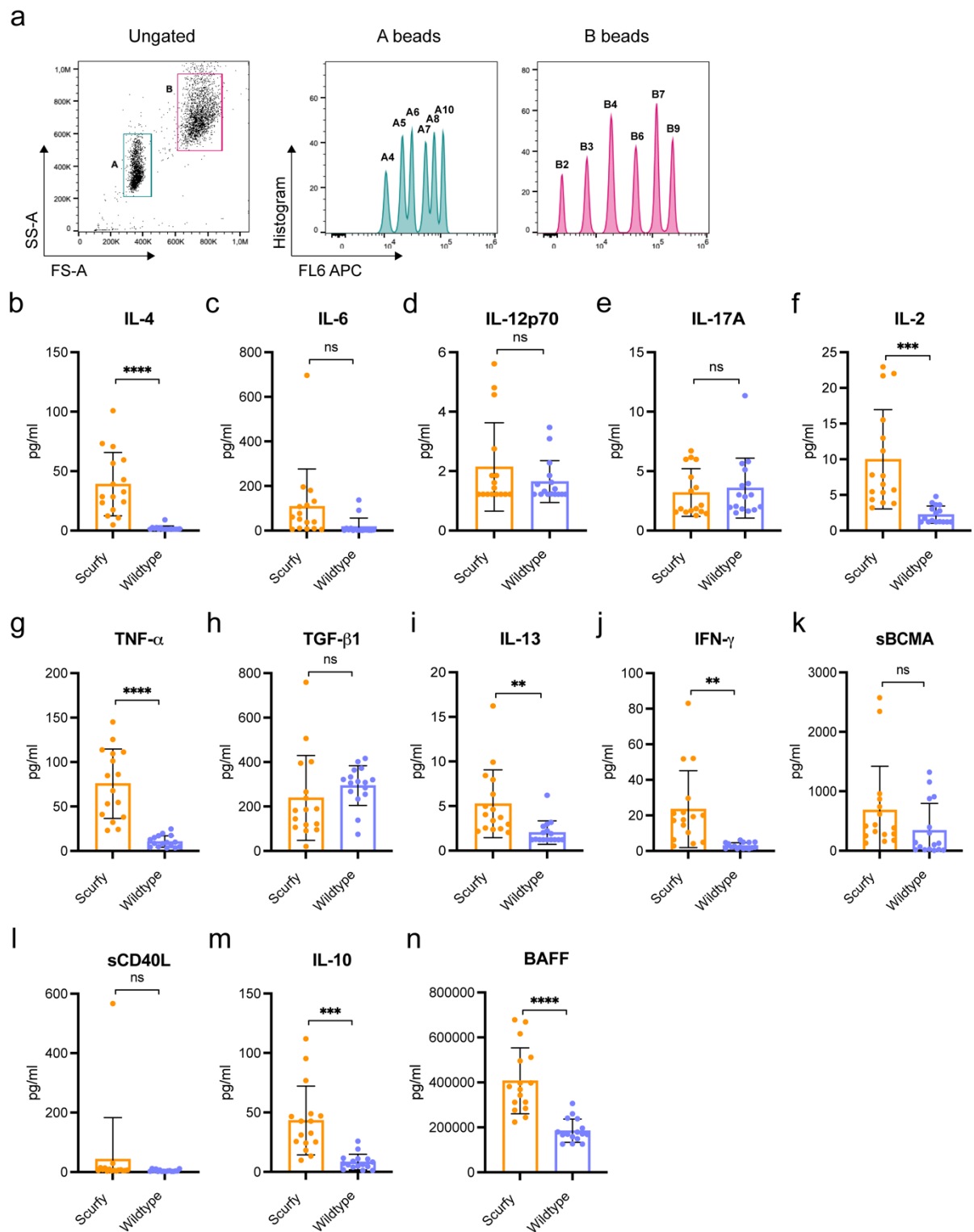


Figure 13. B cell-related inflammatory cytokines are present in serum of scurfy mice. (a) LEGENDplex assays were performed according to the manufacturer's protocol (Biolegend). Representative gating strategy of positive control (standard). Fluorescently labeled Beads A and Beads B were gated. Different bead populations were gated using histogram and APC plot. A Beads were separated in A4, A5, A6, A7, A8, A10 and B Beads in B2, B3, B4, B6, B7 and B9 to characterize the different cytokines according to the fluorescence signal. (b-n) Quantitative analysis of different B cells relevant cytokines in serum of 18-21-day old scurfy mice and WT littermates. Data presented as mean \pm SD, two-tailed unpaired *t* test with Welch's correction was used (** $p < 0.01$, *** $p < 0.001$, **** $p < 0.0001$, ns, not significant).

3.8 Scurfy mice develop AIBD-related antigen-specific B cells

Scurfy mice produce high titers of autoantibodies due to their lack of regulatory mechanisms (Figure 1). Haeberle et al. recently demonstrated that scurfy mice have autoantibodies present in their serum that are specific against known AIBD antigens. Performing IIF microscopy of serum from scurfy mice and WT littermates, linear staining along the BMZ became visible with scurfy serum (Vicari 2019, Master thesis).

To further elucidate the pathological mechanisms leading to BMZ-specific autoantibodies, ELISpot assays were used to identify antigen-specific B cells in the spleen and sdLN of 18-day old scurfy mice and WT littermates. B cells were isolated from scurfy and WT spleens. 200.000 cells per well of total splenocytes (spleen), isolated B cells (B cells), cells remaining after isolation (non-B cells) and total sdLN cells were collected for ELISpot assay. Antigen specificity was tested on murine vWFA2 protein, Laminin α 3 and BP180 c-terminal protein, which are relevant to human forms of AIBD. After spot detection, plates were analyzed on a dedicated ELISpot reader, quality control was performed and data were quantitatively analyzed. Representative images of an ELISpot assay with murine vWFA2 protein, Laminin α 3 and BP180 c-terminal protein showed positive spots for spleen, B cells and sdLN of scurfy mice in contrast to non-B cells and WT mice where almost no spots were detectable (Figure 14 a, c, e). Quantitative analysis revealed significantly more spots in the spleen compared to non-B cells of the spleen and WT spleen for all AIBD antigens (Figure 14 b, d, f). In addition, significantly more spots were detected in the sdLN of scurfy mice compared to WT mice for all AIBD antigens (Figure 14 b, d, f).

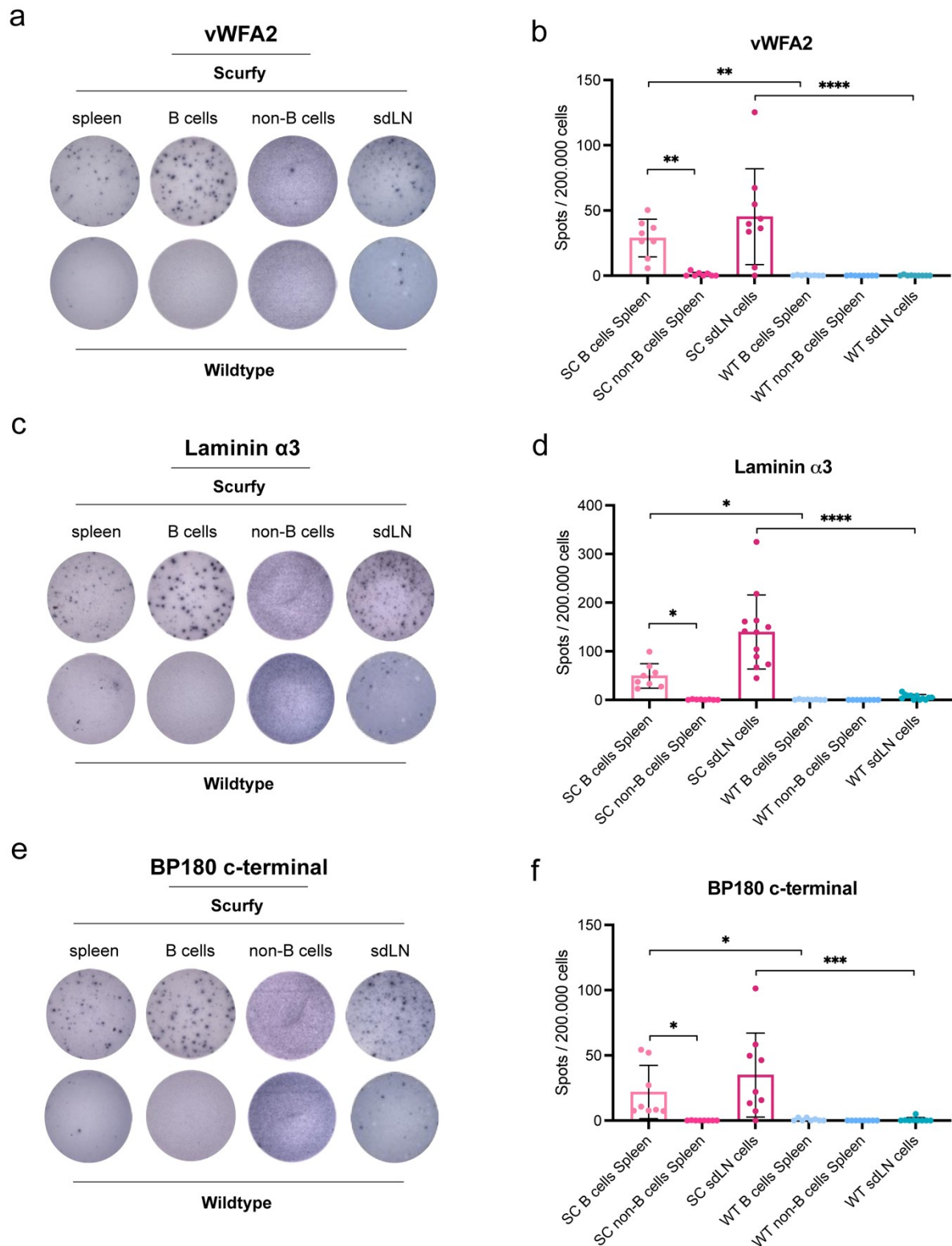


Figure 14. Treg deficiency in scurfy mice leads to AIBD-related antigen-specific B cells in spleen and sdLN. (a) Representative pictures of Enzyme linked immunospot (ELISpot) assay on vWFA2 protein with different cell populations of 18-day old scurfy mice and WT littermates. (b) Quantitative analysis of ELISpot assay with vWFA2. (c) Representative images of ELISpot assay on Laminin α 3 protein with different cell populations of 18-day old scurfy mice and WT littermates. (d) Quantitative analysis of ELISpot assay with Laminin α 3. (e) Representative pictures of ELISpot assay on BP180 c-terminal protein with different cell populations of 18-day old scurfy mice and WT littermates. (f) Quantitative analysis of ELISpot assay with BP180 c-terminal. Data presented as mean \pm SD, one-way ANOVA followed by Bonferroni's multiple comparisons test was performed (* p <0.05, ** p <0.01, *** p <0.001, **** p <0.0001).

3.9 Isolated scurfy autoantibody H510 targets antigen expressed in lower BMZ

To gain further insight into the disease mechanisms leading to AIBD through loss of Treg function, spontaneously developed autoantibodies in scurfy mice were investigated. Splenocytes from sick scurfy mice were harvested and fused with myeloma cells to generate antibody-producing hybridoma cells (Haeberle et al. 2018). After positive selection, the murine monoclonal antibody (mAb) H510 was isolated. The following experiments were performed with purified mAb H510, which was generated and purified by an external company (Absolute Antibody, UK).

IIF microscopy was performed on WT salt-split skin to further characterize the binding capacity of mAb H510 and the localization of the target antigen in the skin. Salt-split assay with H510 could previously show linear staining along the dermal side of the BMZ in WT skin (Vicari 2019, Master thesis). Due to binding of H510 to WT skin and palate (Vicari 2019, Master thesis), next, the binding capacity of H510 was tested on several different WT organs including other organs with stratified epithelia by IIF microscopy, which indicated a specific linear staining pattern along the BMZ on esophagus but not on other organs as the stomach (Table 1, Figure 15).

Table 1. Indirect immunofluorescence with H510 on different tissues.
(Table was modified published in Vicari et al. 2021)

WT tissue	IIF with H510
skin	+
eye	-
palate	+
esophagus	+
stomach	-
duodenum	-
small intestine	-
colon	-
liver	-
lung	-
kidney	-
bladder	-

Abbreviations: IIF, indirect immunofluorescence; WT, wildtype

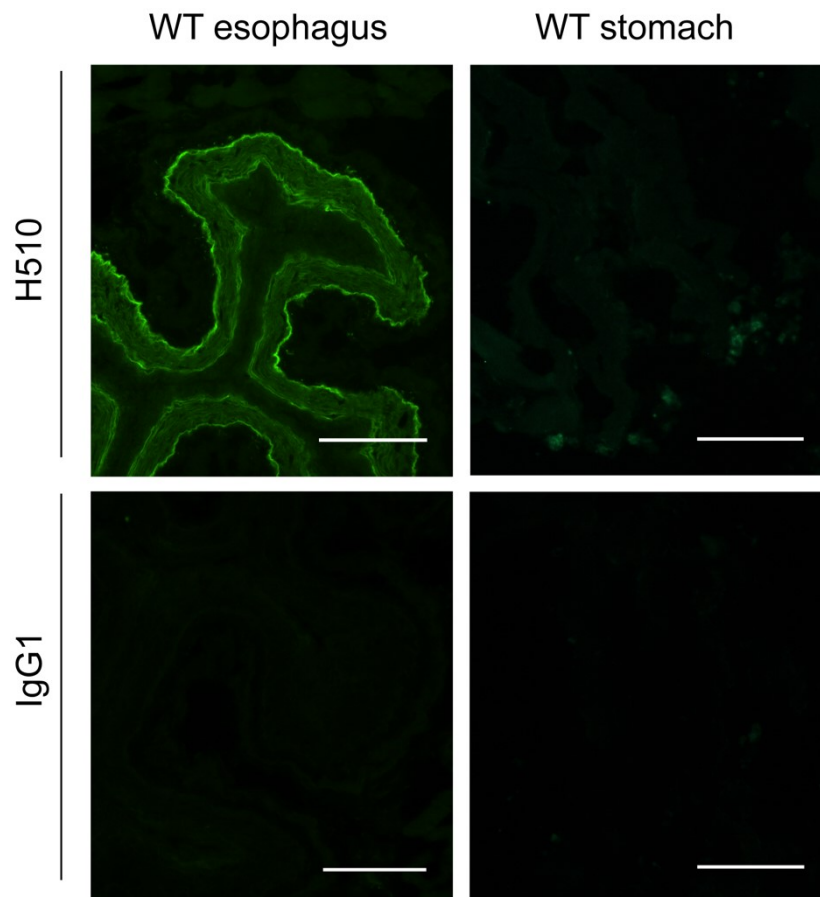


Figure 15. mAb H510 targets antigen along dermal-epidermal junction. Representative IIF staining on WT esophagus and stomach with mAb H510 (upper panel) and comparable IIF staining with control IgG1 (lower panel). Bar = 100 μ m (left panel is shown as published in Vicari et al. 2021).

Due to the skin specificity of mAb H510 in IIF, the expression of the target antigen in keratinocytes and fibroblasts was investigated. Primary murine keratinocytes were isolated from WT neonatal skin and cultured for one week before use. Primary murine fibroblasts were isolated from WT ears and also cultured for one week. The purity of both cell types was checked by expression of the marker K14 for keratinocytes and vimentin for fibroblasts. Representative dot plots showed gating of keratinocytes and fibroblasts with K14⁺ and vimentin⁺ cells pre-gated on alive cells (Figure 16 a). Quantitative analysis revealed positive K14 staining on murine keratinocytes and positive vimentin staining on fibroblasts (Figure 16 b, c). Additionally, western blot analysis was performed on lysed keratinocytes and fibroblasts showing positive signal for K14 on keratinocytes and positive signal for vimentin on fibroblasts (Figure 16 d). Using IIF microscopy, it could be already demonstrated that the mAb displayed an intracellular binding pattern in murine keratinocytes but not in fibroblasts (Vicari 2019, Master thesis). To further study the specific expression of the antigen only in keratinocytes, both cell types were fixed and permeabilized for IIF co-staining with cell specific markers. Cells

were stained with mAb H510 or control IgG1 and anti-K14 and anti-Vimentin antibodies (Figure 17). Co-staining of murine keratinocytes revealed positive co-staining with K14 and H510 (Figure 17 a). In contrast, co-staining on murine fibroblasts showed positive staining for vimentin but no signal with mAb H510 (Figure 17 b).

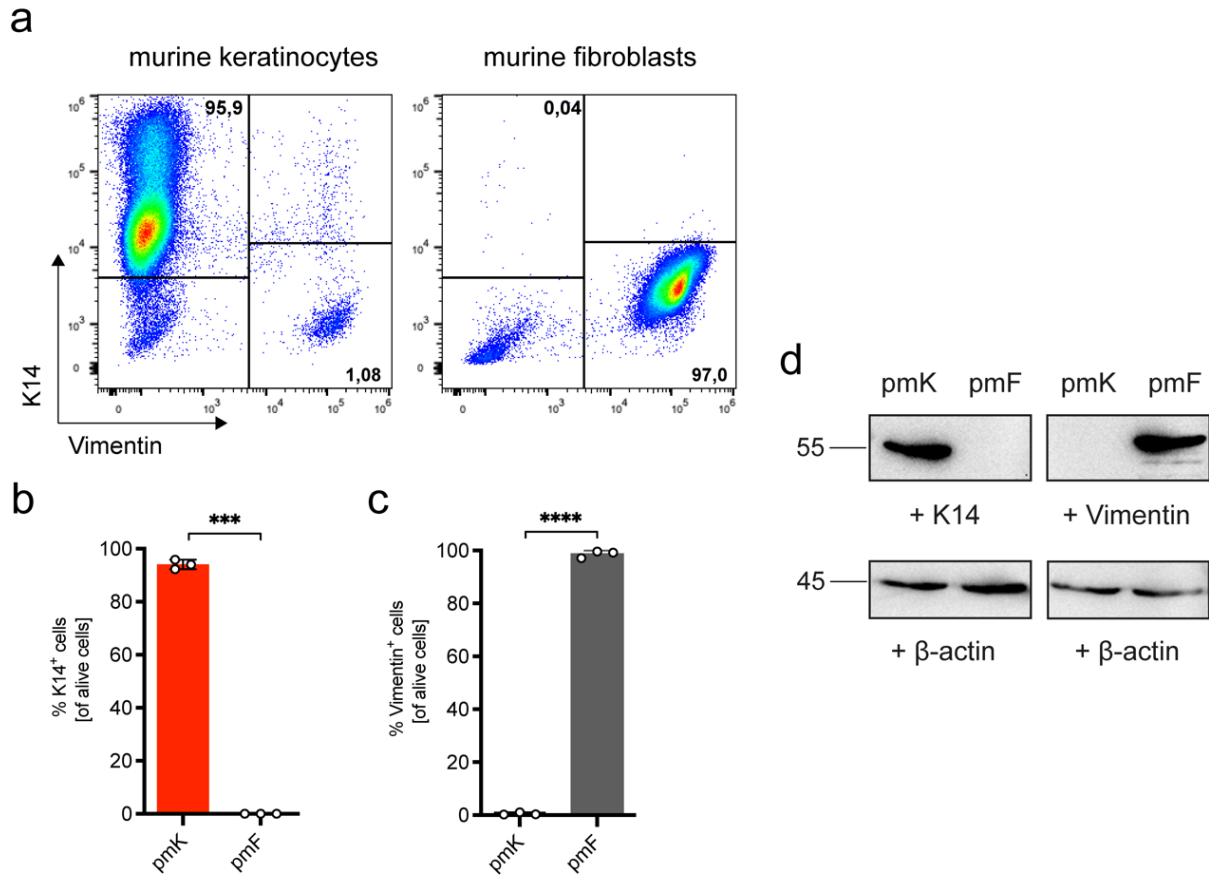


Figure 16. Isolated primary murine keratinocytes and fibroblasts are highly purified. (a) Representative dot plots of isolated primary murine keratinocytes (pmK) and primary murine fibroblasts (pmF) showed gating of K14⁺ cells and vimentin⁺ cells gated on alive cells. (b) Quantitative analysis of pmK and pmF after one week of culture shown as percentage of K14⁺ cells gated on alive cells. (c) Quantitative analysis of pmK and pmF after one week of culture shown as percentage of vimentin⁺ cells gated on alive cells. (d) Western blots on lysed pmK and pmF with anti-K14 antibody and anti-vimentin antibody. β-actin was used as control for total loaded protein. Data presented as mean ± SD, two-tailed unpaired *t* test with Welch's correction was used (***p*<0.001, *****p*<0.0001).

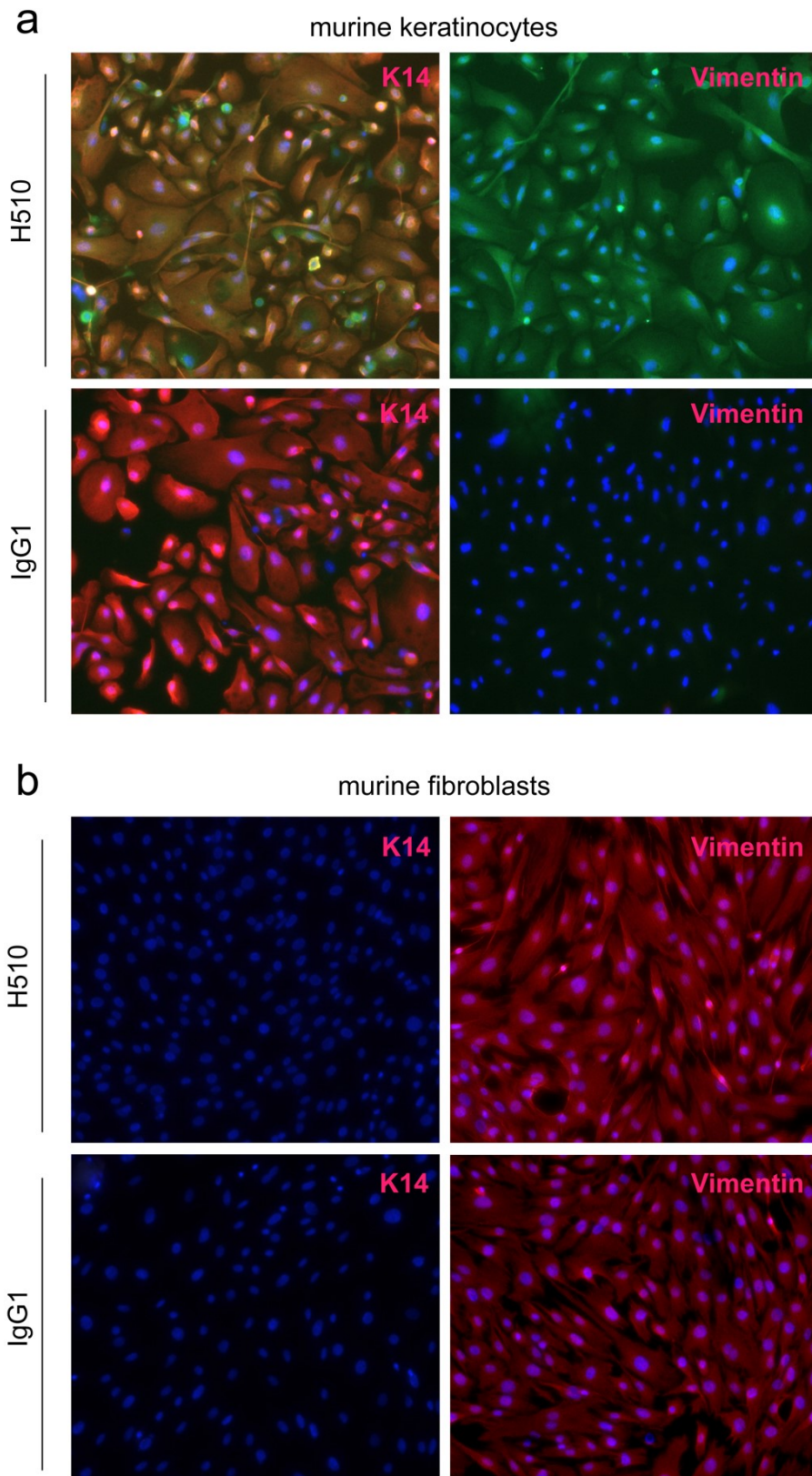


Figure 17. Binding pattern of mAb H510 is co-localized with K14 in murine keratinocytes. (a) IIF staining on fixed and permeabilized primary murine keratinocytes after one week of culture. Co-staining was performed with mAb H510 (green) or control IgG1 (green) and anti-K14 (red) or anti-Vimentin (red) antibody showing positive co-staining (yellow) with H510 and anti-K14. (b) IIF staining on fixed and permeabilized primary murine fibroblasts after one week of culture. Co-staining was performed with mAb H510 (green) or control IgG1 (green) and anti-K14 (red) and anti-Vimentin (red) antibody showing no co-staining with H510 and anti-Vimentin. Bar = 100 μ m.

3.10 Pathogenic autoantibody H510 targets murine vWFA2 of Col7

We could previously prove that mAb H510 is pathogenic: Intradermal injection of mAb H510 into WT neonatal mice revealed subepidermal blister formation in the skin specifically induced by this autoantibody (Vicari 2019, Master thesis). Based on the binding of mAb H510 to the dermal side of the BMZ, Col7, which is located dermally and is the known antigen in the human disease EBA, was considered as a possible antigen. As a first approach, a peptide competition assay was performed to test whether H510 binds to murine Col7. H510, anti-vWFA2 as a positive control and control IgG1 as a negative control were incubated with murine vWFA2 protein and then used for IIF (Figure 18 a). IIF microscopy with antibodies alone showed linear staining for anti-vWFA2 and H510 (Figure 18 b, upper panel). After incubation with murine vWFA2 protein, no linear staining for anti-vWFA2 and H510 was detected (Figure 18 b, lower panel). Quantitative analysis of peptide competition staining revealed a significantly lower binding capacity of both antibodies to murine skin after incubation with vWFA2 (Figure 18 c).

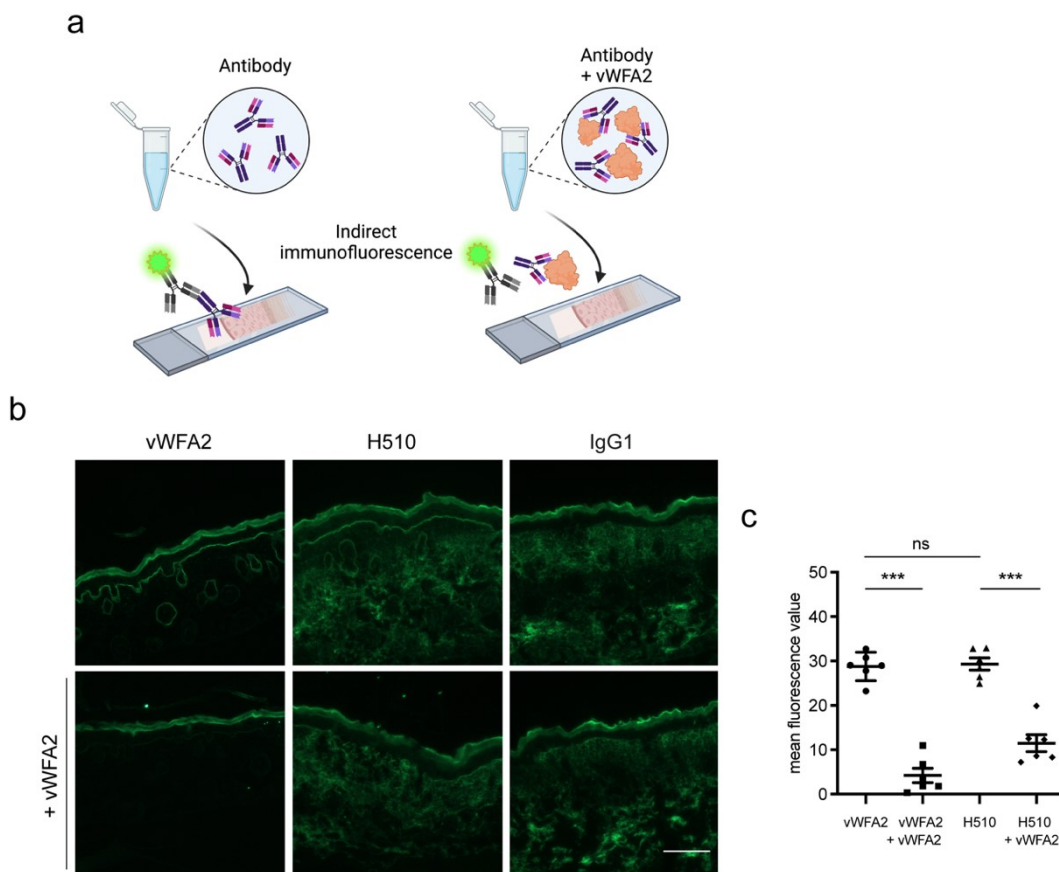


Figure 18. Binding of H510 was blocked after incubation with vWFA2 protein. (a) Schematic illustration of peptide competition assay. Antibody was incubated with murine vWFA2 protein and used for IIF microscopy (created with BioRender). (b) IIF staining with anti-vWFA2, and H510 on WT neonatal skin (upper panel) showed linear staining. IIF staining with anti-vWFA2 and H510 after incubation with vWFA2 protein (lower panel) showed inhibited binding. Bar = 100 μ m. (c) Quantitative analysis of fluorescence intensity in IIF displayed as mean fluorescence value before and after peptide competition. Data presented as mean \pm SD, two-tailed unpaired *t* test with Welch's correction was used (***p* < 0.001, ns, not significant) (Figures b and c are shown as published in Vicari et al. 2021).

To verify that mAb H510 binds to murine Col7 in the skin, skin from Col7 knock-out (Col7^{-/-}) mice was used. First, IIF microscopy was performed to further characterize the specific binding in skin. In addition to skin from Col7^{-/-} mice, skin from WT mice was used as a positive control for IIF with mAb H510, anti-mouse IgG1 (mIgG1), anti-vWFA2, and anti-rabbit IgG1 (rIgG1). IIF on WT skin showed linear staining along the DEJ for H510 and anti-vWFA2 (Figure 19 a, upper panel). In contrast, no staining along the DEJ was detected on Col7^{-/-} skin with H510 and anti-vWFA2 (Figure 19 a, lower panel). Western blot analysis was used to confirm this at the protein level. Skin lysate from WT and Col7^{-/-} mice was taken and western blots were analyzed with H510, anti-vWFA2 and control IgG1. A positive band was detected for WT skin with H510 and anti-vWFA2, but not in Col7^{-/-} skin lysate (Figure 19 b).

Col7 is a large structural protein of the skin which consists of a non-collagenous domain 1 (NC1) including vWFA2, an NC2 domain and a triple-helical domain (THD) (Figure 19 c). To further specify which part of Col7 is specifically targeted by mAb H510, HEK293T cells were transfected. After successful expression of murine NC1, NC2 and THD in HEK293T cells, the cells were lysed and used for western blot analysis. An anti-His-tag antibody was used to prove the expression of the three different domains targeted by a histidine-tag (Figure 19 c). Western blot analysis using H510 and anti-vWFA2 yielded a distinct band at 138 kDa for NC1 domain and not for NC2 or THD (Figure 19 c). In addition, western blot analysis of vWFA2 protein with H510 and anti-vWFA2 showed a positive signal at 21 kDa (Figure 19 d). For additional verification, ELISA was performed with vWFA2 protein and Laminin γ 1 protein as a negative control. H510 showed significantly higher binding to vWFA2 protein in the ELISA (Figure 19 e).

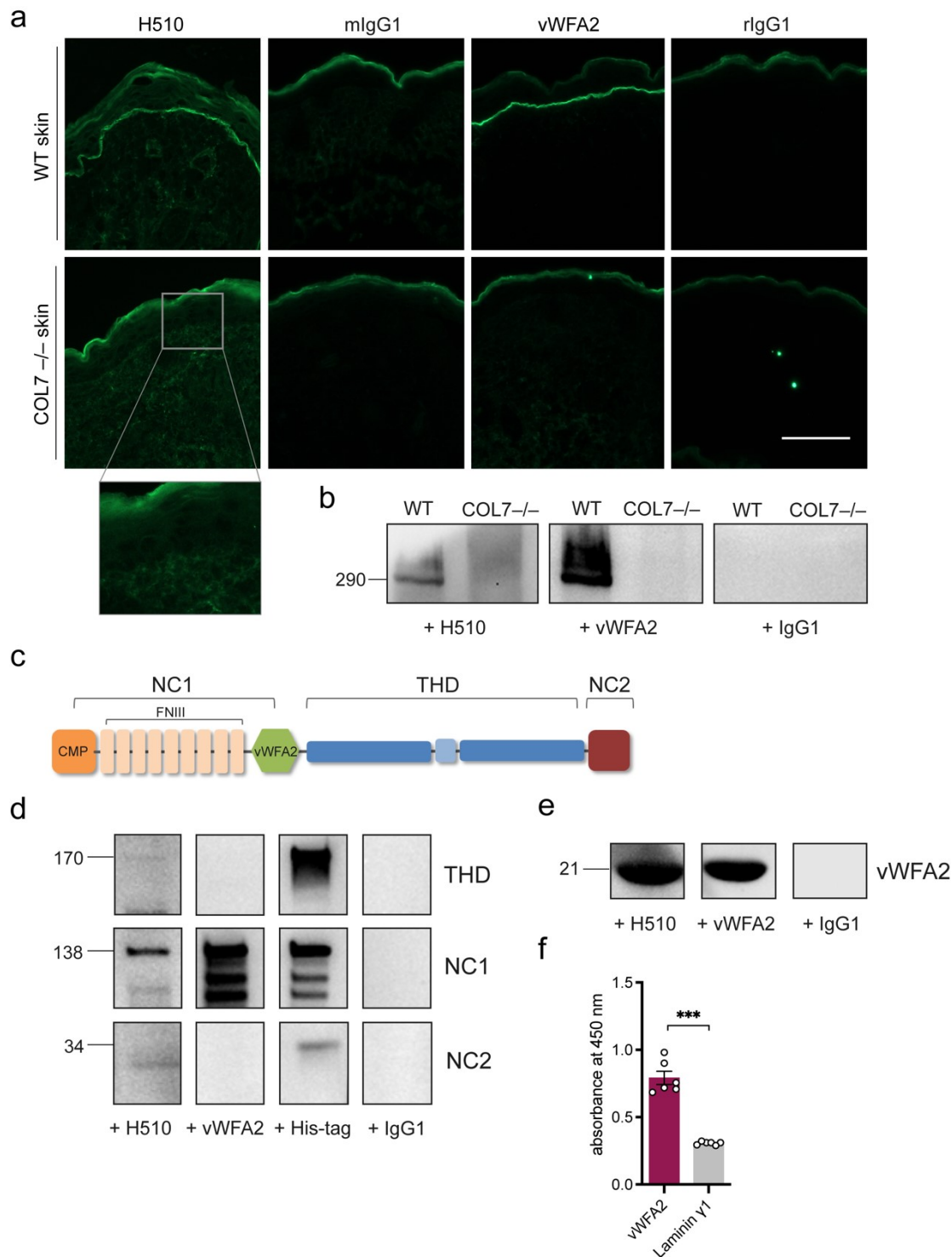


Figure 19. mAb H510 recognizes murine vWFA2 of Col7. (a) IIF staining on WT skin (upper panel) and Col7 knock-out (-/-) skin with mAb H510, anti-vWFA2, control mouse IgG1 (mlgG1) and rabbit IgG1 (rlgG1). Linear staining of H510 and anti-vWFA2 was not visible in Col7^{-/-} skin. Bar = 100 μm. (b) Western blot analysis with lysate of WT skin and Col7^{-/-} with H510, anti-vWFA2 and control IgG1. (c) Schematic illustration of α-chain of Col7 (NC1/2, Non-collagenous domain 1/2; FNIII(1-9), fibronectin-like domains; THD, triple-helical domain; CMP, cartilage-matrix-protein-like domain; vWFA2, von-Willebrand-Factor-A-like domain 2). (d) Western blot analysis on HEK293T cells expressing murine THD, NC1 and NC2. (e) Western blot analysis with murine vWFA2 protein. (f) ELISA with mAb H510 on murine vWFA2 and Laminin γ1 protein as negative control. Data presented as mean ± SD, two-tailed unpaired *t* test with Welch's correction was used (***p*<0.001) (Figures a-e are shown as published in Vicari et al. 2021).

3.11 Pathologic mechanism of H510 is independent of inflammatory immune cells

To investigate how the autoantibody H510 is able to induce a pathogenic blister formation in WT neonatal mice by targeting the murine vWFA2 of Col7, the contribution of the complement system was analyzed. Complement activation is known to be involved in the pathological mechanism leading to the disease EBA in humans (Koga et al. 2018; Mihai et al. 2018). Considering complement activation by the autoantibody H510, DIF microscopy of skin samples from H510-injected mice was performed. Anti-mouse complement 3 antibody (anti-C3) was used to detect complement deposition along the DEJ (Figure 20). Compared to DIF staining with anti-mouse IgG1 antibody to detect H510 in the skin, no linear fluorescence could be detected for C3 staining in representative sections (Figure 20 a). Summary of all experiments performed showed deposition of H510 along the DEJ in six out of eight injected mice, but no C3 deposition was visible (Figure 20 b).

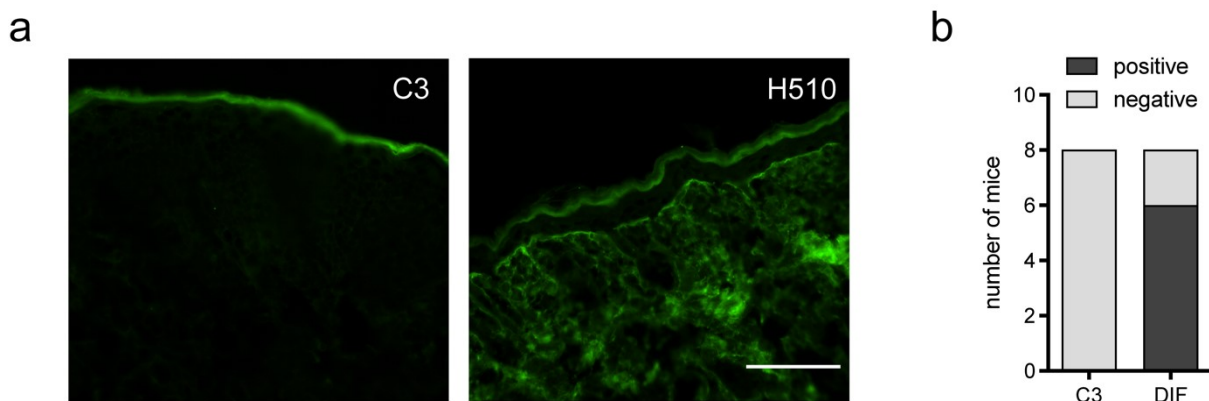


Figure 20. Complement 3 is not present along the DEJ after H510 injection. (a) Direct immunofluorescence (DIF) of WT neonatal skin after injection of H510 with murine anti-C3 antibody (left) and anti-IgG1 antibody (right) showed no linear staining for C3 staining but linear staining of IgG1. (b) Summary of C3 staining and DIF of neonatal WT mice injected with mAb H510. (Figure is shown as published in a modified version in Vicari et al. 2021).

Considering the pro-inflammatory form of EBA, leukocyte extravasation occurs and FcγR are activated by anti-Col7 antibodies resulting in tissue damage (Koga et al. 2018). To get further insights into the mechanism of blister formation by H510 and whether immune cells are involved, neonatal FcγR knock-out (FcγR^{-/-}) mice were injected with H510 or the corresponding control IgG1 (Figure 21 a). After 48 h, mice were sacrificed and the skin was collected and embedded in paraffin (Figure 21 a). To examine the skin for blister formation, H&E staining was performed on paw skin sections and back skin sections. Subepidermal blistering was observed in the paw skin of FcγR^{-/-} mice injected with H510 but not with control IgG1 (Figure 21 b). In summary, subepidermal split formation was found in the skin of the majority of H510-injected mice (Figure 21 c). Furthermore, linear deposition of H510 along the

DEJ in the skin of injected FcγR^{-/-} mice was detected by DIF microscopy (Figure 21 d). All mice injected with H510 showed linear staining along the DEJ by DIF microscopy, in contrast to control IgG1-injected mice (Figure 21 e).

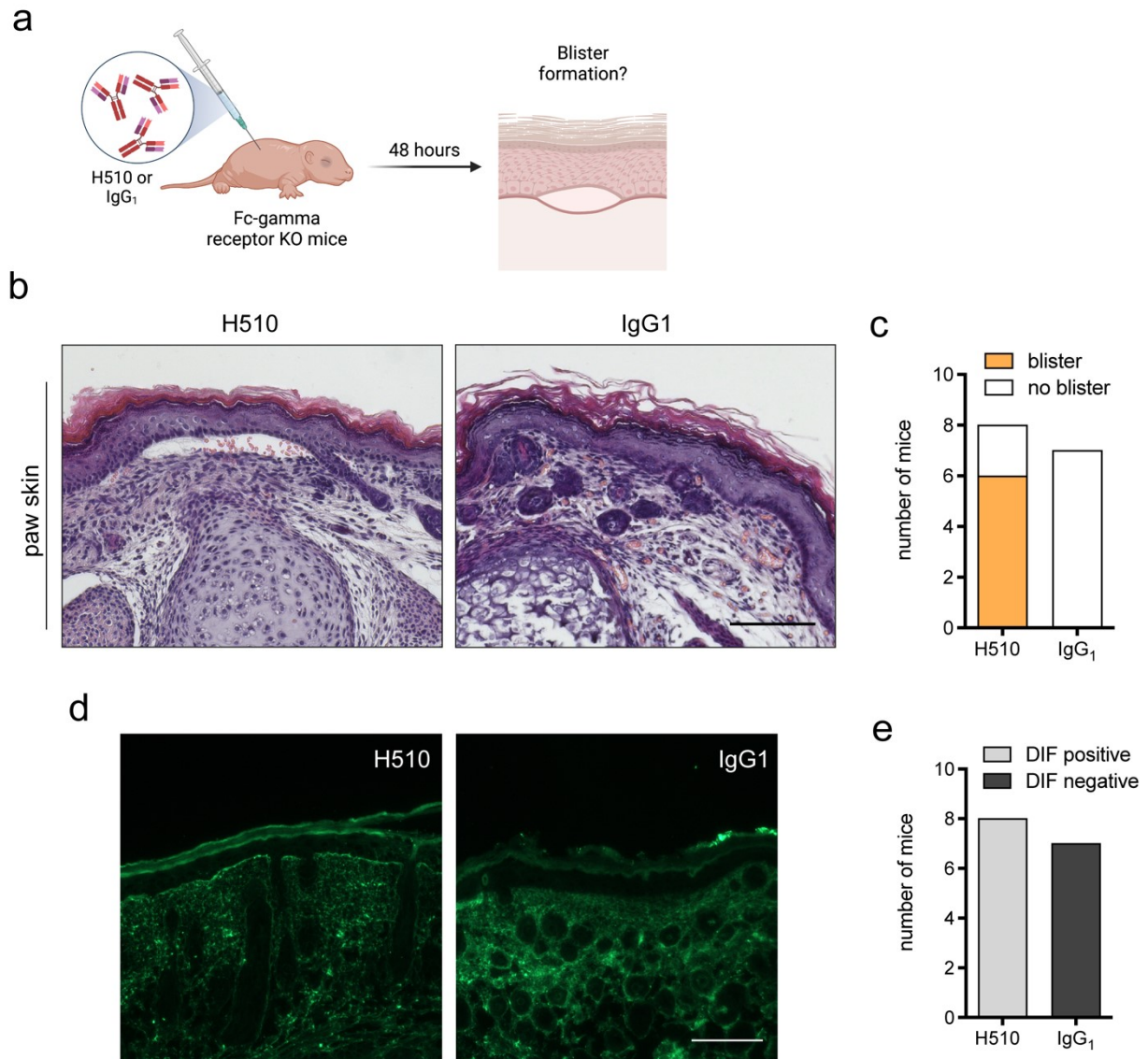


Figure 21. H510 induces subepidermal blisters independently from immune cells. (a) Schematic overview of experimental setup. Subcutaneous injection of mAb H510 or murine control IgG1 in neonatal Fcγ-receptor knock-out mice (FcγR^{-/-}) mice. After 48 h, mice were sacrificed, skin was taken and embedded in paraffin (created with BioRender). (b) Histology of paw skin of injected FcγR^{-/-} neonatal mice showed subepidermal blister formation. (c) Summary of blister formation in skin of FcγR^{-/-} neonatal mice which were injected with mAb H510 or control IgG1 showed blister in 6 of 8 H510-injected mice. (d) Direct immunofluorescence (DIF) of back skin of injected FcγR^{-/-} neonatal mice revealed linear staining along dermal-epidermal junction. (e) Summary of DIF analysis showed linear staining in 8 of 8 H510-injected mice. Bar = 100 μm.

4 DISCUSSION

4.1 Treg deficiency leads to altered B cell compartment in scurfy mice

Scurfy mice develop several autoimmune diseases due to their dysfunction in Treg resulting in an expansion of autoreactive CD4⁺ T cells (Figure 1). These potent spontaneous autoimmune responses result in high numbers of immune cells circulating in lymphoid organs and causing tissue inflammation. Scurfy mice show severe enlargement of the spleen and lymph nodes, resembling autoimmune responses in secondary lymphoid organs.

Treg deficiency in scurfy mice leads to high titers of autoantibodies and the development of AIBD (Hadaschik et al. 2015; Haeberle et al. 2018; Muramatsu et al. 2018). Therefore, the contribution of B cells getting activated by autoreactive CD4⁺ T cells and their production of autoantibodies was further investigated. FACS analysis was performed to screen for B cell subsets in 18-21-day old scurfy mice at different developmental stages in BM, spleen and sdLN. Scurfy mice developed higher frequencies of innate B1 B cells in the sdLN compared to WT littermates. B1 B cells have been shown to rapidly respond to non-specific inflammatory stimuli by migrating to secondary lymphoid tissues and differentiating into antibody-producing cells (Morris et al. 2019). Additionally, a potential pathogenic role of B1 B cells in autoimmune diseases such as SLE or multiple sclerosis has recently been described (Morris et al. 2019) suggesting a possible contribution to disease progression in scurfy mice.

Compared to WT littermates, fewer B2 B cells were found in the BM and spleen of sick scurfy mice. Consistent with previous studies, Treg deficiency in scurfy mice results in impaired B cell development in BM and spleen (Riewaldt et al. 2012), whereas B2 B cell frequencies in sdLN were comparable to WT mice. Further analysis of B cell maturation revealed no differences in the frequencies of mature or transitional B cells in BM and spleen between scurfy and WT mice. In contrast, analysis of the sdLN revealed a lower percentage of mature B cell populations in scurfy mice compared to WT littermates. Several studies described defective B cell development in scurfy mice, while others indicated residual B lymphopoietic activity at least in the BM (Leonardo et al. 2010; Riewaldt et al. 2012) consistent with these data. These discrepancies within early B cell lymphopoiesis could be due to differences in the microbiome of scurfy mice and variations in the kinetics of spontaneously developed autoimmune disease (Riewaldt et al. 2012).

Within the secondary lymphoid organs, follicular aggregates of B cells are visible, which in healthy conditions are present as primary lymphoid follicles with quiescent B cells (Matsuno et al. 2010). After challenge with antigen, GC with surrounding mantle zone form secondary lymphoid follicles (Matsuno et al. 2010). Histology of the sdLN and spleen of scurfy mice showed increased follicle formation, indicating ongoing immune and GC responses. Surprisingly, follicular B cell populations in spleen and sdLN of scurfy mice were not altered compared to WT littermates. Histology of the spleen of scurfy mice revealed altered MZ structures in contrast to the visible MZ surrounding follicles in WT mice. Consistent with this, FACS analysis indicated significantly decreased levels of MZ B cells in both spleen and sdLN of scurfy mice. Innate-like MZ B cells are known to be activated T cell-independently following antibody production and expansion of these cells has been demonstrated in several autoimmune mouse models (Hoffman et al. 2016; Palm and Kleinau 2021). However, the impaired MZ B cell compartment in scurfy mice may indicate that at this stage of disease severity, pathogenic autoantibodies are already produced and MZ B cell function is no longer essential for disease progression (Palm et al. 2016; Wither et al. 2000).

Within GC reactions, Tfh cells interact with B cells resulting in B cell proliferation and differentiation into memory B cells or antibody-producing plasma cells (Shlomchik and Weisel 2012). Similar to the elevated secondary follicle formation in scurfy mice, significantly higher levels of GC B cells were found in the sdLN and spleen in line with the increased number of autoreactive T cell populations that develop as a result of Treg defect. In addition, FACS analysis revealed that GC B cells of scurfy mice produce elevated levels of IgG1 antibodies explaining the increased autoantibody titers present in scurfy mice attacking structures as skin proteins, DNA or platelets (Aschermann et al. 2013; Huter et al. 2010; Yilmaz et al. 2019). Furthermore, scurfy mice showed higher frequencies of memory B cells in the BM and spleen and elevated levels of plasma cells in the sdLN compared to their WT littermates. Due to antigen-mediated crosslinking of IgG on membranes, memory B cells have been shown to have a lower threshold for activation, resulting in fast differentiation into antibody-secreting plasma cells (Deenick et al. 2013; Vitetta et al. 1991). Besides, memory B cells resemble strong APCs comparable to DCs, which appears to be important for chronic phases of autoimmune responses (Hofmann et al. 2018). These results suggest that scurfy mice have increased levels of memory B cell in the BM and spleen that differentiate into plasma cells that reside the sdLN and produce skin-specific autoantibodies, leading to autoimmune skin disease.

Cytokine secretion plays a major role in B cell-mediated autoimmune diseases. As Treg deficiency in scurfy mice leads to Th2-driven immune responses in the skin (Haeberle et al. 2017), the contribution of cytokines to B cell development, activation and survival was further investigated using multiplex FACS analysis of scurfy and WT serum. In conclusion, the

expansion of cytokines produced by Th2-primed Be-2 cells was confirmed, showing higher levels of IL-4, IL-2, IL-13 and TNF- α in the serum of scurfy mice. In particular, IL-4 and IL-6 play important roles in B cell proliferation and survival (Rush and Hodgkin 2001; Van Snick 1990), explaining the elevated levels of autoreactive memory B cells or plasma cells promoting AIBD in scurfy mice. In addition, IFN- γ levels were highly increased in scurfy mice enhancing inflammatory responses. Although IFN- γ produced by Th1-primed cells has been shown to inhibit B cell responses and IgG1 secretion, this mechanism does not affect resting B cells (Abed et al. 1994; Bradley et al. 1996; Kawano et al. 1994). The large increase of BAFF levels in scurfy serum enhances B cell overactivation, which has been reported to be involved in autoimmune diseases and essential for autoantibody production (Darce et al. 2007; Groom et al. 2007), indicating the importance of B cells for disease progression in scurfy mice. Unexpectedly, IL-10 levels were significantly higher in scurfy serum. Breg have been reported to produce IL-10 for regulation of inflammation and reduction of autoimmunity (Rosser et al. 2014) by conversion of CD4⁺ T cells into Treg (Chen et al. 2003). Since scurfy mice suffer from *Foxp3* mutation and therefore lack functional Treg, IL-10 production by B cells could be a potential counter-regulatory mechanism to try to dampen the strong autoimmune reactions. Increased Breg levels have been investigated in BP patients (Maglie et al. 2023). However, it has been reported that Breg have inflammatory capabilities rather than regulatory functions due to the secretion of IFN- γ , IL-4 and TNF- α instead of expected IL-10 production (Liu et al. 2018). Further analysis of Breg in scurfy mice would be interesting to characterize the onset of AIBD and possible regulatory mechanisms replacing missing Treg control.

Consistent with the results in scurfy serum, BAFF levels were also shown to be upregulated in BP patients (Asashima et al. 2006; Qian et al. 2014), confirming the development of AIBD in this mouse model and the similarity of disease mechanisms important for future studies.

Further analysis of the skin pathology that develops due to Treg deficiency revealed that scurfy mice suffer from strong inflammation, immune cell infiltration, erosions, and skin blistering (Haeberle et al. 2017; Haeberle et al. 2018). FACS analysis indicated the presence of B cells in the skin of scurfy mice. Skin-infiltrating B cells have previously been studied in chronic inflammatory autoimmune diseases (Nagel et al. 2009). A mouse model of skin inflammation showed heterogenous populations of skin-resident B cells characterized by co-expression of IgM and CD11b and increased expression of MHC class II, CD1 and CD80/86, which are important for T cell activation (Geherin et al. 2012). Increased frequencies of B cells in the skin of scurfy mice suggest a potential accumulation of antibody-secreting cells at the site of inflammation. These B cells may be able to release autoantibodies locally to enhance disease progression in the skin (Geherin et al. 2012). Further characterization of skin-resident B cells, which develop under impaired central tolerance leading to autoimmune disease in scurfy mice, will help to identify potential targets to prevent strong inflammatory responses in tissues.

4.2 Scurfy mice develop antigen-specific B cells relevant for AIBD onset

B cell responses are frequently studied to elucidate mechanisms in various antibody-mediated autoimmune diseases (Shlomchik 2008). It has been reported that up to 20% of mature B cells are capable of binding self-antigens (Meffre and Wardemann 2008). Mice are protected against autoimmune diseases by deletion of B cells with high affinity against self-antigens or by lack of T cell help (Taylor et al. 2012). Analysis of antigen-specific B cells describes the binding of BCR to a specific antigen (Boonyaratanakornkit and Taylor 2019), resulting in autoantibody production and potential autoimmunity. Haeberle et al. recently demonstrated that scurfy mice develop skin-specific autoantibodies in their serum attacking AIBD-related antigens. Therefore, the localization and quantification of antigen-specific B cells in sick scurfy mice was further investigated. ELISpot assays were performed with three proteins related to different forms of AIBD and B cells from spleen and sdLN of scurfy mice and WT littermates. Of note, ELISpot assays require antibody-secreting B cells, as the assay detects antibodies produced by a single antigen-specific B cell per spot (Boonyaratanakornkit and Taylor 2019; Saletti et al. 2013). B cells isolated from the spleen of scurfy mice showed significantly more specific B cells against vWFA2, Laminin α 3 and BP180 c-terminal domain compared to WT littermates. Non-B cells as a negative control confirmed significant B cell binding in this assay. Compared to the spleen, more antigen-specific B cells were detected from the sdLN. This indicates a stronger autoimmune response within the sdLN of scurfy mice, which is in line with the increased plasma cell levels in lymph nodes that produce skin-specific autoantibodies resulting in AIBD development. In pemphigus vulgaris patients, Desmoglein 3-specific B cell populations in peripheral blood have been reported to contribute to disease progression (Pollmann et al. 2019). Therefore, additional studies of antigen-specific autoreactive B cells in AIBD will provide further insight into mechanistic processes and potential therapeutic targets for treatment at early time points prior to antibody production.

4.3 Injection of autoantibody H510 mimics EBA in mice

To focus on the onset of AIBD in scurfy mice, which develop multiple autoimmune diseases simultaneously, hybridomas were generated using scurfy splenocytes to produce monoclonal antibodies for further analyses (Haeberle et al. 2018). Several antibodies were isolated and tested for skin specificity using IIF microscopy. Moreover, one of these spontaneously developed autoantibodies against BP230 was shown to be pathogenic *in vivo*, leading to the development of AIBD in scurfy mice (Haeberle et al. 2018). As this observation can be regarded

as “proof-of-principle” that uncontrolled activation of autoreactive CD4⁺ T cells can finally lead to autoantibody-mediated AIBD with a clearly defined autoantigen, further pathogenic autoantibodies were isolated and screened. One spontaneously generated mAb (H510) was successfully isolated and purified.

First, mAb H510 was tested in IIF on salt-split murine palate, as it is the gold standard for diagnosis of AIBD (Gammon et al. 1990), revealing binding of H510 to the blister floor (Vicari 2019, Master thesis). In addition, binding of H510 to the BMZ of esophageal epithelium was detected. These results suggest that H510 targets its antigen in the lower *L. lucida*, excluding potential antigens at the blister roof such as BP230, relevant for human BP (Goletz et al. 2017; Thoma-Uszynski et al. 2004). By performing IIF microscopy on primary murine keratinocytes and fibroblasts, antigen expression in skin cells was examined. Co-staining on both cell types with mAb H510, anti-K14 and anti-vimentin indicated antigen expression of H510 in primary murine keratinocytes but not in fibroblasts.

Previous experiments showed that injection of H510 in WT neonatal mice induced a pathogenic subepidermal blister formation in the skin (Vicari 2019, Master thesis). However, H510 was only able to induce microscopic blistering. In mouse immunization experiments with different autoantibodies involved in AIBD, macroscopic blisters were detected suggesting difficult accessibility of the autoantigen and binding of H510 to a small epitope (Ludwig et al. 2011; Pollmann and Eming 2017; Vorobyev et al. 2015).

Since binding of H510 to the dermal side of the DEJ implies a target antigen in the lower *L. lucida*, Col7 was considered as a possible autoantigen, which is the target in the human disease EBA. As a first approach, a peptide competition assay with H510 and the murine vWFA2 protein, which is part of the NC1 domain of Col7, showed a significant blocking of the antibody binding capacity after protein incubation. Western blot analysis, IIF microscopy and ELISA using skin from Col7^{-/-} mice and vWFA2 protein confirmed the specific binding of mAb H510 to vWFA2 of Col7, which had developed spontaneously under Treg deficiency in scurfy mice.

In an experimental model of EBA, it was previously reported that depletion of Treg did not affect the production of anti-Col7 autoantibodies (Chen et al. 2006). The authors concluded that the development of autoimmunity against Col7 is independent of Treg function. However, the discrepancy with our results may be explained by the fact that this study used Treg depletion by anti-CD25 antibodies. Since CD25 is an activation marker for T cells, depletion via CD25 targets Treg as well as activated conventional effector T cells (Li et al. 2015). Nevertheless, Treg depletion is never as complete as in scurfy mice lacking functional Treg due to a missense mutation in the *Foxp3* gene, the major factor for Treg function.

H510 belongs to the IgG1 subclass and thus shares this feature with circulating autoantibodies against Col7 in EBA patients which mainly belong to the IgG1 and IgG4 subclasses (Bernard et al. 1991; Mooney and Gammon 1990). This allows a translational connection between the disease in EBA patients and our EBA mouse model for further mechanistic insights and the development of IgG subclass-specific immunotherapies (Sitaru 2007). The dominant part of Col7 attacked by pathogenic autoantibodies in almost all EBA patients is the NC1 domain containing the vWFA2 (Chen et al. 1997; Gammon et al. 1993; Komorowski et al. 2013). Moreover, vWFA2 has been shown to be the binding site for type I Collagen, Laminin 332, and a β 1-Integrin, thereby ensuring the stability of the BMZ in the skin (Gebauer et al. 2020; Villone et al. 2008). The pathogenicity of autoantibodies against vWFA2 was demonstrated after immunization experiments in mice, strengthening the potential impact of H510 for further elucidation of the pathological mechanism leading to disease onset in human EBA (Iwata et al. 2013).

4.4 H510 induces skin blistering independent from inflammatory immune cells

As the injection of mAb H510 mimics the human disease EBA, it is interesting to further dissect the mechanism leading to pathogenic blister formation. It has been previously investigated that the complement system is involved in pathogenic mechanisms leading to the severe blistering disease EBA in patients (Koga et al. 2018; Mihai et al. 2018). Due to the lack of C3 deposition along the DEJ after *in vivo* experiments with H510, a contribution of complement C3 to pathogenic blister formation could be excluded. Considering the most common form of EBA induced by inflammatory tissue damage, extravasation of leukocytes to the DEJ occurs following Fc γ R activation on neutrophils by anti-Col7 antibodies (Figure 3) (Koga et al. 2018). Injection of mAb H510 into Fc γ R $^{-/-}$ mice resulted in subepidermal blister formation in the skin of the majority of injected mice, indicating a pathological mechanism independent of inflammatory immune cells.

In previous studies, several experimental models have demonstrated a pathogenic capacity of anti-Col7 antibodies *in vivo* (Kasperkiewicz et al. 2016; Ludwig 2012). Transfer of rabbit-anti-mouse Col7 IgG antibodies, representing a mouse model for EBA, indicated the development of inflammatory EBA (Kasperkiewicz et al. 2016; Sitaru et al. 2005; Vorobyev et al. 2015). These mouse models are mainly characterized by inflammation-triggered blister formation through activation of neutrophils via Fc γ R-mediated pathways (Kasperkiewicz et al. 2012; Yu et al. 2010). Of note, depletion of Treg in this mouse model led to excessive skin inflammation and blistering (Bieber et al. 2017).

As the pathogenic mechanism of H510 appears to be independent of inflammation, the injection experiments represent a mouse model for the classical/mechano-bullous form of EBA rather than the BP-like variant in which inflammatory immune cells contribute to disease onset. The mechanisms leading to non-inflammatory EBA are still elusive, and the pathways leading to blister formation by potential direct autoantibody binding are yet unknown (Kasperkiewicz et al. 2016; Koga et al. 2018; Prost-Squarcioni et al. 2018). Therefore, this anti-Col7 antibody developed under Treg defect has a high impact on further studies elucidating the pathogenic cascades leading to classical/mechano-bullous EBA in patients.

In addition, pursuing injection experiments with genetically modified mAb H510 are planned to reinforce the absence of inflammatory mediators and immune cells during blister formation. Silencing the Fc part of this anti-Col7 antibody following injection into WT neonatal mice will allow the study of skin blistering without immune cell binding to the antibody itself. Furthermore, the elucidation of a possible direct interference mechanism of the antibody with Col7 in the skin will be of great interest in the future.

4.5 Conclusion and outlook

In summary, the data from the first part of this project demonstrate that Treg deficiency in scurfy mice results not only in an expansion of autoreactive CD4⁺ T cells, but also in an altered B cell compartment, including elevated levels of germinal center B cells, memory B cells and plasma cells which all contribute to the production of autoreactive autoantibodies leading to autoimmune disease in these mice. Moreover, analysis of the inflamed skin revealed the presence of tissue-resident B cells that may also directly contribute to the pathological phenotype. Antigen-specific B cells against proteins relevant for various autoimmune blistering diseases were found in the spleen and skin-draining lymph nodes of sick scurfy mice suggesting relevance for specific autoantibody production and disease development. From these results, it can be hypothesized that autoreactive B cells under defective Treg control strongly contribute to the early onset of AIBD. Further studies will define different B cell interactions and further classification of antigen-specific B cells may provide potential targets for therapeutic approaches.

The data from the second part of this project demonstrated that a spontaneously developed pathogenic autoantibody targeting murine vWFA2 of Col7 could be isolated from scurfy mice. Injection of this antibody into mice serves as a mouse model for the classical/mechano-bullous form of EBA without contribution of inflammatory mediators. Currently, the majority of patients are treated with systemic corticosteroids, which come with many side effects due to its effect on the whole body (Koga et al. 2018). Further characterization of the pathological mechanism

leading to this so far unidentified disease development will allow studies for better treatment options for EBA patients.

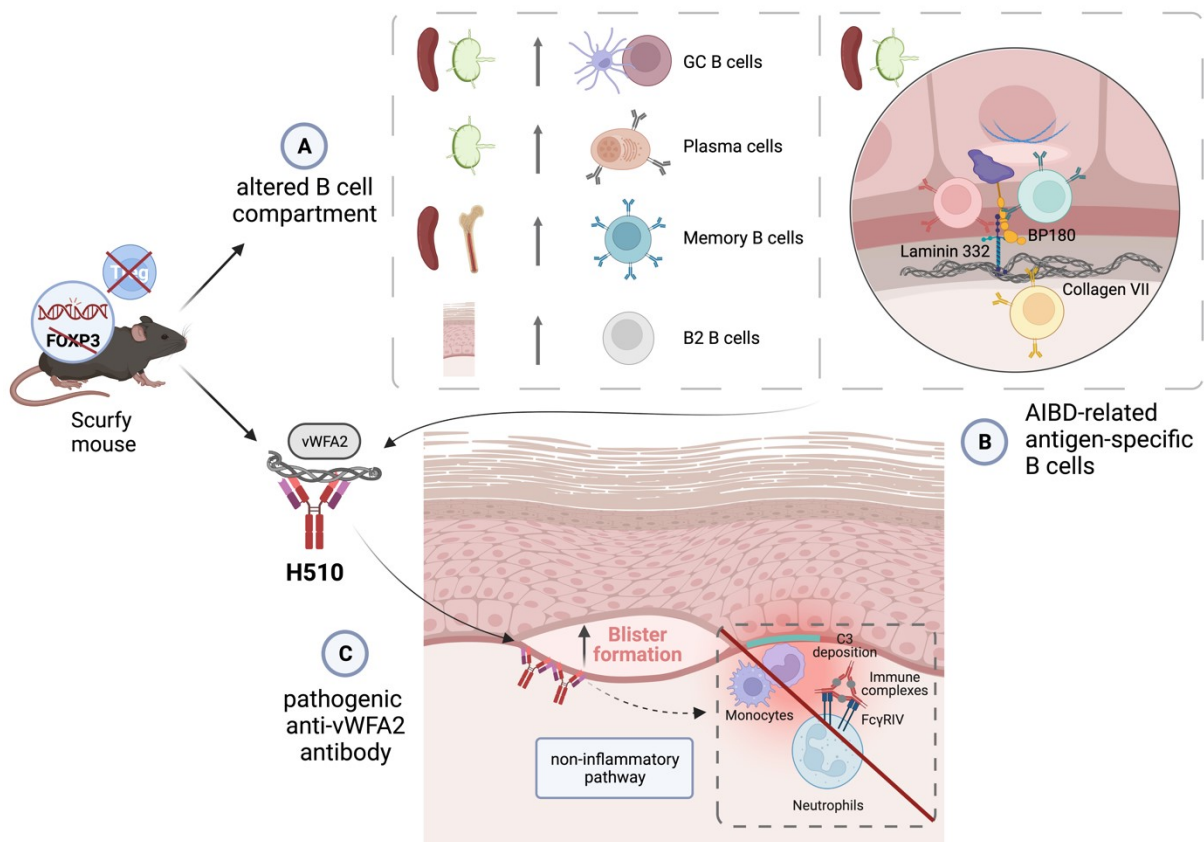


Figure 22. Schematic project summary. (A) Treg-deficient scurfy mice have an altered B cell compartment compared to WT littermates. Expanded frequencies of germinal center (GC) B cells in spleen and skin-draining lymph nodes (sdLN), plasma cells in sdLN, memory B cells in spleen and bone marrow and B2 B cells in skin were found. (B) In detail, out of altered B cell compartment, antigen-specific B cells against Laminin 332, BP180 and Collagen VII (Col7) were characterized being relevant for AIBD progression in scurfy mice. (C) Pathogenic murine autoantibody H510 was isolated out of scurfy mice targeting murine von-Willebrand-Factor-A-like domain 2 (vWFA2) of Col7 leading to subepidermal blisters in WT neonatal mice in a non-inflammatory manner (created with BioRender).

5 SUMMARY

Previous studies have shown that regulatory T cell-deficient scurfy mice develop several autoimmune diseases including autoimmune blistering disease (AIBD), associated with the production of high titers of anti-basement membrane antibodies.

To approach the cellular mechanisms of autoimmunity, this project demonstrated that scurfy mice are characterized by elevated levels of several B cell subpopulations, including germinal center B cells, memory B cells, and plasma cells. Focusing on the site of AIBD manifestation, scurfy mice showed significantly higher numbers of B cells in the skin. To further specify the role of B cells in the pathogenesis of AIBD, scurfy mice exhibited antigen-specific B cells against human relevant AIBD-related proteins present in the skin. Among others, Collagen type VII (Col7), the immunodominant antigen of the human disease Epidermolysis bullosa acquisita (EBA), was identified.

To study the immune response to this antigen in more detail, the scurfy-derived monoclonal antibody H510 was used which had previously been shown to be pathogenic *in vivo* as injection of H510 into wildtype neonatal mice resulted in subepidermal blisters. In the present project the murine von-Willebrand-Factor-A-like domain 2 of Col7 was identified as the target epitope of H510. Focusing on the pathogenic mechanism, injection into Fcγ-receptor knock-out mice could not abrogate the blister-inducing capacity of this anti-Col7 antibody, suggesting that H510 acts independently of cell-induced inflammation.

In conclusion, this project demonstrates the relevance of antigen-specific B cells for AIBD induction in scurfy mice, highlighting their potential role as a therapeutic target in human AIBD. Furthermore, the identification of the pathogenic anti-Col7 antibody H510 provides a new EBA mouse model that might become an important tool to further study this rare human AIBD and allow for potential development of novel therapeutic targets.

6 ZUSAMMENFASSUNG

Frühere Studien haben gezeigt, dass Scurfy Mäuse mit einem Mangel an regulatorischen T-Zellen verschiedene Autoimmunerkrankungen entwickeln, darunter auch Blasenbildende Autoimmundermatosen (BAID), welche mit der Produktion hoher Titer von Antikörpern gegen die Basalmembran einhergehen.

Um die zellulären Mechanismen der Autoimmunerkrankungen in diesen Mäusen weiter aufzuklären, wurde in diesem Projekt nachgewiesen, dass Scurfy Mäuse eine erhöhte Konzentration verschiedener B-Zell-Subpopulationen aufweisen, darunter B-Zellen aus dem Keimzentrum, B-Gedächtniszellen und Plasmazellen. Im Hinblick auf den Ort der BAID-Manifestation wiesen Scurfy Mäuse eine signifikant höhere Anzahl von B-Zellen in der Haut auf. Um die Rolle der B-Zellen in der Pathogenese der BAID weiter zu spezifizieren, konnten in Scurfy Mäusen antigenspezifische B-Zellen gegen humane, mit der BAID in Zusammenhang stehende Proteine in der Haut nachgewiesen werden. Unter anderem konnte Kollagen Typ VII (Col7), das immundominante Antigen der humanen Erkrankung Epidermolysis bullosa acquisita (EBA), identifiziert werden.

Um die Immunantwort auf dieses Antigen genauer zu untersuchen, wurde der monoklonale Scurfy-Antikörper H510 verwendet, der sich zuvor als pathogen erwiesen hatte, da die Injektion von H510 in neonatale Wildtyp Mäuse zu subepidermalen Blasen führte. Im vorliegenden Projekt wurde die murine von-Willebrand-Factor-A-like Domäne 2 von Col7 als das Zielepitop von H510 identifiziert. Im Hinblick auf den pathogenen Mechanismus konnte die Injektion in Fcy-Rezeptor Knock-out Mäuse die blasenauslösende Wirkung dieses anti-Col7 Antikörpers nicht aufheben, was darauf hindeutet, dass H510 unabhängig von der zellinduzierten Entzündung wirkt.

Zusammenfassend lässt sich sagen, dass dieses Projekt die Bedeutung antigenspezifischer B-Zellen für die Auslösung von BAID in Scurfy Mäusen aufzeigt und ihre potenzielle Rolle als therapeutisches Ziel bei humanen BAID unterstreicht. Des Weiteren liefert die Identifizierung des pathogenen anti-Col7 Antikörpers H510 ein neues EBA-Mausmodell, das für die weitere Erforschung dieser seltenen humanen BAID und die Entwicklung neuer therapeutischer Zielstrukturen zukünftig von entscheidender Bedeutung sein kann.

7 REFERENCES

- Abed, N. S., Chace, J. H., Fleming, A. L. and Cowdery, J. S. (1994). **Interferon-gamma regulation of B lymphocyte differentiation: activation of B cells is a prerequisite for IFN-gamma-mediated inhibition of B cell differentiation.** *Cell Immunol* 153 (2), 356-366, doi: 10.1006/cimm.1994.1034.
- Amagai, M., Klaus-Kovtun, V. and Stanley, J. R. (1991). **Autoantibodies against a novel epithelial cadherin in pemphigus vulgaris, a disease of cell adhesion.** *Cell* 67 (5), 869-877, doi: 10.1016/0092-8674(91)90360-b.
- Arellano, B., Graber, D. J. and Sentman, C. L. (2016). **Regulatory T cell-based therapies for autoimmunity.** *Discov Med* 22 (119), 73-80.
- Asashima, N., Fujimoto, M., Watanabe, R., Nakashima, H., Yazawa, N., Okochi, H. and Tamaki, K. (2006). **Serum levels of BAFF are increased in bullous pemphigoid but not in pemphigus vulgaris.** *Br J Dermatol* 155 (2), 330-336, doi: 10.1111/j.1365-2133.2006.07305.x.
- Aschermann, S., Lehmann, C. H., Mihai, S., Schett, G., Dudziak, D. and Nimmerjahn, F. (2013). **B cells are critical for autoimmune pathology in Scurfy mice.** *Proc Natl Acad Sci U S A* 110 (47), 19042-19047, doi: 10.1073/pnas.1313547110.
- Bernard, P., Prost, C., Aucouturier, P., Durepaire, N., Denis, F. and Bonnetblanc, J. M. (1991). **The subclass distribution of IgG autoantibodies in cicatricial pemphigoid and epidermolysis bullosa acquisita.** *J Invest Dermatol* 97 (2), 259-263, doi: 10.1111/1523-1747.ep12480369.
- Bertram, F., Brocker, E. B., Zillikens, D. and Schmidt, E. (2009). **Prospective analysis of the incidence of autoimmune bullous disorders in Lower Franconia, Germany.** *J Dtsch Dermatol Ges* 7 (5), 434-440, doi: 10.1111/j.1610-0387.2008.06976.x.
- Bettini, M. and Vignali, D. A. (2009). **Regulatory T cells and inhibitory cytokines in autoimmunity.** *Curr Opin Immunol* 21 (6), 612-618, doi: 10.1016/j.coi.2009.09.011.
- Bieber, K., Sun, S., Witte, M., Kasprick, A., Beltsiou, F., Behnen, M., Laskay, T., Schulze, F. S., Pipi, E., Reichhelm, N., Pagel, R., Zillikens, D., Schmidt, E., Sparwasser, T., Kalies, K. and Ludwig, R. J. (2017). **Regulatory T Cells Suppress Inflammation and Blistering in Pemphigoid Diseases.** *Front Immunol* 8, 1628, doi: 10.3389/fimmu.2017.01628.
- Boonyaratankornkit, J. and Taylor, J. J. (2019). **Techniques to Study Antigen-Specific B Cell Responses.** *Front Immunol* 10, 1694, doi: 10.3389/fimmu.2019.01694.
- Bouaziz, J. D., Yanaba, K., Venturi, G. M., Wang, Y., Tisch, R. M., Poe, J. C. and Tedder, T. F. (2007). **Therapeutic B cell depletion impairs adaptive and autoreactive CD4+ T cell activation in mice.** *Proc Natl Acad Sci U S A* 104 (52), 20878-20883, doi: 10.1073/pnas.0709205105.
- Bradley, L. M., Dalton, D. K. and Croft, M. (1996). **A direct role for IFN-gamma in regulation of Th1 cell development.** *J Immunol* 157 (4), 1350-1358.
- Brink, R. (2014). **The imperfect control of self-reactive germinal center B cells.** *Curr Opin Immunol* 28, 97-101, doi: 10.1016/j.coi.2014.03.001.
- Brunkow, M. E., Jeffery, E. W., Hjerrild, K. A., Paepfer, B., Clark, L. B., Yasayko, S. A., Wilkinson, J. E., Galas, D., Ziegler, S. F. and Ramsdell, F. (2001). **Disruption of a new**

- forkhead/winged-helix protein, scurfin, results in the fatal lymphoproliferative disorder of the scurfy mouse.** *Nat Genet* 27 (1), 68-73, doi: 10.1038/83784.
- Chan, O. and Shlomchik, M. J. (1998). **A new role for B cells in systemic autoimmunity: B cells promote spontaneous T cell activation in MRL-lpr/lpr mice.** *J Immunol* 160 (1), 51-59.
- Chang, S. E., Guo, L., Tian, J., Liu, Y., Guo, Z., Zheng, B. and Han, S. (2012). **Autoimmune bone marrow environment severely inhibits B cell development by inducing extensive cell death and inhibiting proliferation.** *Autoimmunity* 45 (3), 210-217, doi: 10.3109/08916934.2011.632455.
- Chen, L., Peterson, J. D., Zheng, W. Y., Lin, S. X. and Chan, L. S. (2006). **Autoimmunity to type VII collagen in SKH1 mice is independent of regulatory T cells.** *Clin Exp Immunol* 145 (2), 322-331, doi: 10.1111/j.1365-2249.2006.03115.x.
- Chen, M., Chan, L. S., Cai, X., O'Toole, E. A., Sample, J. C. and Woodley, D. T. (1997). **Development of an ELISA for rapid detection of anti-type VII collagen autoantibodies in epidermolysis bullosa acquisita.** *J Invest Dermatol* 108 (1), 68-72, doi: 10.1111/1523-1747.ep12285634.
- Chen, M., Doostan, A., Bandyopadhyay, P., Remington, J., Wang, X., Hou, Y., Liu, Z. and Woodley, D. T. (2007). **The cartilage matrix protein subdomain of type VII collagen is pathogenic for epidermolysis bullosa acquisita.** *Am J Pathol* 170 (6), 2009-2018, doi: 10.2353/ajpath.2007.061212.
- Chen, W., Jin, W., Hardegen, N., Lei, K. J., Li, L., Marinos, N., McGrady, G. and Wahl, S. M. (2003). **Conversion of peripheral CD4⁺CD25⁻ naive T cells to CD4⁺CD25⁺ regulatory T cells by TGF-beta induction of transcription factor Foxp3.** *J Exp Med* 198 (12), 1875-1886, doi: 10.1084/jem.20030152.
- Choe, J. and Choi, Y. S. (1998). **IL-10 interrupts memory B cell expansion in the germinal center by inducing differentiation into plasma cells.** *Eur J Immunol* 28 (2), 508-515, doi: 10.1002/(SICI)1521-4141(199802)28:02<508::AID-IMMU508>3.0.CO;2-I.
- Chung, J. B., Silverman, M. and Monroe, J. G. (2003). **Transitional B cells: step by step towards immune competence.** *Trends Immunol* 24 (6), 343-349, doi: 10.1016/s1471-4906(03)00119-4.
- Chung, Y., Tanaka, S., Chu, F., Nurieva, R. I., Martinez, G. J., Rawal, S., Wang, Y. H., Lim, H., Reynolds, J. M., Zhou, X. H., Fan, H. M., Liu, Z. M., Neelapu, S. S. and Dong, C. (2011). **Follicular regulatory T cells expressing Foxp3 and Bcl-6 suppress germinal center reactions.** *Nat Med* 17 (8), 983-988, doi: 10.1038/nm.2426.
- Damsker, J. M., Hansen, A. M. and Caspi, R. R. (2010). **Th1 and Th17 cells: adversaries and collaborators.** *Ann N Y Acad Sci* 1183, 211-221, doi: 10.1111/j.1749-6632.2009.05133.x.
- Darce, J. R., Arendt, B. K., Wu, X. and Jelinek, D. F. (2007). **Regulated expression of BAFF-binding receptors during human B cell differentiation.** *J Immunol* 179 (11), 7276-7286, doi: 10.4049/jimmunol.179.11.7276.
- Debes, G. F. and McGettigan, S. E. (2019). **Skin-Associated B Cells in Health and Inflammation.** *J Immunol* 202 (6), 1659-1666, doi: 10.4049/jimmunol.1801211.

- Deenick, E. K., Avery, D. T., Chan, A., Berglund, L. J., Ives, M. L., Moens, L., Stoddard, J. L., Bustamante, J., Boisson-Dupuis, S., Tsumura, M., Kobayashi, M., Arkwright, P. D., Averbuch, D., Engelhard, D., Roesler, J., Peake, J., Wong, M., Adelstein, S., Choo, S., Smart, J. M., French, M. A., Fulcher, D. A., Cook, M. C., Picard, C., Durandy, A., Klein, C., Holland, S. M., Uzel, G., Casanova, J. L., Ma, C. S. and Tangye, S. G. (2013). **Naive and memory human B cells have distinct requirements for STAT3 activation to differentiate into antibody-secreting plasma cells.** *J Exp Med* 210 (12), 2739-2753, doi: 10.1084/jem.20130323.
- Edwards, J. C. and Cambridge, G. (2005). **Prospects for B-cell-targeted therapy in autoimmune disease.** *Rheumatology (Oxford)* 44 (2), 151-156, doi: 10.1093/rheumatology/keh446.
- Egbuniwe, I. U., Karagiannis, S. N., Nestle, F. O. and Lacy, K. E. (2015). **Revisiting the role of B cells in skin immune surveillance.** *Trends Immunol* 36 (2), 102-111, doi: 10.1016/j.it.2014.12.006.
- Elkon, K. and Casali, P. (2008). **Nature and functions of autoantibodies.** *Nat Clin Pract Rheumatol* 4 (9), 491-498, doi: 10.1038/ncprheum0895.
- Fang, H., Zhang, Y., Li, N., Wang, G. and Liu, Z. (2018). **The Autoimmune Skin Disease Bullous Pemphigoid: The Role of Mast Cells in Autoantibody-Induced Tissue Injury.** *Front Immunol* 9, 407, doi: 10.3389/fimmu.2018.00407.
- Fetter, T., Niebel, D., Braegelmann, C. and Wenzel, J. (2020). **Skin-Associated B Cells in the Pathogenesis of Cutaneous Autoimmune Diseases-Implications for Therapeutic Approaches.** *Cells* 9 (12), doi: 10.3390/cells9122627.
- Fontenot, J. D., Gavin, M. A. and Rudensky, A. Y. (2003). **Foxp3 programs the development and function of CD4⁺CD25⁺ regulatory T cells.** *Nat Immunol* 4 (4), 330-336, doi: 10.1038/ni904.
- Gammon, W. R., Heise, E. R., Burke, W. A., Fine, J. D., Woodley, D. T. and Briggaman, R. A. (1988). **Increased frequency of HLA-DR2 in patients with autoantibodies to epidermolysis bullosa acquisita antigen: evidence that the expression of autoimmunity to type VII collagen is HLA class II allele associated.** *J Invest Dermatol* 91 (3), 228-232, doi: 10.1111/1523-1747.ep12470317.
- Gammon, W. R., Kowalewski, C., Chorzelski, T. P., Kumar, V., Briggaman, R. A. and Beutner, E. H. (1990). **Direct immunofluorescence studies of sodium chloride-separated skin in the differential diagnosis of bullous pemphigoid and epidermolysis bullosa acquisita.** *J Am Acad Dermatol* 22 (4), 664-670, doi: 10.1016/0190-9622(90)70094-x.
- Gammon, W. R., Murrell, D. F., Jenison, M. W., Padilla, K. M., Prisayanh, P. S., Jones, D. A., Briggaman, R. A. and Hunt, S. W., 3rd (1993). **Autoantibodies to type VII collagen recognize epitopes in a fibronectin-like region of the noncollagenous (NC1) domain.** *J Invest Dermatol* 100 (5), 618-622, doi: 10.1111/1523-1747.ep12472291.
- Gebauer, J. M., Flachsenberg, F., Windler, C., Richer, B., Baumann, U. and Seeger, K. (2020). **Structural and biophysical characterization of the type VII collagen vWFA2 subdomain leads to identification of two binding sites.** *FEBS Open Bio* 10 (4), 580-592, doi: 10.1002/2211-5463.12807.

- Geherin, S. A., Fintushel, S. R., Lee, M. H., Wilson, R. P., Patel, R. T., Alt, C., Young, A. J., Hay, J. B. and Debes, G. F. (2012). **The skin, a novel niche for recirculating B cells.** *J Immunol* 188 (12), 6027-6035, doi: 10.4049/jimmunol.1102639.
- Georgi, M., Jainta, S., Brocker, E. B. and Zillikens, D. (2001). **[Autoantigens of subepidermal bullous autoimmune dermatoses].** *Hautarzt* 52 (12), 1079-1089, doi: 10.1007/s001050170017.
- Giltiay, N. V., Chappell, C. P. and Clark, E. A. (2012). **B-cell selection and the development of autoantibodies.** *Arthritis Res Ther* 14 Suppl 4 (Suppl 4), S1, doi: 10.1186/ar3918.
- Godfrey, V. L., Wilkinson, J. E., Rinchik, E. M. and Russell, L. B. (1991a). **Fatal lymphoreticular disease in the scurfy (sf) mouse requires T cells that mature in a sf thymic environment: potential model for thymic education.** *Proc Natl Acad Sci U S A* 88 (13), 5528-5532, doi: 10.1073/pnas.88.13.5528.
- Godfrey, V. L., Wilkinson, J. E. and Russell, L. B. (1991b). **X-linked lymphoreticular disease in the scurfy (sf) mutant mouse.** *Am J Pathol* 138 (6), 1379-1387.
- Goletz, S., Hashimoto, T., Zillikens, D. and Schmidt, E. (2014). **Anti-p200 pemphigoid.** *J Am Acad Dermatol* 71 (1), 185-191, doi: 10.1016/j.jaad.2014.02.036.
- Goletz, S., Zillikens, D. and Schmidt, E. (2017). **Structural proteins of the dermal-epidermal junction targeted by autoantibodies in pemphigoid diseases.** *Exp Dermatol* 26 (12), 1154-1162, doi: 10.1111/exd.13446.
- Groom, J. R., Fletcher, C. A., Walters, S. N., Grey, S. T., Watt, S. V., Sweet, M. J., Smyth, M. J., Mackay, C. R. and Mackay, F. (2007). **BAFF and MyD88 signals promote a lupuslike disease independent of T cells.** *J Exp Med* 204 (8), 1959-1971, doi: 10.1084/jem.20062567.
- Guo, R., Wang, W., Yu, L., Zhu, Z. and Tu, P. (2021). **Different regulatory effects of CD40 ligand and B-cell activating factor on the function of B cells.** *Int Immunopharmacol* 91, 107337, doi: 10.1016/j.intimp.2020.107337.
- Guo, W., Smith, D., Aviszus, K., Detanico, T., Heiser, R. A. and Wysocki, L. J. (2010). **Somatic hypermutation as a generator of antinuclear antibodies in a murine model of systemic autoimmunity.** *J Exp Med* 207 (10), 2225-2237, doi: 10.1084/jem.20092712.
- Hadaschik, E. N., Wei, X., Leiss, H., Heckmann, B., Niederreiter, B., Steiner, G., Ulrich, W., Enk, A. H., Smolen, J. S. and Stummvoll, G. H. (2015). **Regulatory T cell-deficient scurfy mice develop systemic autoimmune features resembling lupus-like disease.** *Arthritis Res Ther* 17, 35, doi: 10.1186/s13075-015-0538-0.
- Haeberle, S., Raker, V., Haub, J., Kim, Y. O., Weng, S. Y., Yilmaz, O. K., Enk, A., Steinbrink, K., Schuppan, D. and Hadaschik, E. N. (2017). **Regulatory T cell deficient scurfy mice exhibit a Th2/M2-like inflammatory response in the skin.** *J Dermatol Sci* 87 (3), 285-291, doi: 10.1016/j.jdermsci.2017.07.001.
- Haeberle, S., Wei, X., Bieber, K., Goletz, S., Ludwig, R. J., Schmidt, E., Enk, A. H. and Hadaschik, E. N. (2018). **Regulatory T-cell deficiency leads to pathogenic bullous pemphigoid antigen 230 autoantibody and autoimmune bullous disease.** *J Allergy Clin Immunol* 142 (6), 1831-1842 e1837, doi: 10.1016/j.jaci.2018.04.006.

- Hammers, C. M. and Stanley, J. R. (2016). **Mechanisms of Disease: Pemphigus and Bullous Pemphigoid**. *Annu Rev Pathol* 11, 175-197, doi: 10.1146/annurev-pathol-012615-044313.
- Harris, D. P., Haynes, L., Sayles, P. C., Duso, D. K., Eaton, S. M., Lepak, N. M., Johnson, L. L., Swain, S. L. and Lund, F. E. (2000). **Reciprocal regulation of polarized cytokine production by effector B and T cells**. *Nat Immunol* 1 (6), 475-482, doi: 10.1038/82717.
- Hashimoto, T., Takahashi, H. and Sakaguchi, S. (2018). **Regulatory T-cell deficiency and autoimmune skin disease: Beyond the scurfy mouse and immune dysregulation, polyendocrinopathy, enteropathy, X-linked syndrome**. *J Allergy Clin Immunol* 142 (6), 1754-1756, doi: 10.1016/j.jaci.2018.08.028.
- Hennerici, T., Pollmann, R., Schmidt, T., Seipelt, M., Tackenberg, B., Mobs, C., Ghoreschi, K., Hertl, M. and Eming, R. (2016). **Increased Frequency of T Follicular Helper Cells and Elevated Interleukin-27 Plasma Levels in Patients with Pemphigus**. *PLoS One* 11 (2), e0148919, doi: 10.1371/journal.pone.0148919.
- Hertl, M., Eming, R. and Veldman, C. (2006). **T cell control in autoimmune bullous skin disorders**. *J Clin Invest* 116 (5), 1159-1166, doi: 10.1172/JCI28547.
- Hiepe, F., Dorner, T., Hauser, A. E., Hoyer, B. F., Mei, H. and Radbruch, A. (2011). **Long-lived autoreactive plasma cells drive persistent autoimmune inflammation**. *Nat Rev Rheumatol* 7 (3), 170-178, doi: 10.1038/nrrheum.2011.1.
- Hirose, M., Kasprick, A., Beltsiou, F., Dieckhoff Schulze, K., Schulze, F. S., Samavedam, U. K., Hundt, J. E., Pas, H. H., Jonkman, M. F., Schmidt, E., Kalies, K., Zillikens, D., Ludwig, R. J. and Bieber, K. (2017). **Reduced skin blistering in experimental epidermolysis bullosa acquisita after anti-TNF treatment**. *Mol Med* 22, 918-926, doi: 10.2119/molmed.2015.00206.
- Hoffman, W., Lakkis, F. G. and Chalasani, G. (2016). **B Cells, Antibodies, and More**. *Clin J Am Soc Nephrol* 11 (1), 137-154, doi: 10.2215/CJN.09430915.
- Hofmann, K., Clauder, A. K. and Manz, R. A. (2018). **Targeting B Cells and Plasma Cells in Autoimmune Diseases**. *Front Immunol* 9, 835, doi: 10.3389/fimmu.2018.00835.
- Hori, S., Nomura, T. and Sakaguchi, S. (2003). **Control of regulatory T cell development by the transcription factor Foxp3**. *Science* 299 (5609), 1057-1061, doi: 10.1126/science.1079490.
- Hsu, H. C., Yang, P., Wang, J., Wu, Q., Myers, R., Chen, J., Yi, J., Guentert, T., Tousson, A., Stanus, A. L., Le, T. V., Lorenz, R. G., Xu, H., Kolls, J. K., Carter, R. H., Chaplin, D. D., Williams, R. W. and Mountz, J. D. (2008). **Interleukin 17-producing T helper cells and interleukin 17 orchestrate autoreactive germinal center development in autoimmune BXD2 mice**. *Nat Immunol* 9 (2), 166-175, doi: 10.1038/ni1552.
- Huter, E. N., Natarajan, K., Torgerson, T. R., Glass, D. D. and Shevach, E. M. (2010). **Autoantibodies in scurfy mice and IPEX patients recognize keratin 14**. *J Invest Dermatol* 130 (5), 1391-1399, doi: 10.1038/jid.2010.16.
- Iwata, H., Bieber, K., Tiburzy, B., Chrobok, N., Kalies, K., Shimizu, A., Leineweber, S., Ishiko, A., Vorobyev, A., Zillikens, D., Kohl, J., Westermann, J., Seeger, K., Manz, R. and Ludwig, R. J. (2013). **B cells, dendritic cells, and macrophages are required to**

- induce an autoreactive CD4 helper T cell response in experimental epidermolysis bullosa acquisita.** *J Immunol* 191 (6), 2978-2988, doi: 10.4049/jimmunol.1300310.
- Iwata, H., Witte, M., Samavedam, U. K., Gupta, Y., Shimizu, A., Ishiko, A., Schroder, T., Seeger, K., Dahlke, M., Rades, D., Zillikens, D. and Ludwig, R. J. (2015). **Radiosensitive Hematopoietic Cells Determine the Extent of Skin Inflammation in Experimental Epidermolysis Bullosa Acquisita.** *J Immunol* 195 (5), 1945-1954, doi: 10.4049/jimmunol.1501003.
- Jain, A., Kovacs, J. A., Nelson, D. L., Migueles, S. A., Pittaluga, S., Fanslow, W., Fan, X., Wong, D. W., Massey, J., Hornung, R., Brown, M. R., Spinner, J. J., Liu, S., Davey, V., Hill, H. A., Ochs, H. and Fleisher, T. A. (2011). **Partial immune reconstitution of X-linked hyper IgM syndrome with recombinant CD40 ligand.** *Blood* 118 (14), 3811-3817, doi: 10.1182/blood-2011-04-351254.
- Kanitakis, J. (2002). **Anatomy, histology and immunohistochemistry of normal human skin.** *Eur J Dermatol* 12 (4), 390-399; quiz 400-391.
- Kasperkiewicz, M., Ellebrecht, C. T., Takahashi, H., Yamagami, J., Zillikens, D., Payne, A. S. and Amagai, M. (2017). **Pemphigus.** *Nat Rev Dis Primers* 3, 17026, doi: 10.1038/nrdp.2017.26.
- Kasperkiewicz, M., Nimmerjahn, F., Wende, S., Hirose, M., Iwata, H., Jonkman, M. F., Samavedam, U., Gupta, Y., Moller, S., Rentz, E., Hellberg, L., Kalies, K., Yu, X., Schmidt, E., Hasler, R., Laskay, T., Westermann, J., Kohl, J., Zillikens, D. and Ludwig, R. J. (2012). **Genetic identification and functional validation of FcγR4 as key molecule in autoantibody-induced tissue injury.** *J Pathol* 228 (1), 8-19, doi: 10.1002/path.4023.
- Kasperkiewicz, M., Sadik, C. D., Bieber, K., Ibrahim, S. M., Manz, R. A., Schmidt, E., Zillikens, D. and Ludwig, R. J. (2016). **Epidermolysis Bullosa Acquisita: From Pathophysiology to Novel Therapeutic Options.** *J Invest Dermatol* 136 (1), 24-33, doi: 10.1038/JID.2015.356.
- Kawano, Y., Noma, T. and Yata, J. (1994). **Regulation of human IgG subclass production by cytokines. IFN-gamma and IL-6 act antagonistically in the induction of human IgG1 but additively in the induction of IgG2.** *J Immunol* 153 (11), 4948-4958.
- Koch, P. J., Walsh, M. J., Schmelz, M., Goldschmidt, M. D., Zimbelmann, R. and Franke, W. W. (1990). **Identification of desmoglein, a constitutive desmosomal glycoprotein, as a member of the cadherin family of cell adhesion molecules.** *Eur J Cell Biol* 53 (1), 1-12.
- Koga, H., Prost-Squarcioni, C., Iwata, H., Jonkman, M. F., Ludwig, R. J. and Bieber, K. (2018). **Epidermolysis Bullosa Acquisita: The 2019 Update.** *Front Med (Lausanne)* 5, 362, doi: 10.3389/fmed.2018.00362.
- Komorowski, L., Muller, R., Vorobyev, A., Probst, C., Recke, A., Jonkman, M. F., Hashimoto, T., Kim, S. C., Groves, R., Ludwig, R. J., Zillikens, D., Stocker, W. and Schmidt, E. (2013). **Sensitive and specific assays for routine serological diagnosis of epidermolysis bullosa acquisita.** *J Am Acad Dermatol* 68 (3), e89-95, doi: 10.1016/j.jaad.2011.12.032.
- Kraal, G. and Mebius, R. (2006). **New insights into the cell biology of the marginal zone of the spleen.** *Int Rev Cytol* 250, 175-215, doi: 10.1016/S0074-7696(06)50005-1.

- Kurosaki, T., Kometani, K. and Ise, W. (2015). **Memory B cells**. *Nat Rev Immunol* 15 (3), 149-159, doi: 10.1038/nri3802.
- Lanzavecchia, A. (1985). **Antigen-specific interaction between T and B cells**. *Nature* 314 (6011), 537-539, doi: 10.1038/314537a0.
- Laurent, S. A., Hoffmann, F. S., Kuhn, P. H., Cheng, Q., Chu, Y., Schmidt-Supprian, M., Hauck, S. M., Schuh, E., Krumbholz, M., Rubsamen, H., Wanngren, J., Khademi, M., Olsson, T., Alexander, T., Hiepe, F., Pfister, H. W., Weber, F., Jenne, D., Wekerle, H., Hohlfeld, R., Lichtenthaler, S. F. and Meinl, E. (2015). **gamma-Secretase directly sheds the survival receptor BCMA from plasma cells**. *Nat Commun* 6, 7333, doi: 10.1038/ncomms8333.
- LeBien, T. W. and Tedder, T. F. (2008). **B lymphocytes: how they develop and function**. *Blood* 112 (5), 1570-1580, doi: 10.1182/blood-2008-02-078071.
- Leonardo, S. M., Josephson, J. A., Hartog, N. L. and Gauld, S. B. (2010). **Altered B cell development and anergy in the absence of Foxp3**. *J Immunol* 185 (4), 2147-2156, doi: 10.4049/jimmunol.1000136.
- Li, Z., Li, D., Tsun, A. and Li, B. (2015). **FOXP3+ regulatory T cells and their functional regulation**. *Cell Mol Immunol* 12 (5), 558-565, doi: 10.1038/cmi.2015.10.
- Lim, H. W., Hillsamer, P., Banham, A. H. and Kim, C. H. (2005). **Cutting edge: direct suppression of B cells by CD4+ CD25+ regulatory T cells**. *J Immunol* 175 (7), 4180-4183, doi: 10.4049/jimmunol.175.7.4180.
- Linterman, M. A., Pierson, W., Lee, S. K., Kallies, A., Kawamoto, S., Rayner, T. F., Srivastava, M., Divekar, D. P., Beaton, L., Hogan, J. J., Fagarasan, S., Liston, A., Smith, K. G. and Vinuesa, C. G. (2011). **Foxp3+ follicular regulatory T cells control the germinal center response**. *Nat Med* 17 (8), 975-982, doi: 10.1038/nm.2425.
- Liu, Z., Dang, E., Li, B., Qiao, H., Jin, L., Zhang, J. and Wang, G. (2018). **Dysfunction of CD19(+)/CD24(hi)/CD27(+) B regulatory cells in patients with bullous pemphigoid**. *Sci Rep* 8 (1), 703, doi: 10.1038/s41598-018-19226-z.
- Liu, Z. and Davidson, A. (2011). **BAFF and selection of autoreactive B cells**. *Trends Immunol* 32 (8), 388-394, doi: 10.1016/j.it.2011.06.004.
- Ludwig, R. J. (2012). **Model systems duplicating epidermolysis bullosa acquisita: a methodological review**. *Autoimmunity* 45 (1), 102-110, doi: 10.3109/08916934.2011.606451.
- Ludwig, R. J., Recke, A., Bieber, K., Muller, S., Marques Ade, C., Banczyk, D., Hirose, M., Kasperkiewicz, M., Ishii, N., Schmidt, E., Westermann, J., Zillikens, D. and Ibrahim, S. M. (2011). **Generation of antibodies of distinct subclasses and specificity is linked to H2s in an active mouse model of epidermolysis bullosa acquisita**. *J Invest Dermatol* 131 (1), 167-176, doi: 10.1038/jid.2010.248.
- Lund, F. E. (2008). **Cytokine-producing B lymphocytes-key regulators of immunity**. *Curr Opin Immunol* 20 (3), 332-338, doi: 10.1016/j.coi.2008.03.003.
- Lund, F. E., Garvy, B. A., Randall, T. D. and Harris, D. P. (2005). **Regulatory roles for cytokine-producing B cells in infection and autoimmune disease**. *Curr Dir Autoimmun* 8, 25-54, doi: 10.1159/000082086.

- MacLeod, M., Kwakkenbos, M. J., Crawford, A., Brown, S., Stockinger, B., Schepers, K., Schumacher, T. and Gray, D. (2006). **CD4 memory T cells survive and proliferate but fail to differentiate in the absence of CD40**. *J Exp Med* 203 (4), 897-906, doi: 10.1084/jem.20050711.
- Maglie, R., Solimani, F., Didona, D., Pipito, C., Antiga, E. and Di Zenzo, G. (2023). **The cytokine milieu of bullous pemphigoid: Current and novel therapeutic targets**. *Front Med (Lausanne)* 10, 1128154, doi: 10.3389/fmed.2023.1128154.
- Martin, F., Oliver, A. M. and Kearney, J. F. (2001). **Marginal zone and B1 B cells unite in the early response against T-independent blood-borne particulate antigens**. *Immunity* 14 (5), 617-629, doi: 10.1016/s1074-7613(01)00129-7.
- Martin, S. W. and Goodnow, C. C. (2002). **Burst-enhancing role of the IgG membrane tail as a molecular determinant of memory**. *Nat Immunol* 3 (2), 182-188, doi: 10.1038/ni752.
- Maruyama, M., Lam, K. P. and Rajewsky, K. (2000). **Memory B-cell persistence is independent of persisting immunizing antigen**. *Nature* 407 (6804), 636-642, doi: 10.1038/35036600.
- Marzano, A. V., Cozzani, E., Fanoni, D., De Pita, O., Vassallo, C., Berti, E., Parodi, A., Crosti, C. and Cugno, M. (2013). **Diagnosis and disease severity assessment of epidermolysis bullosa acquisita by ELISA for anti-type VII collagen autoantibodies: an Italian multicentre study**. *Br J Dermatol* 168 (1), 80-84, doi: 10.1111/bjd.12011.
- Matsuno, K., Ueta, H., Shu, Z., Xue-Dong, X., Sawanobori, Y., Kitazawa, Y., Bin, Y., Yamashita, M. and Shi, C. (2010). **The microstructure of secondary lymphoid organs that support immune cell trafficking**. *Arch Histol Cytol* 73 (1), 1-21, doi: 10.1679/aohc.73.1.
- Mauri, C., Gray, D., Mushtaq, N. and Londei, M. (2003). **Prevention of arthritis by interleukin 10-producing B cells**. *J Exp Med* 197 (4), 489-501, doi: 10.1084/jem.20021293.
- McHeyzer-Williams, L. J., Milpied, P. J., Okitsu, S. L. and McHeyzer-Williams, M. G. (2015). **Class-switched memory B cells remodel BCRs within secondary germinal centers**. *Nat Immunol* 16 (3), 296-305, doi: 10.1038/ni.3095.
- Medgyesi, D., Hobeika, E., Biesen, R., Kollert, F., Taddeo, A., Voll, R. E., Hiepe, F. and Reth, M. (2014). **The protein tyrosine phosphatase PTP1B is a negative regulator of CD40 and BAFF-R signaling and controls B cell autoimmunity**. *J Exp Med* 211 (3), 427-440, doi: 10.1084/jem.20131196.
- Meffre, E. (2011). **The establishment of early B cell tolerance in humans: lessons from primary immunodeficiency diseases**. *Ann N Y Acad Sci* 1246, 1-10, doi: 10.1111/j.1749-6632.2011.06347.x.
- Meffre, E. and Wardemann, H. (2008). **B-cell tolerance checkpoints in health and autoimmunity**. *Curr Opin Immunol* 20 (6), 632-638, doi: 10.1016/j.coi.2008.09.001.
- Mihai, S., Hirose, M., Wang, Y., Thurman, J. M., Holers, V. M., Morgan, B. P., Kohl, J., Zillikens, D., Ludwig, R. J. and Nimmerjahn, F. (2018). **Specific Inhibition of Complement Activation Significantly Ameliorates Autoimmune Blistering Disease in Mice**. *Front Immunol* 9, 535, doi: 10.3389/fimmu.2018.00535.

- Montecino-Rodriguez, E. and Dorshkind, K. (2012). **B-1 B cell development in the fetus and adult**. *Immunity* 36 (1), 13-21, doi: 10.1016/j.immuni.2011.11.017.
- Mooney, E. and Gammon, W. R. (1990). **Heavy and light chain isotypes of immunoglobulin in epidermolysis bullosa acquisita**. *J Invest Dermatol* 95 (3), 317-319, doi: 10.1111/1523-1747.ep12485033.
- Morris, G., Puri, B. K., Olive, L., Carvalho, A. F., Berk, M. and Maes, M. (2019). **Emerging role of innate B1 cells in the pathophysiology of autoimmune and neuroimmune diseases: Association with inflammation, oxidative and nitrosative stress and autoimmune responses**. *Pharmacol Res* 148, 104408, doi: 10.1016/j.phrs.2019.104408.
- Muramatsu, K., Ujiie, H., Kobayashi, I., Nishie, W., Izumi, K., Ito, T., Yoshimoto, N., Natsuga, K., Iwata, H. and Shimizu, H. (2018). **Regulatory T-cell dysfunction induces autoantibodies to bullous pemphigoid antigens in mice and human subjects**. *J Allergy Clin Immunol* 142 (6), 1818-1830 e1816, doi: 10.1016/j.jaci.2018.03.014.
- Nagel, A., Hertl, M. and Eming, R. (2009). **B-cell-directed therapy for inflammatory skin diseases**. *J Invest Dermatol* 129 (2), 289-301, doi: 10.1038/jid.2008.192.
- Nguyen, L. T., Jacobs, J., Mathis, D. and Benoist, C. (2007). **Where FoxP3-dependent regulatory T cells impinge on the development of inflammatory arthritis**. *Arthritis Rheum* 56 (2), 509-520, doi: 10.1002/art.22272.
- Nicholson, L. B. (2016). **The immune system**. *Essays Biochem* 60 (3), 275-301, doi: 10.1042/EBC20160017.
- Nutt, S. L., Hodgkin, P. D., Tarlinton, D. M. and Corcoran, L. M. (2015). **The generation of antibody-secreting plasma cells**. *Nat Rev Immunol* 15 (3), 160-171, doi: 10.1038/nri3795.
- Ochs, H. D., Ziegler, S. F. and Torgerson, T. R. (2005). **FOXP3 acts as a rheostat of the immune response**. *Immunol Rev* 203, 156-164, doi: 10.1111/j.0105-2896.2005.00231.x.
- Ohkura, N., Kitagawa, Y. and Sakaguchi, S. (2013). **Development and maintenance of regulatory T cells**. *Immunity* 38 (3), 414-423, doi: 10.1016/j.immuni.2013.03.002.
- Oliver, A. M., Martin, F., Gartland, G. L., Carter, R. H. and Kearney, J. F. (1997). **Marginal zone B cells exhibit unique activation, proliferative and immunoglobulin secretory responses**. *Eur J Immunol* 27 (9), 2366-2374, doi: 10.1002/eji.1830270935.
- Palm, A. E. and Kleinau, S. (2021). **Marginal zone B cells: From housekeeping function to autoimmunity?** *J Autoimmun* 119, 102627, doi: 10.1016/j.jaut.2021.102627.
- Palm, A. K., Friedrich, H. C. and Kleinau, S. (2016). **Nodal marginal zone B cells in mice: a novel subset with dormant self-reactivity**. *Sci Rep* 6, 27687, doi: 10.1038/srep27687.
- Pillai, S. and Cariappa, A. (2009). **The follicular versus marginal zone B lymphocyte cell fate decision**. *Nat Rev Immunol* 9 (11), 767-777, doi: 10.1038/nri2656.
- Pillai, S., Mattoo, H. and Cariappa, A. (2011). **B cells and autoimmunity**. *Curr Opin Immunol* 23 (6), 721-731, doi: 10.1016/j.coi.2011.10.007.

- Pollmann, R. and Eming, R. (2017). **Research Techniques Made Simple: Mouse Models of Autoimmune Blistering Diseases**. *J Invest Dermatol* 137 (1), e1-e6, doi: 10.1016/j.jid.2016.11.003.
- Pollmann, R., Walter, E., Schmidt, T., Waschke, J., Hertl, M., Mobs, C. and Eming, R. (2019). **Identification of Autoreactive B Cell Subpopulations in Peripheral Blood of Autoimmune Patients With Pemphigus Vulgaris**. *Front Immunol* 10, 1375, doi: 10.3389/fimmu.2019.01375.
- Prost-Squarcioni, C., Caux, F., Schmidt, E., Jonkman, M. F., Vassileva, S., Kim, S. C., Iranzo, P., Daneshpazhooh, M., Terra, J., Bauer, J., Fairley, J., Hall, R., Hertl, M., Lehman, J. S., Marinovic, B., Patsatsi, A., Zillikens, D., International Bullous Diseases, G., Werth, V., Woodley, D. T. and Murrell, D. F. (2018). **International Bullous Diseases Group: consensus on diagnostic criteria for epidermolysis bullosa acquisita**. *Br J Dermatol* 179 (1), 30-41, doi: 10.1111/bjd.16138.
- Qian, H., Kusuhara, M., Li, X., Tsuruta, D., Tsuchisaka, A., Ishii, N., Koga, H., Hayakawa, T., Ohara, K., Karashima, T., Ohyama, B., Ohata, C., Furumura, M. and Hashimoto, T. (2014). **B-cell activating factor detected on both naive and memory B cells in bullous pemphigoid**. *Exp Dermatol* 23 (8), 596-605, doi: 10.1111/exd.12421.
- Riewaldt, J., Duber, S., Boernert, M., Krey, M., Dembinski, M., Weiss, S., Garbe, A. I. and Kretschmer, K. (2012). **Severe Developmental B Lymphopoietic Defects in Foxp3-Deficient Mice are Refractory to Adoptive Regulatory T Cell Therapy**. *Front Immunol* 3, 141, doi: 10.3389/fimmu.2012.00141.
- Rosser, E. C., Oleinika, K., Tonon, S., Doyle, R., Bosma, A., Carter, N. A., Harris, K. A., Jones, S. A., Klein, N. and Mauri, C. (2014). **Regulatory B cells are induced by gut microbiota-driven interleukin-1beta and interleukin-6 production**. *Nat Med* 20 (11), 1334-1339, doi: 10.1038/nm.3680.
- Rush, J. S. and Hodgkin, P. D. (2001). **B cells activated via CD40 and IL-4 undergo a division burst but require continued stimulation to maintain division, survival and differentiation**. *Eur J Immunol* 31 (4), 1150-1159, doi: 10.1002/1521-4141(200104)31:4<1150::aid-immu1150>3.0.co;2-v.
- Sakaguchi, S., Sakaguchi, N., Asano, M., Itoh, M. and Toda, M. (1995). **Immunologic self-tolerance maintained by activated T cells expressing IL-2 receptor alpha-chains (CD25). Breakdown of a single mechanism of self-tolerance causes various autoimmune diseases**. *J Immunol* 155 (3), 1151-1164.
- Sakaguchi, S., Yamaguchi, T., Nomura, T. and Ono, M. (2008). **Regulatory T cells and immune tolerance**. *Cell* 133 (5), 775-787, doi: 10.1016/j.cell.2008.05.009.
- Saletti, G., Cuburu, N., Yang, J. S., Dey, A. and Czerkinsky, C. (2013). **Enzyme-linked immunospot assays for direct ex vivo measurement of vaccine-induced human humoral immune responses in blood**. *Nat Protoc* 8 (6), 1073-1087, doi: 10.1038/nprot.2013.058.
- Samavedam, U. K., Kalies, K., Scheller, J., Sadeghi, H., Gupta, Y., Jonkman, M. F., Schmidt, E., Westermann, J., Zillikens, D., Rose-John, S. and Ludwig, R. J. (2013). **Recombinant IL-6 treatment protects mice from organ specific autoimmune disease by IL-6 classical signalling-dependent IL-1ra induction**. *J Autoimmun* 40, 74-85, doi: 10.1016/j.jaut.2012.08.002.

- Schmidt, E., Kasperkiewicz, M. and Joly, P. (2019). **Pemphigus**. *Lancet* 394 (10201), 882-894, doi: 10.1016/S0140-6736(19)31778-7.
- Schmidt, E. and Zillikens, D. (2011). **The diagnosis and treatment of autoimmune blistering skin diseases**. *Dtsch Arztebl Int* 108 (23), 399-405, I-III, doi: 10.3238/arztebl.2011.0399.
- Schmidt, E. and Zillikens, D. (2013). **Pemphigoid diseases**. *Lancet* 381 (9863), 320-332, doi: 10.1016/S0140-6736(12)61140-4.
- Schneider, P., Takatsuka, H., Wilson, A., Mackay, F., Tardivel, A., Lens, S., Cachero, T. G., Finke, D., Beermann, F. and Tschopp, J. (2001). **Maturation of marginal zone and follicular B cells requires B cell activating factor of the tumor necrosis factor family and is independent of B cell maturation antigen**. *J Exp Med* 194 (11), 1691-1697, doi: 10.1084/jem.194.11.1691.
- Shlomchik, M. J. (2008). **Sites and stages of autoreactive B cell activation and regulation**. *Immunity* 28 (1), 18-28, doi: 10.1016/j.immuni.2007.12.004.
- Shlomchik, M. J. and Weisel, F. (2012). **Germinal center selection and the development of memory B and plasma cells**. *Immunol Rev* 247 (1), 52-63, doi: 10.1111/j.1600-065X.2012.01124.x.
- Sitaru, C. (2007). **Experimental models of epidermolysis bullosa acquisita**. *Exp Dermatol* 16 (6), 520-531, doi: 10.1111/j.1600-0625.2007.00564.x.
- Sitaru, C., Mihai, S., Otto, C., Chiriac, M. T., Hausser, I., Dotterweich, B., Saito, H., Rose, C., Ishiko, A. and Zillikens, D. (2005). **Induction of dermal-epidermal separation in mice by passive transfer of antibodies specific to type VII collagen**. *J Clin Invest* 115 (4), 870-878, doi: 10.1172/JCI21386.
- Stebegg, M., Kumar, S. D., Silva-Cayetano, A., Fonseca, V. R., Linterman, M. A. and Graca, L. (2018). **Regulation of the Germinal Center Response**. *Front Immunol* 9, 2469, doi: 10.3389/fimmu.2018.02469.
- Takahashi, H., Kouno, M., Nagao, K., Wada, N., Hata, T., Nishimoto, S., Iwakura, Y., Yoshimura, A., Yamada, T., Kuwana, M., Fujii, H., Koyasu, S. and Amagai, M. (2011). **Desmoglein 3-specific CD4+ T cells induce pemphigus vulgaris and interface dermatitis in mice**. *J Clin Invest* 121 (9), 3677-3688, doi: 10.1172/JCI57379.
- Taylor, J. J., Martinez, R. J., Titcombe, P. J., Barsness, L. O., Thomas, S. R., Zhang, N., Katzman, S. D., Jenkins, M. K. and Mueller, D. L. (2012). **Deletion and anergy of polyclonal B cells specific for ubiquitous membrane-bound self-antigen**. *J Exp Med* 209 (11), 2065-2077, doi: 10.1084/jem.20112272.
- Thai, L. H., Le Gallou, S., Robbins, A., Crickx, E., Fadeev, T., Zhou, Z., Cagnard, N., Megret, J., Bole, C., Weill, J. C., Reynaud, C. A. and Mahevas, M. (2018). **BAFF and CD4(+) T cells are major survival factors for long-lived splenic plasma cells in a B-cell-depletion context**. *Blood* 131 (14), 1545-1555, doi: 10.1182/blood-2017-06-789578.
- Theofilopoulos, A. N., Kono, D. H. and Baccala, R. (2017). **The multiple pathways to autoimmunity**. *Nat Immunol* 18 (7), 716-724, doi: 10.1038/ni.3731.
- Thoma-Uszynski, S., Uter, W., Schwietzke, S., Hofmann, S. C., Hunziker, T., Bernard, P., Treudler, R., Zouboulis, C. C., Schuler, G., Borradori, L. and Hertl, M. (2004). **BP230-**

- and BP180-specific auto-antibodies in bullous pemphigoid.** *J Invest Dermatol* 122 (6), 1413-1422, doi: 10.1111/j.0022-202X.2004.22603.x.
- Trigo-Guzman, F. X., Conti, A., Aoki, V., Maruta, C. W., Santi, C. G., Resende Silva, C. M., Gontijo, B., Woodley, D. T. and Rivitti, E. A. (2003). **Epidermolysis bullosa acquisita in childhood.** *J Dermatol* 30 (3), 226-229, doi: 10.1111/j.1346-8138.2003.tb00376.x.
- van Beek, N., Zillikens, D. and Schmidt, E. (2018). **Diagnosis of autoimmune bullous diseases.** *J Dtsch Dermatol Ges* 16 (9), 1077-1091, doi: 10.1111/ddg.13637.
- van Bruggen, N. and Ouyang, W. (2014). **Th17 cells at the crossroads of autoimmunity, inflammation, and atherosclerosis.** *Immunity* 40 (1), 10-12, doi: 10.1016/j.immuni.2013.12.006.
- Van Snick, J. (1990). **Interleukin-6: an overview.** *Annu Rev Immunol* 8, 253-278, doi: 10.1146/annurev.iy.08.040190.001345.
- Vicari, E. (2019). **Charakterisierung des Antigens und der Pathogenität eines murinen Autoantikörpers in der Scurfy Maus.** Unveröffentlichte Masterthesis. Johannes Gutenberg-Universität Mainz.
- Villone, D., Fritsch, A., Koch, M., Bruckner-Tuderman, L., Hansen, U. and Bruckner, P. (2008). **Supramolecular interactions in the dermo-epidermal junction zone: anchoring fibril-collagen VII tightly binds to banded collagen fibrils.** *J Biol Chem* 283 (36), 24506-24513, doi: 10.1074/jbc.M802415200.
- Vitetta, E. S., Berton, M. T., Burger, C., Kepron, M., Lee, W. T. and Yin, X. M. (1991). **Memory B and T cells.** *Annu Rev Immunol* 9, 193-217, doi: 10.1146/annurev.iy.09.040191.001205.
- Vorobyev, A., Ujiie, H., Recke, A., Buijsrogge, J. J. A., Jonkman, M. F., Pas, H. H., Iwata, H., Hashimoto, T., Kim, S. C., Hoon Kim, J., Groves, R., Samavedam, U., Gupta, Y., Schmidt, E., Zillikens, D., Shimizu, H. and Ludwig, R. J. (2015). **Autoantibodies to Multiple Epitopes on the Non-Collagenous-1 Domain of Type VII Collagen Induce Blisters.** *J Invest Dermatol* 135 (6), 1565-1573, doi: 10.1038/jid.2015.51.
- Winter, O., Dame, C., Jundt, F. and Hiepe, F. (2012). **Pathogenic long-lived plasma cells and their survival niches in autoimmunity, malignancy, and allergy.** *J Immunol* 189 (11), 5105-5111, doi: 10.4049/jimmunol.1202317.
- Wither, J. E., Roy, V. and Brennan, L. A. (2000). **Activated B cells express increased levels of costimulatory molecules in young autoimmune NZB and (NZB x NZW)F(1) mice.** *Clin Immunol* 94 (1), 51-63, doi: 10.1006/clim.1999.4806.
- Witte, M., Zillikens, D. and Schmidt, E. (2018). **Diagnosis of Autoimmune Blistering Diseases.** *Front Med (Lausanne)* 5, 296, doi: 10.3389/fmed.2018.00296.
- Wollenberg, I., Agua-Doce, A., Hernandez, A., Almeida, C., Oliveira, V. G., Faro, J. and Graca, L. (2011). **Regulation of the germinal center reaction by Foxp3+ follicular regulatory T cells.** *J Immunol* 187 (9), 4553-4560, doi: 10.4049/jimmunol.1101328.
- Wong, F. S., Wen, L., Tang, M., Ramanathan, M., Visintin, I., Daugherty, J., Hannum, L. G., Janeway, C. A., Jr. and Shlomchik, M. J. (2004). **Investigation of the role of B-cells in type 1 diabetes in the NOD mouse.** *Diabetes* 53 (10), 2581-2587, doi: 10.2337/diabetes.53.10.2581.

- Woodley, D. T., Chang, C., Saadat, P., Ram, R., Liu, Z. and Chen, M. (2005). **Evidence that anti-type VII collagen antibodies are pathogenic and responsible for the clinical, histological, and immunological features of epidermolysis bullosa acquisita.** *J Invest Dermatol* 124 (5), 958-964, doi: 10.1111/j.0022-202X.2005.23702.x.
- Xie, S., Li, J., Wang, J. H., Wu, Q., Yang, P., Hsu, H. C., Smythies, L. E. and Mountz, J. D. (2010). **IL-17 activates the canonical NF-kappaB signaling pathway in autoimmune B cells of BXD2 mice to upregulate the expression of regulators of G-protein signaling 16.** *J Immunol* 184 (5), 2289-2296, doi: 10.4049/jimmunol.0903133.
- Yancey, K. B. (1995). **Adhesion molecules. II: Interactions of keratinocytes with epidermal basement membrane.** *J Invest Dermatol* 104 (6), 1008-1014, doi: 10.1111/1523-1747.ep12606244.
- Yang, M., Hase, H., Legarda-Addison, D., Varughese, L., Seed, B. and Ting, A. T. (2005). **B cell maturation antigen, the receptor for a proliferation-inducing ligand and B cell-activating factor of the TNF family, induces antigen presentation in B cells.** *J Immunol* 175 (5), 2814-2824, doi: 10.4049/jimmunol.175.5.2814.
- Yang, M., Sun, L., Wang, S., Ko, K. H., Xu, H., Zheng, B. J., Cao, X. and Lu, L. (2010). **Novel function of B cell-activating factor in the induction of IL-10-producing regulatory B cells.** *J Immunol* 184 (7), 3321-3325, doi: 10.4049/jimmunol.0902551.
- Yildirim-Toruner, C. and Diamond, B. (2011). **Current and novel therapeutics in the treatment of systemic lupus erythematosus.** *J Allergy Clin Immunol* 127 (2), 303-312; quiz 313-304, doi: 10.1016/j.jaci.2010.12.1087.
- Yilmaz, O. K., Haeberle, S., Zhang, M., Fritzler, M. J., Enk, A. H. and Hadaschik, E. N. (2019). **Scurfy Mice Develop Features of Connective Tissue Disease Overlap Syndrome and Mixed Connective Tissue Disease in the Absence of Regulatory T Cells.** *Front Immunol* 10, 881, doi: 10.3389/fimmu.2019.00881.
- Yu, X., Holdorf, K., Kasper, B., Zillikens, D., Ludwig, R. J. and Petersen, F. (2010). **FcgammaRIIA and FcgammaRIIB are required for autoantibody-induced tissue damage in experimental human models of bullous pemphigoid.** *J Invest Dermatol* 130 (12), 2841-2844, doi: 10.1038/jid.2010.230.
- Yuan, H., Zhou, S., Liu, Z., Cong, W., Fei, X., Zeng, W., Zhu, H., Xu, R., Wang, Y., Zheng, J. and Pan, M. (2017). **Pivotal Role of Lesional and Perilesional T/B Lymphocytes in Pemphigus Pathogenesis.** *J Invest Dermatol* 137 (11), 2362-2370, doi: 10.1016/j.jid.2017.05.032.
- Yurasov, S., Wardemann, H., Hammersen, J., Tsuiji, M., Meffre, E., Pascual, V. and Nussenzweig, M. C. (2005). **Defective B cell tolerance checkpoints in systemic lupus erythematosus.** *J Exp Med* 201 (5), 703-711, doi: 10.1084/jem.20042251.
- Zillikens, D., Wever, S., Roth, A., Weidenthaler-Barth, B., Hashimoto, T. and Brocker, E. B. (1995). **Incidence of autoimmune subepidermal blistering dermatoses in a region of central Germany.** *Arch Dermatol* 131 (8), 957-958, doi: 10.1001/archderm.131.8.957.

8 PERSONAL PUBLICATIONS

Partial of this dissertation have already been published in the following article:

1. Vicari, E., Haeberle, S., Bolduan, V., Ramcke, T., Vorobyev, A., Goletz, S., Iwata, H., Ludwig, R. J., Schmidt, E., Enk, A. H. and Hadaschik, E. N. (2022). **Pathogenic Autoantibody Derived from Regulatory T Cell–Deficient Scurfy Mice Targets Type VII Collagen and Leads to Epidermolysis Bullosa Acquisita–Like Blistering Disease**. *J Invest Dermatol* 142 (3 Pt B), 980-984 e984, doi: 10.1016/j.jid.2021.08.441.

This publication is based on the results in chapters 3.9 (Table 1, Figure 15), 3.10 and 3.11 (Figure 20). Furthermore, discussion about pathogenicity of the autoantibody is partially based on this publication (chapter 4.3, 4.4). My personal contribution to this publication consisted in conceptualization, formal analysis, investigation, methodology, project administration, validation, visualization, writing and original draft preparation as well as review and editing.

Further publications:

2. Ramcke, T., Bolduan, V., Vicari, E., Yilmaz, K., Bertlich, I., Goletz, S., Mindorf, S., Hoffmann, J., Schmidt, E., Enk, A. and Hadaschik, E. (2022). **Anti-BP230 Only Bullous Pemphigoid Constitutes a Distinct Disease Subgroup with Characteristic Serological and Clinical Features**. *J Invest Dermatol* 142 (11), 3110-3113 e3118, doi: 10.1016/j.jid.2022.05.1084.
3. Ramcke, T., Vicari, E., Bolduan, V., Enk, A. and Hadaschik, E. (2022). **Bullous pemphigoid (BP) patients with selective IgG autoreactivity against BP230: Review of a rare but valuable cohort with impact on the comprehension of the pathogenesis of BP**. *J Dermatol Sci* 105 (2), 72-79, doi: 10.1016/j.jdermsci.2021.11.011.
4. Klaus, T., Wilson, A. S., Vicari, E., Hadaschik, E., Klein, M., Helbich, S. S. C., Kamenjarin, N., Hodapp, K., Schunke, J., Haist, M., Butsch, F., Probst, H. C., Enk, A. H., Mahnke, K., Waisman, A., Bednarczyk, M., Bros, M., Bopp, T. and Grabbe, S. (2022). **Impaired Treg-DC interactions contribute to autoimmunity in leukocyte adhesion deficiency type 1**. *JCI Insight* 7 (24), doi: 10.1172/jci.insight.162580.

9 ACKNOWLEDGMENTS

I would like to express my gratitude to all the people who supported me during my PhD.

First of all, I would like to thank Prof. Dr. Eva Hadaschik and Prof. Dr. Alexander Enk for giving me the opportunity to perform this dissertation in the research lab of the Department of Dermatology at Heidelberg University Hospital. Thank you for your guidance, support and expertise over the last years promoting my project and scientific career. My special gratitude goes to Eva, who was the perfect boss, always sympathetic, always motivating and enthusiastic, even when experiments failed several times. I am very grateful for your trust in letting me work independently and for your great supervision and scientific expertise during my time in the lab.

I would also like to thank our collaborators from Lübeck, Prof. Dr. Ralf Ludwig and Dr. Artem Vorobyev, for promoting my project with their expertise and the connection to Dr. Hiroaki Iwata in Japan, whom I would like to thank for providing me with important samples that pushed my project forward. Furthermore, I would like to thank Prof. Enno Schmidt and PD Dr. Stephanie Goletz for the fruitful cooperation and excellent expertise in the field of AIBD.

In addition, I would like to acknowledge all the members of my lab group, Torben Ramcke, Sophia Johannisson, Vanessa Bolduan and Lena Beideck who supported me with my experiments. Thank you for all the discussions, brainstorming, analysis of results and finally for every lunch break, conference or SFB retreat, we joined together. Without you, my time in the lab would not have been the same. Special thanks go to Steffi Häberle for her excellent training in the lab, project planning and great support during my PhD. A big thank you for always motivating and cheering me up, and for all the quality time beyond the lab. I would never have started this project without you being my colleague and friend even after you left our group. Furthermore, I would like to thank the whole research lab for the nice and inspiring discussions, lab meetings and help with my experiments. Special thanks to Dr. Florian Kurschus and Sonja Moos for the great discussions, setting up helpful hypotheses and experimental planning.

I am above all grateful to my boyfriend Chris for always being by my side, believing in me, encouraging me to start with this project, motivating me, and cheering me up when nothing worked in the lab. Thanks so much for your patience, encouragement, and unlimited support to follow my path.

Last but not least, I would like to thank my parents and my sister for always listening to me, for their never-ending support and for encouraging me to pursue my goals. Without you, I would not be at this point of writing my doctoral thesis.

10 EIDESSTATTLICHE VERSICHERUNG

1. Bei der eingereichten Dissertation zu dem Thema "Contribution of B cells to autoimmune blistering diseases in regulatory T cell-deficient scurfy mice" handelt es sich um meine eigenständig erbrachte Leistung.
2. Ich habe nur die angegebenen Quellen und Hilfsmittel benutzt und mich keiner unzulässigen Hilfe Dritter bedient. Insbesondere habe ich wörtlich oder sinngemäß aus anderen Werken übernommene Inhalte als solche kenntlich gemacht.
3. Die Arbeit oder Teile davon habe ich bislang nicht an einer Hochschule des In- oder Auslands als Bestandteil einer Prüfungs- oder Qualifikationsleistung vorgelegt.
4. Die Richtigkeit der vorstehenden Erklärungen bestätige ich.
5. Die Bedeutung der eidesstattlichen Versicherung und die strafrechtlichen Folgen einer unrichtigen oder unvollständigen eidesstattlichen Versicherung sind mir bekannt. Ich versichere an Eides statt, dass ich nach bestem Wissen die reine Wahrheit erkläre und nichts verschwiegen habe.

Ort und Datum

Unterschrift